Title
Identifying the mechanisms of activated transcription factor 6 - mediated cardioprotection

Permalink
https://escholarship.org/uc/item/1ps6h6tb

Author
Belmont, Peter Joseph

Publication Date
2010

Peer reviewed|Thesis/dissertation

UNIVERSITY OF CALIFORNIA, SAN DIEGO
SAN DIEGO STATE UNIVERSITY

Identifying the Mechanisms of
Activated Transcription Factor 6 - Mediated Cardioprotection

A dissertation submitted in partial satisfaction of the requirements for the degree

Doctor of Philosophy

in

Biology

by

Peter Joseph Belmont

Committee in charge:

      University of California, San Diego
            Professor Joan Heller Brown
            Professor Maho Niwa

      San Diego State University
            Professor Christopher C. Glembotski, Chair
            Professor Sanford Bernstein
            Professor Robert Zeller

2010

The dissertation of Peter Joseph Belmont is approved, and it is acceptable in quality and form for publication of microfilm:

_____

_____

_____

_____

Chair

University of California, San Diego

San Diego State University

2010

DEDICATION

This thesis, and all of my future work as a scientist, is dedicated to my father, Peter Joseph Belmont I, who passed away on January 14, 2006. It was due to his hard work and selflessness that I was afforded every opportunity growing up, and it was his encouragement and belief in me that got me to this point. Nobody was ever prouder of me than my father. As he was battling cancer, he made me promise that I would complete this degree and take care of my mother and sisters. I know he is smiling down on me and this work.

EPIGRAPH

You can be whatever you want to be in life, as long as you put your mind to it.

-Gloria Jean Belmont

TABLE OF CONTENTS

LIST OF ABBREVIATIONS

A1ATmut - α-1 antitrypsin mutant

AdV – Adenoviral

ANP – Atrial natriuretic peptide

ATF6 – Activating transcription factor 6

BNP – Brain natriuretic peptide

CHOP - C/EBP homologous protein

Derl1 – Derlin-1

Derl2 – Derlin-2

Derl3 – Derlin-3

DN – Dominant-negative

ER – Endoplasmic reticulum

ERAD – Endoplasmic reticulum-associated degradation

ERSE- ER-stress-response element

ERSE-II - ER-stress-response element II

ERSR – Endoplasmic reticulum stress response

ERSRG – Endoplasmic reticulum stress response gene

GO – Gene ontology

GRP78 – Glucose-regulated protein 78

GRP94 – Glucose-regulated protein 94

Hsp90 - Heat shock protein 90

IRE-1 - inositol-requiring protein-1

MCIP1 – Modulatory calcineurin interacting protein-1

MER – Mutant mouse estrogen receptor

MI – Myocardial infarction

miCon – microRNA control (non-specific)

miDerl3 – microRNA directed to Derl3

miRNA – MicroRNA

NFAT - Nuclear factor of activated T cells

NRVMC - Neonatal rat ventricular myocyte cultures

NTG - Non-transgenic

PAO – Preamyloid Oligomers

PE – Phenylephrine

PERK - Protein kinase R (PKR)-like ER kinase

PI – Propidium Iodide

RCAN1 – Regulator of calcineurin 1

sI – Simulated ischemia

sI/R – Simulated ischemia/reperfusion

siRNA – Small interfering RNA

TG – Transgenic

TM - Tunicamycin

UPR – Unfolded Protein Response

UPRE - Unfolded protein response element

DN – Dominant negative

LIST OF FIGURES

LIST OF TABLES

ACKNOWLEDGMENTS

This thesis was made possible because of the opportunity Professor Glembotski gave me to work in his lab. He has always been a great person to work both for and with, and has always had faith in my potential. In my first days in the lab it was Jason Wall who showed me the ropes, working patiently with me, even before I could confidently use a pipette. He will always have my gratitude for his mentorship and sage advice. Over the years there have been individuals that need to be thanked for their contributions to my scientific development: Dr. Jason Wall, Dr. Joshua Martindale, Dr. Ross Whittaker, Marie Marcinko, Donna Thuerauf, and Dr. Joan Chen. There have also been many individuals in the laboratory who have worked with me in collaboration and friendship: Michelle Frankson, Rayne Fernandez, Mimi Ly, Sherleen Cepada, Matt Glassy, Jungkang Jin, Kat Nasiadko, Archana Tadimalla, Shirin Doroudgar, John Vekich, Nikki Leonard, Dr. Nicole Gellings Lowe, Tera Tran, An Ta, Ali Obeid, and Annie Huynh. I would also like to give a special thanks to Matt San Pedro, a talented and dedicated undergraduate who worked closely with me during a portion of my last year in the program, and showed rapid development as a scientist.

I am grateful for the guidance and support of my doctoral thesis committee. From the University California San Diego: Professors Joan Heller Brown, PhD, whose lab has graciously prepared neonatal myocytes for our cell culture experiments, and Professor Maho Niwa, PhD, who has shared her expertise on the unfolded protein response; and from San Diego State University: Professor Sanford I. Bernstein, PhD,

I would also like to thank my amazing mother, Gloria, who has always put my siblings and me before herself, and who taught me that I can achieve whatever I put my mind to; my wife and best friend Katie, whom I have been in love with ever since we met 9 years ago in Boston, as she has stood by me throughout this entire process; my sisters Denise and Jessica; my grandfather Henry; the Rhodes family, who have all warmly taken me in as one of their own; and all of my family and friends in New York, Boston, San Diego, and elsewhere, who have given me encouragement, happiness, and support throughout this journey.

Peter J. Belmont, Matthew N. San Pedro, Wenqiong J. Chen, Donna J. Thuerauf, Nicole Gellings Lowe, Natalie Gude, Brett Hilton, Roland Wolkowicz, Mark A. Sussman, and Christopher C. Glembotski. "Roles for ER associated degradation and Derlin-3 in the heart during ER stress," Circulation Research Nov 25, 2009 [Epub ahead of print].

CURRICULUM VITA

1996-2000   Boston College
                   B.S. Biology

2007-2009   San Diego State University
                   Masters Program in Business Administration

2004-2010   University of California, San Diego and San Diego State
                   University
                   Ph.D. Biology

PUBLICATIONS

Belmont PJ, San Pedro M, Chen WJ, Theuerauf DJ, Gellings Lowe N, Gude N, Hilton B, Wolkowicz R, Sussman MA, Glembotski, CC. Degradation in Endoplasmic Reticulum Stress Protein 3 (Derl3) is an ATF6-Inducible Stress Response Gene which Enhances ERAD in Cardiomyocytes. Circ Res. 2009 Nov 25. [Epub ahead of print]

Doroudgar S, Thuerauf DJ, Marcinko MC, **Belmont PJ**, Glembotski CC. Ischemia activates the ATF6 branch of the endoplasmic reticulum (ER) stress response. J Biol Chem. 2009 Oct 23;284(43):29735-45. Epub 2009 Jul 21.

Tadimalla A, **Belmont PJ**, Thuerauf DJ, Glassy MS, Martindale JJ, Gude N, Sussman MA, Glembotski CC. Mesencephalic astrocyte-derived neurotrophic factor is an ischemia-inducible secreted endoplasmic reticulum stress response protein in the heart. Circ Res. 2008 Nov 21;103(11):1249-58.

Belmont PJ, Tadimalla A, Chen WJ, Martindale JJ, Thuerauf DJ, Marcinko M, Gude N, Sussman MA, Glembotski CC. Coordination of growth and endoplasmic reticulum stress signaling by regulator of calcineurin 1 (RCAN1), a novel ATF6-inducible gene. J Biol Chem. 2008 May 16;283(20):14012-21.

Thuerauf DJ, Marcinko M, **Belmont PJ**, Glembotski CC. Effects of the Isoform-specific Characteristics of ATF6a and ATF6bon ER Stress Response Gene Expression and Cell Viability. J Biol Chem. 2007 Aug 3;282(31):22865-78.

Wall JA, Wei J, Ly M, **Belmont PJ**, Martindale JJ, Tran D, Sun J, Chen WJ, Yu W, Oeller P, Briggs S, Gustafsson AB, Sayen MR, Gottlieb RA, Glembotski CC. Proteomic Analysis of MKK6 Transgenic Mouse Hearts Reveals Alterations in the Expression of Electron Transport Chain Components and Mitochondrial Respiration. Am J Physiol Heart Circ Physiol. 2006 Nov;291(5):H2462-72.

FIELD OF STUDY

Studies in Cellular and Molecular Biology
Professor Christopher C. Glembotski

ABSTRACT OF THE DISSERTATION

Identifying the Mechanisms of

Activated Transcription Factor 6 - Mediated Cardioprotection

by

Peter Joseph Belmont

Doctor of Philosophy in Biology

University of California, San Diego, 2010

San Diego State University, 2010

Professor Christopher C. Glembotski, Chair

Optimal conditions are required for proper protein folding in the ER. Cellular stresses can compromise these conditions, leading to an increase in misfolded proteins within the ER lumen, a condition known as ER stress. One such stress experienced by cardiac myocytes is myocardial infarction (MI), in which nutrients and oxygen are deprived to a particular region of the heart due to a coronary blockage. Upon ER stress, a protective signaling pathway known as the unfolded protein response (UPR) is triggered by three major ER membrane-bound stress sensors, PERK, IRE1, and ATF6. Pre-activating ATF6 prior to stress has been shown to decrease cell death, and

increase cardiac performance following the stress; however, the consequence of ATF6 activation on overall gene expression, and the specific mechanisms of ATF6-mediated protection, have not been investigated. This work focused on identifying ATF6-activated genes in the hearts of transgenic mice. In addition, this work identified two novel mechanisms of ATF6-mediated protection. The first involves the activation of RCAN1, a protein whose role in calcineurin-NFAT hypertrophic signaling is well known, but whose role in ER stress signaling had not been studied. RCAN1 was shown to be ER stress- and ATF6-inducible. This represents the first known study identifying a potential interface between ER stress and hypertrophic signaling. In addition, this work identified Derlin-3 (Derl3), a component of ER-associated degradation (ERAD), as another novel target of ATF6, as it displayed among the most dynamic up-regulation by ATF6 ever seen in the heart. Derl3 was also up-regulated in the heart following MI and in cultured myocytes following simulated ischemia (sI). Derl3 overexpression increased clearance of known misfolded proteins and attenuated apoptotic signaling and death in response to sI, while knock-down exacerbated death. These results indicated that enhancing components of ERAD can protect against cardiac stress, solidifying the critical importance of ERAD and protein quality control in the heart. Finally, this work was the first to investigate the role of ATF6 in microRNA gene regulation in the heart, uncovering potential novel connections between microRNAs and ER stress signaling.

I.   Introduction

Proteins are principally responsible for all cellular functions. To carry out their

functions, each protein possesses a unique three-dimensional shape, or native

conformation. This native conformation is obtained through folding of the polypeptide

chain, which is encoded by the genome. Optimal cellular conditions are required for

proteins to be properly synthesized and folded into their native conformation,

including the correct balance of oxygen, nutrients and ATP, and the correct

glycosylation and redox status within the cell. Upon exposure to stresses that perturb

these cellular conditions, protein folding can become compromised, leading to

incorrectly shaped, or misfolded, proteins. Misfolded proteins are unable to carry out

their native functions, and often, misfolded proteins can aggregate in the cell; both of

these outcomes have been shown to lead to a diverse number of pathologies, as

described below.

A.   Protein Folding

1.   Misfolded Proteins and Pathology:

The accumulation of misfolded proteins can be damaging to the cell, and has

been implicated in a number of pathologies and disease states in several tissue types.

For instance, systemic and localized amyloidoses can effect most tissues in the body;

neurodegenerative diseases such as Alzheimer's, Parkinson's, Huntington's, ALS,

bipolar disorder, and dementia can effect the brain and nervous system; atherosclerosis

can effect the arteries; sickle cell anemia can effect erythrocytes; and other disease

states such as diabetes mellitus can effect the pancreas.[1] In addition, protein

misfolding has been implicated in aging,[2] and it has been suggested that chaperones

and other protein quality control factors play roles in mediating the progression of age-related diseases that arise due to protein misfolding and aggregation.[2]

2. Protein Folding in the Endoplasmic Reticulum:

The endoplasmic reticulum (ER) is the first compartment in the secretory pathway, and is the site of synthesis of roughly 35% of all cellular proteins, including the majority of all secreted and membrane-bound proteins.[3] The ER is intimately involved with ribosomal protein synthesis, co- and post-translational modifications, and protein folding. To effectively carry out these functions, the ER lumen contains a diverse set of specialized chaperones, folding enzymes, and proteases, which aid in signal peptide cleavage, proper protein folding, and post-translational modifications, such as disulfide bond formations and N-linked glycosylations.[4] The ER plays a critical role in protein quality control (PQC), as proteins are only efficiently exported once they reach their native conformation in the ER.[4] Due to the prolific protein production that occurs within this organelle, protein concentrations can reach up to 100 mg/ml.[3]

B. Endoplasmic Reticulum Stress:

The accumulation of misfolded proteins within the ER is termed ER stress. Prolonged, unresolved ER stress has been shown to be detrimental to the cell, resulting in the initiation of apoptotic signaling emanating from ER components, ultimately leading to cell death.[5-8] Misfolded proteins in the ER can lead to several pathological states. In all, over 70 disease states have been identified which consist of mutations in a protein synthesized in the ER, or in a protein which plays a functional role in the ER
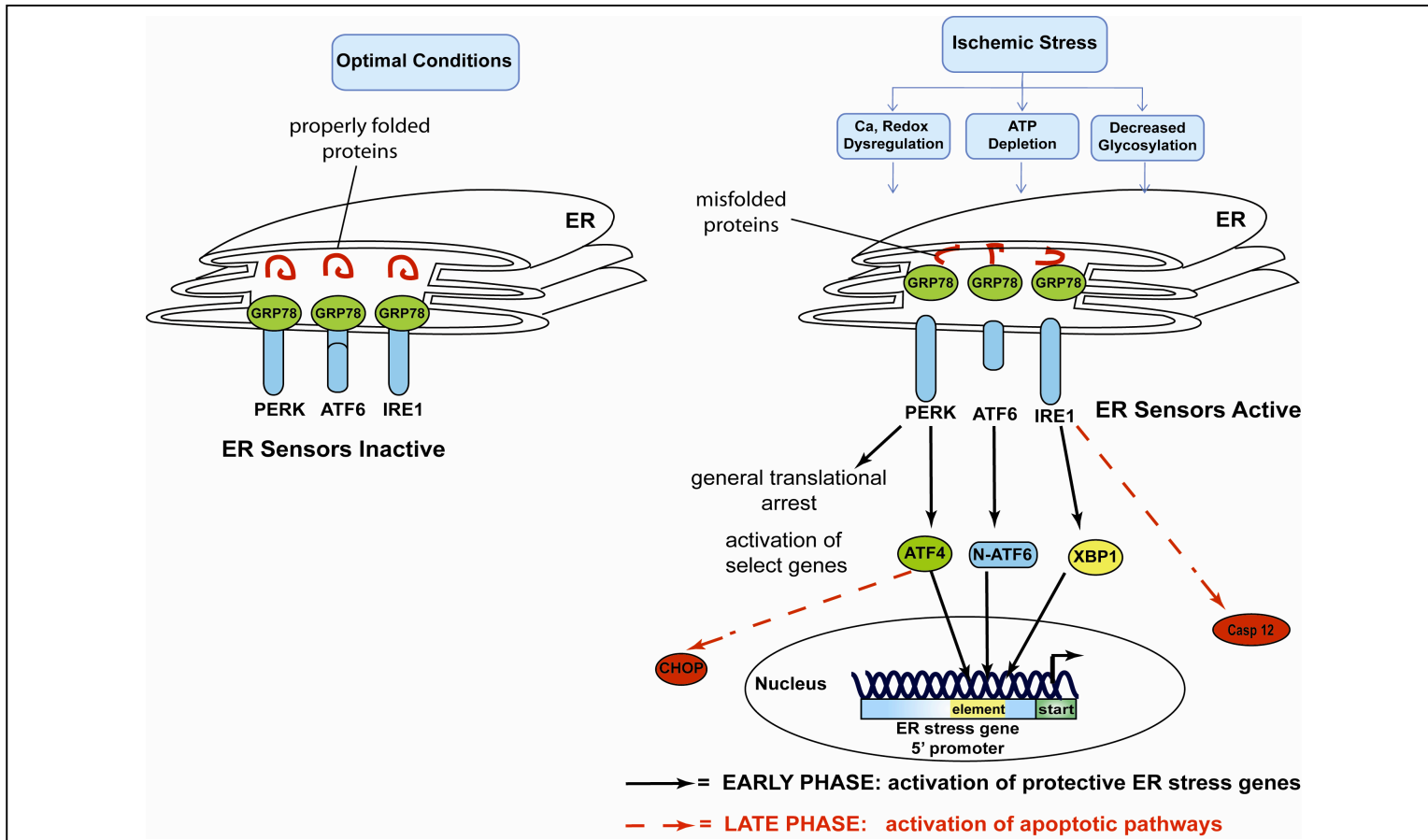
Figure 1. Activation of the Three Main Regulators of the Unfolded Protein Response.

Representation of the three main regulators of the unfolded protein response (UPR), PERK, ATF6, and IRE1, in their inactivate state during basal, unstressed conditions (left) or in response to ischemic stress (right). Ischemic stress results in dysregulations of ER Ca2+ and redox status, ATP depletion, and decreased protein glycosylation, all of which can lead to an increase in misfolded proteins and activation of the three major sensors of ER stress. Early phases of activation consist of protective signaling (black arrows), whereas prolonged, unresolved stress consists of pro-apoptotic signaling (red arrows).

2.   Activation of PERK by the UPR:

Upon GRP78 release, PERK can homodimerize, resulting in autophosphorylation and activation. Activated PERK phosphorylates the α subunit of eukaryotic initiation factor 2 (eIF2), a ribosomal protein which, under basal conditions, plays a role in translational initiation.[12] This phosphorylation decreases eIF2 activity, resulting in general translational repression, which reduces the overall protein synthesis and folding load in the ER, a response thought to facilitate recovery from the stress and a return to homeostasis and efficient protein folding in the ER. While phosphorylation of eIF2 results in general inhibition of translation of most mRNAs, it actually leads to an increase in translation of an mRNA encoding activated transcription factor 4 (ATF4),[13] possibly due to the presence of open reading frames within the 5' untranslated region (5' UTR) of the ATF4 mRNA. While ATF4 has been shown to facilitate the transcription of several protective ER stress response genes, prolonged ATF4 activation is responsible for the transcription of several pro-apoptotic genes, including CCAAT/enhancer-binding protein-homologous protein (CHOP), itself a b-ZIP transcription factor which mediates apoptotic cell death.[14] For instance, CHOP is known to down-regulate the anti-apoptotic protein Bcl2, and up-regulate the pro-apoptotic Bim, as well as to perturb the cellular redox state by down-regulating glutathione and increasing production of reactive oxygen species.[15]

3.   Activation of IRE1 by the UPR:

Upon dislocation of GRP78, IRE1 also homodimerizes, leading to autophosphorylation events, much like PERK; however, autophosporylation of IRE1 results in unique endoribonuclease activity, which leads to the induction of the un-

conventional splicing of x-box binding protein-1 (XBP1) via cleavage of its intron, which leads to the translation of an alternative, spliced form of XBP1.[16,17] Spliced XBP1 is known to be a potent transcription factor regulating the expression of ER stress response genes.[18] Prolonged activation of IRE1 can also lead to pro-apoptotic signaling. Upon prolonged activation, the cytosolic domain of IRE1 can bind to the adaptor protein tumor necrosis factor associated factor 2 (TRAF2), which leads to the activation of the pro-apoptotic C-Jun N-terminal kinase (JNK) pathway.[19]

4. Activation of ATF6 by the UPR:

Upon dislocation of GRP78, ATF6 is shuttled to the Golgi apparatus, where it is cleaved by site-1 and 2 proteases (S1P, S2P), producing a 50-kilodalton, N-terminal fragment. Upon cleavage, N-terminal ATF6 translocates to the nucleus, where it regulates the transcription of several ER stress response genes.[20] This N-terminal portion possesses both a DNA binding domain and a transactivation domain.[21] Interestingly, the N-terminal portion also contains a domain which confers its rapid degradation upon engagement in transcription. This domain bears distinct similarity to the VN8 region of the herpes simplex viral protein 16 (VP16), a transcription factor which displays rapid proteasomal degradation upon activation.[20] In all, the transition from inactive, membrane-bound ATF6 to its N-terminal, transcriptionally active form is a complex process which involves several cellular compartments.

C.   Gene Induction by ATF6

1.   Promoter Elements Recognized by ATF6:

The N-terminal portion of ATF6 has been shown to bind with high affinity to specific nucleotide sequences, or elements, within the 5' flanking promoter regions of genes. Such elements include the ER stress response element (ERSE, CCAAT-N9-CCACG)[22], the ER stress response element-II (ERSEII, ATTGG-N-CCACG)[23], and the unfolded protein response element (UPRE, TGACGTGGA)[24]. Spliced XBP1 has also been shown to bind with high affinity to several of these elements,[25] and it has been suggested that XBP1 binds preferentially to UPREs.[25] In addition, it has been suggested that ATF6 and XBP1, both basic leucine zipper (bZIP) domain-containing transcription factors, can homo- and hetero-dimerize.[26] Genes that contain such elements within their 5' flanking promoter regions have been classified as ER stress response genes (ERSRGs). The characterization of genes which contain each of these canonical elements has recently been carried out as a part of this dissertation.[27] Several of the genes with these canonical elements have already been shown to play functional roles in ERSR signaling, while the function of several others is yet to be defined. In addition, there is likely a large number of genes which do not contain any of the mentioned canonical elements, but which do function as ER stress response genes.

2.   ATF6-Regulated Genes:

Upon its activation and translocation to the nucleus, ATF6 regulates the expression of many proteins that help to restore a proper protein folding environment, including molecular chaperones such as GRP78 and GRP94; isomerases such as protein disulfide isomerase (PDI); and proteins such ER degradation enhancer,

mannosidase alpha-like (EDEM), which aid in the detection and destruction of terminally misfolded proteins, a process termed ER-associated degradation (ERAD). Each of these classes of genes has clear implications in restoring a proper protein folding environment in the ER, resuming correct protein folding, and ultimately aiding in recovery from the stress which led to the original perturbation.

D.   Cellular Stressors Which Initiate the Unfolded Protein Response

1.   UPR in Solid Tumors:

Several physiological stressors can lead to ER stress and initiate the unfolded protein response in diverse tissue types and disease states. For instance, solid tumors which display dysregulated growth, are subjected to a low oxygen environment as they grow, a condition known as hypoxia.[3] Hypoxia activates the UPR, which can confer protection to the tumor, leading to increased malignancy and increased drug resistance.[3,28] In this sense, UPR signaling is thought to aid in tumor survival, and because of this, several key UPR signaling nodes have been the targets of anti-cancer therapies **(see Fig 2)**.[29] For instance, the drug Versipelostatin (VST) is a specific inhibitor of GRP78 expression and shows cytotoxic qualities in glucose-deprived tumor cells by inhibiting the induction of key UPR transcription factors.[29]

2.   UPR in the Brain:

UPR markers have been recently shown to be induced in the brain in response to various stresses, such as focal cerebral ischemia,[30] transient cerebral ischemia,[31,32] and brain trauma caused by head injury.[33] The UPR has also been shown to be activated and dysregulated in hepatic cells due to non-alcoholic fatty liver disease (NAFLD).[34]

3.   UPR in the Heart:

Conditions of hypoxia have recently been shown to activate the UPR in the heart. The hearts of mice subjected to *in vivo* myocardial infarction (MI) display a marked increase in the prototypical ER stress protein, GRP78, in the cells surrounding the border zone of the injury.[35] In this study, these results were recapitulated in cell culture models. When neonatal and adult cardiac myocytes were subjected to conditions which simulate in vivo infarction, such as low oxygen and nutrient content, a condition known as simulated ischemia (sI), several hallmarks of the UPR were increased, including GRP78 promoter activation, an increase GRP78 protein, and XBP1 mRNA splicing.[35] In addition, when oxygen and nutrients were replenished, which simulates recovery from an infarction, the cells displayed a decrease in these UPR markers, suggesting that the UPR is activated during ischemia but not reoxygenation.[35] Pre-activation of the ATF6 branch of the UPR has been shown to minimize apoptosis and necrosis, and improve cardiovascular function following the stress, indicating a protective role of the UPR in the heart during stress.[20] In this sense, activation of the UPR can be thought of as beneficial to the heart in response to stress **(Fig. 2)**.
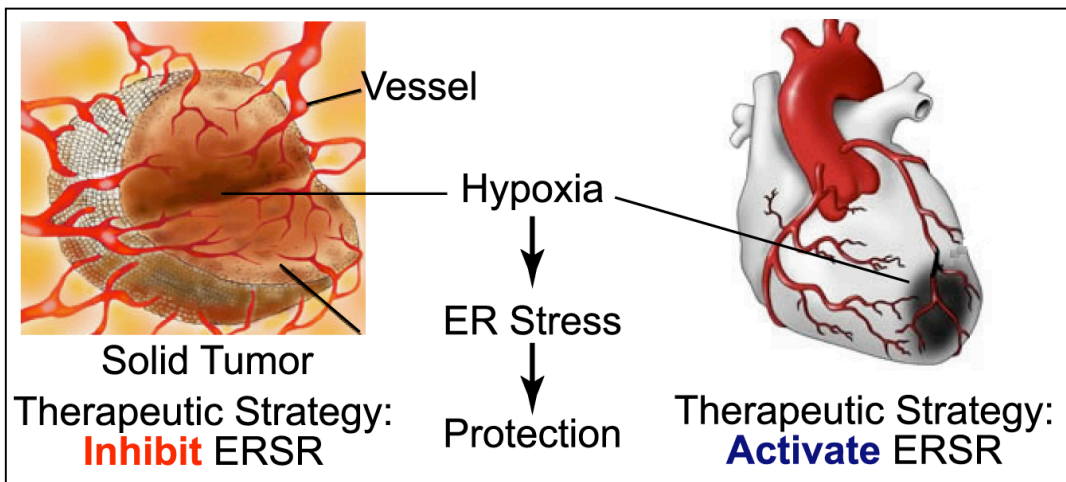
Figure 2. Ischemia-Mediated ER Stress Response.
Hypoxia has been shown to activate the ER stress response in several disease states, including in solid tumors and in the heart in the region of an infarct. While therapeutic strategies in tumors have aimed to inhibit the ERSR to increase cell death, therapeutic strategies in the heart should aim to activate the ERSR, in order to prevent cell death in the area at risk.

E.   Potential Detrimental Effects of ER Stress

1.   Prolonged ER Sress and Apoptosis:

The initial phases of ER stress and ATF6 signaling are thought to be predominantly protective; however, prolonged, unresolved ER stress can lead to conditions which activate proapoptotic factors, [8,36] a process thought to spare neighboring cells. The PERK/Eif2α branch of the ER stress response can lead to induction of the transcription factor C/EBP homologous protein (CHOP),[37] and the IRE1 branch can lead to recruitment of TRAF2 leading to induction of the proapoptotic protein JNK.[19] In addition, IRE1-mediated JNK activation is also thought to induce clustering and eventual cleavage of the ER-resident procaspase-12, leading to induction of the caspase cascade.[19] Less is currently known about pro-apoptotic signaling from the ATF6 branch of the UPR, although it has been shown that prolonged activation of ATF6 can lead to CHOP induction,[38]and it has been suggested that ATF6 may mediate myoblast apoptosis during muscle development.[39]

F.   Overall Hypothesis: The Role of ATF6 in the Heart

More recently, simulated ischemia was shown to activate the ATF6 branch of the ER stress response in cultured cardiac myocytes, and blockage of the ATF6 branch by adenoviral overexpression of a microRNA targeted to ATF6 sensitized cells to ischemia-mediated cell death,[40] indicating an important role for ATF6 in survival from ischemic stress. The overarching hypothesis of this dissertation is that the ATF6 branch of the UPR contributes to protection from ischemic damage in the heart by inducing novel cardioprotective genes which restore ER homeostasis **(Fig. 3)**. By promoting the restoration of a favorable ER protein folding environment, ATF6

prevents the progression to apoptotic signaling and promotes survival. It is the goal of this work to understand the effects of ATF6 overexpression on gene expression in the heart, and in turn, to identify potential novel mechanisms by which ATF6 promotes survival from stress.
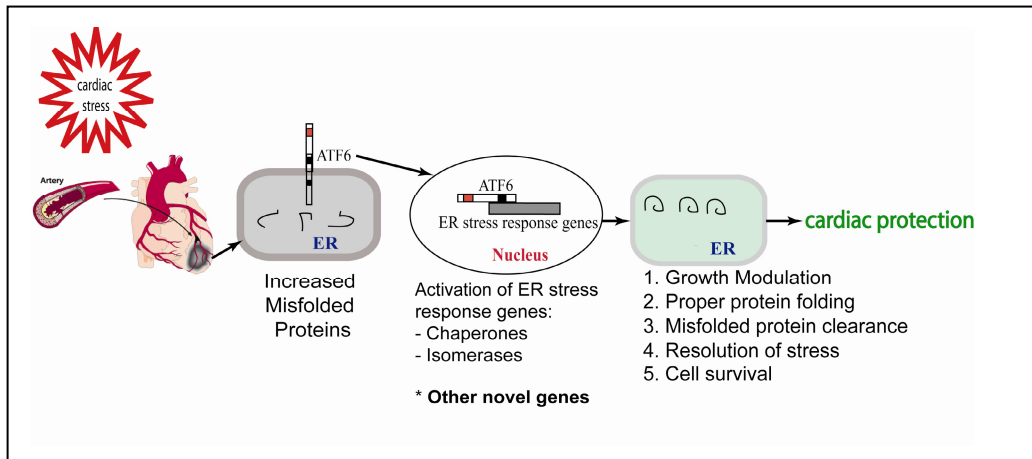
Figure 3. Depiction of the Overall Hypothesis: The ATF6 Branch of the UPR Provides Protection from Cardiac Stress.

Upon cardiac stress, such as myocardial infarction, the region of the heart distal to the blockage becomes compromised, and the cells in this region experience a dysregulation of the ER protein folding environment, leading to an increase in misfolded proteins. This increase leads to activation and translocation of ATF6 to the nucleus, where it induces several protective genes, many of which aid in restoring the ER protein folding environment, ultimately leading to recovery from the stress and cell survival.

G.   Investigating the Protective Effects of ATF6

1.   Transgenic Overexpression of ATF6:

Since ATF6 signaling fosters the restoration of an optimal ER protein folding

environment, recent studies have focused on examining whether overexpression of

ATF6 can protect cells from stress-related injury. To this end, a line of transgenic

mice was generated that possess an inducible form of ATF6.[20] The mice possess a

transgene which encodes the transcriptionally active, N-terminal portion of ATF6,

fused to the mutated mouse estradiol receptor (MER) under the regulation of the

alpha-myosin heavy chain promoter (αMHC), to drive ATF6-MER expression in

cardiac myocytes in vivo, only in the heart. Under basal conditions, the ATF6-MER

fusion protein is expressed in the heart, and remains in an inactive state, as the MER

binds proteins which mask both the DNA binding and transactivation domains of

ATF6. Upon administration of the drug tamoxifen, an estrogen analog, the MER

preferentially binds the smaller tamoxifen molecule, unmasking the activation

domains and producing a transcriptionally active ATF6 protein. A schematic of the

mechanism of action of ATF6-MER is shown in **Fig. 4**.
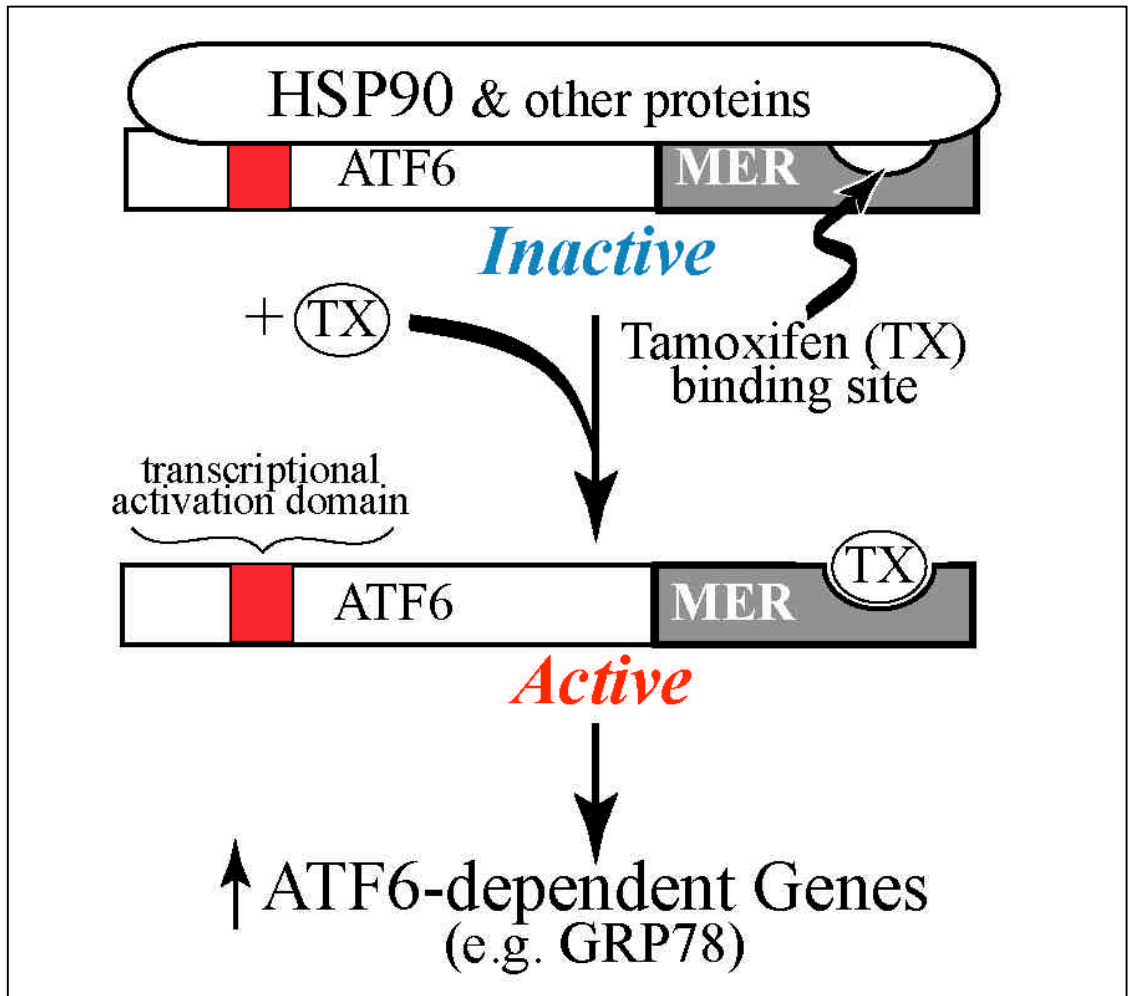
Figure 4. Mechanism of ATF6 Action in Transgenic Mouse Hearts.

The mechanism of tamoxifen-mediated ATF6 activation by tamoxifen is shown. The transcriptional activation domain of ATF6, shown in red, is masked by proteins, such as Hsp90, which bind to the MER fragment in the absence of tamoxifen, rendering the ATF6-MER fusion protein inactive. Tamoxifen displaces these proteins, unmasking the transcriptional activation domain, conferring transcriptional activation to ATF6-MER.

The hearts of transgenic mice treated with tamoxifen displayed marked increases in several protective ER stress response transcripts, such as GRP78, GRP94, PDI, EDEM, and ERP72.[20] In addition, when ATF6 was activated prior to a physiological stress, such as *ex vivo* ischemia/reperfusion (I/R), these hearts exhibited increased functional recovery and decreased apoptotic and necrotic cell death.[20] Taken together, pre-activating ATF6 prior to cardiac stress improved performance and minimized cellular damage. This suggests that increasing signaling from the ATF6 branch of the ER stress response prior to cardiac stress can prepare cardiac myocytes for the harmful effects of the stress, perhaps by enhancing the capacity of the ER to cope with an increase of misfolded proteins. It is the hypothesis of this dissertation that pre-activating the ATF6 branch of the UPR will increase the expression of several protective ER components, leading to restoration of the ER protein folding environment, minimization of misfolded protein aggregates, inhibition of apoptotic signaling, and thus minimization of cell death in the region of the infarct, all of which can preserve cardiac contractility and function following the stress. A depiction of these possible modes of ATF6-mediated protection can be seen in **Fig. 5**.
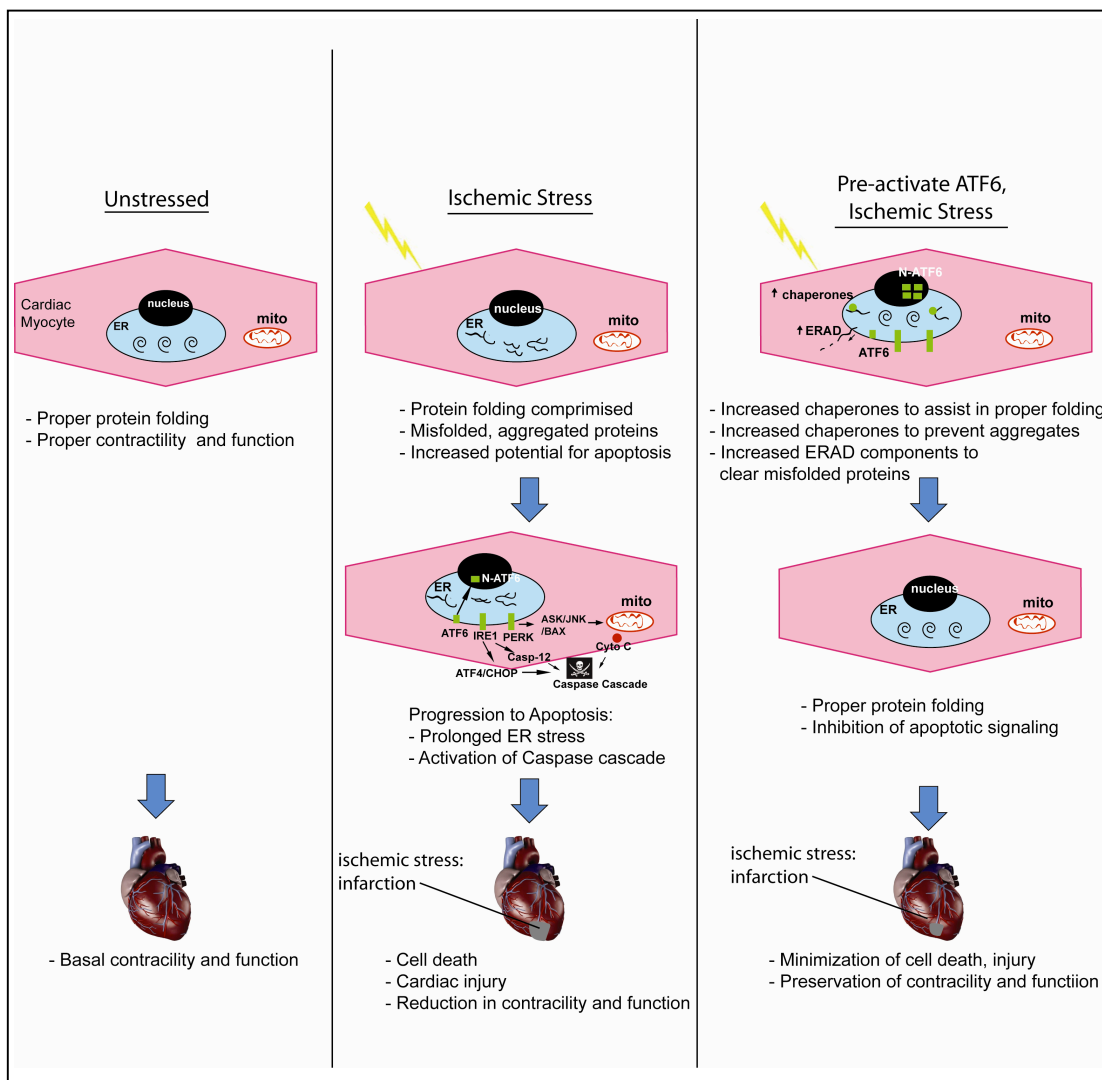
Figure 5. Depiction of Possible Modes of ATF6-Mediated Protection from Cardiac Stress.

Upon basal, unstressed conditions, proteins are properly folded in the ER, and contractility and function are preserved. In response to ischemic stress, such as myocardial infarction, the region of the heart distal to the blockage becomes compromised, and the cells in this region experience a dysregulation of the ER protein folding environment, leading to an increase in misfolded proteins. This increase leads to activation of the three main regulators of the UPR; however, persistent, unresolved stress can lead to an accumulation of misfolded proteins, as well as apoptotic signaling, activation of the caspase cascade, and cell death in the region of the infarct, all of which can be detrimental to contractility and function. Pre-activating the ATF6 branch of the UPR could bolster certain protective elements of the UPR, including an increase in ER chaperones to assist in folding, and an increase in ERAD components to assist in protein quality control, leaving the cells poised to resolve the stress, restore proper folding, thus minimizing apoptotic cell death and maintaining contractility and function.

2.   ATF6 Whole-Genome Microarray:

To determine the specific mechanisms of ATF6-mediated cardioprotection, ATF6-regulated genes were identified in the heart, using a whole-genome microarray analysis.[41] This analysis identified 607 genes that were regulated by ATF6 in the heart, with 381 genes exhibiting up-regulation.

3.   Promoter Element Search:

A search for the known ER stress element motifs was performed on the first 2kb of the 5' flanking promoter regions of each these 607 ATF6-regulated genes. ATF6 has been shown to regulate the expression of genes with elements bearing close similarity to one or more of these canonical ER stress elements, suggesting that the canonical sequence is not required for ATF6 binding and regulation.[24] Therefore, element searches allowed for the canonical element, or one basepair mismatch anywhere on the flanking regions of the ERSE and ERSE-II element, and one basepair mismatch anywhere on the UPRE element. Of the 607 up-regulated genes, 227 contained elements identical to, or one basepair mismatched from the canonical ERSE, ERSEII, or UPRE. A bootstrapping analysis determined that the list of ATF6-regulated genes is significantly enriched in genes containing each of these elements.[27] These genes which were differentially expressed in the ATF6 array and contain ER stress promoter elements are likely to be direct targets of ATF6 regulation, and can be considered as potential mediators of the protective effects of ATF6 during stress.

4.   ATF6 and Growth Modulation:

In addition to regulating known or putative ER stress response genes, ATF6 has also been recently shown to regulate genes which modulate growth. One such gene is regulator of calcineurin-1 (RCAN1), which plays a well-known role in modulating calcineurin/NFAT mediated hypertrophic signaling.[42] RCAN1 was found to be up-regulated by ATF6 in a whole-genome microarray.[41] A promoter analysis indicated that RCAN1 possesses an ERSE-like element within its 5' flanking promoter region, and RCAN1 promoter activity was shown to be regulated by ATF6, in part through this element. ATF6 overexpression was shown to induce RCAN1 in the hearts of transgenic mice, and in cultured cardiac myocytes. ATF6 had anti-hypertrophic properties in cultured cardiac myocytes subjected to the classical hypertrophic agonist phenylephrine (PE), and these growth-modulating effects were shown to be mediated in part by RCAN1. This was the first report highlighting the potential interplay of the ER stress and hypertrophic signaling pathways, and established a potential role for ATF6 in modulating additional growth during ER stress, which would allow the ER to recover from the stress by attenuating new protein synthesis.[41]

5.   ATF6-Mediated Induction of ER-Associated Degradation:

ER-resident chaperones, including GRP78, GRP94, PDI, calnexin and calreticulin are responsible for aiding in the folding of newly synthesized proteins in the ER.[43,44] Several of these chaperones are responsible for detecting misfolded proteins in the ER, in order to prevent protein aggregation and promote folding into the proper conformation.[44] In fact, several chaperones, including GRP78, GRP94, and PDI, have been detected in a multimeric complex with misfolded proteins.[45] While the
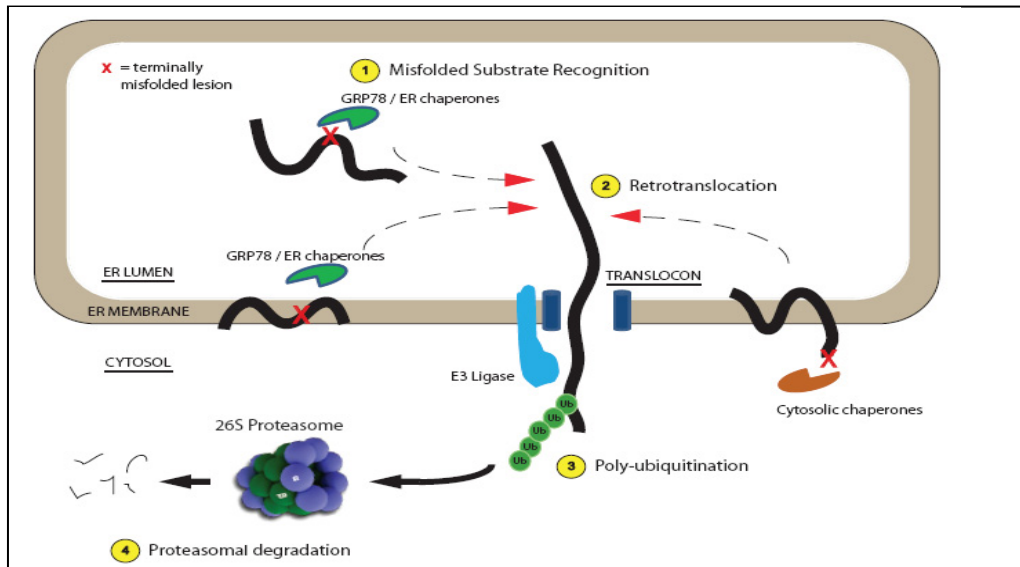
Figure 6. Mechanism of Action of ER-Associated Degradation.

(1) Proteins containing misfolded protein lesions, including exposed hydrophobic or improperly glycosylated regions on their luminal, membrane-bound, or cytosolic domains are recognized by ER-resident or cytosolic chaperones. **(2)** Proteins which cannot be properly folded into their native conformation are then retro-translocated back out of the ER translocon channel. **(3)** Coordinate with retrotranslocation, misfolded proteins are polyubiquitinated by ER membrane-bound E3 ligases. **(4)**. Polyubiquitinated substrates are shuttled to the cytosolic 26S proteasome for degradation.

involvement of microRNAs in several cellular stress responses, including hypoxia,

nutrient deprivation, and DNA damage;[57] however, the role of microRNAs in

modulating ER stress and the unfolded protein response is completely unknown.

There have been no studies of ATF6-regulated miRNAs. In addition, the extent of

microRNA gene expression influencing ER stress signaling is not known. To address

these issues, we have determined the effects of activating the ATF6 branch of the ER

stress response in the hearts of transgenic mice. Preliminary data indicated that ATF6

differentially regulated the expression of several miRNAs. The predicted mRNA

targets of several of these miRNAs overlapped with ATF6-regulated transcripts

identified in the whole-genome transcript array. A diagram depicting the potential

mechanisms by which ATF6 may mediate gene expression via miRNAs can be seen in

Fig. 7.
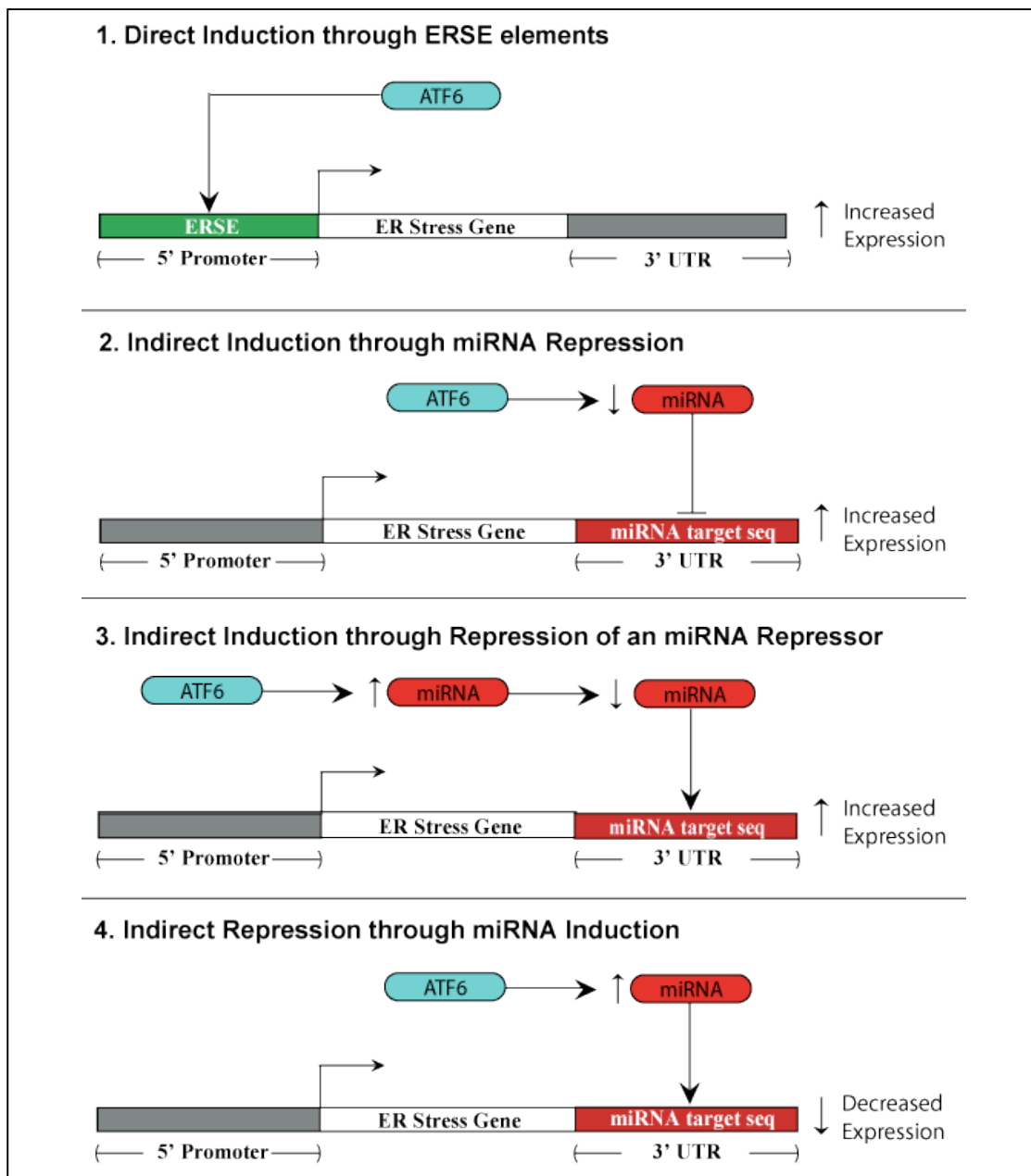
Figure 7. Potential Modes of ATF6 Gene Regulation.
(1) ATF6 can bind directly to ER stress response elements in the 5' regulatory regions of genes, promoting their transcription. **(2)** For genes which do not contain ER stress response elements within their regulatory regions, ATF6 may still be able to induce an increase in transcription by down-regulating miRNAs which normally target a given transcript for degradation. **(3)** It remains possible that ATF6 can promote transcriptional induction by up-regulating a miRNA which targets a repressor miRNA, which normally would enhance degradation of the transcript. **(4)** ATF6 may lead to decreased expression of a transcript by up-regulating a miRNA which targets the 3'untranslated region (UTR) of a gene, enhancing the degradation of its transcript.

It also remains possible that these ATF6-regulated miRNAs may alternatively regulate gene expression by inhibiting protein translation, and not by enhancing mRNA degradation. Accordingly, we also identified the potential miRNA targets which were not represented in the ATF6 transcript array, and assigned Gene Ontology (GO) classifications to these transcripts, in order to determine if these miRNA targets could potentially be enriched for certain gene families. The results of these preliminary miRNA studies are explained in **Chapter D**.

II. Materials and Methods:

A. Animals:

Approximately 100 C57/BL6 mice (Harlan Sprague-Dawley), 8 to 16 weeks of age were studied. All procedures involving animals were carried out in accordance with the San Diego State University Institutional Animal Care and Use Committee. ATF6-MER transgenic mice were generated as previously described.[20]

B. Genotyping:

Genomic DNA from tail biopsies was used as the template for PCR-based genotyping using the following primers:

ATF6-MER primers:

5' primer: CAGACGGTTTTGCTGTCTCAG

3' primer: ACCCATTTCATTTCGTAGCG

GAPDH primers:

5': TGCTGAGTATGTCGTGGAGTCTA

3': AGTGGGAGTTGCTGTTGAAGTCG

C. Tamoxifen Treatments:

Tamoxifen (Sigma, St. Louis, MO) was suspended at 10 mg/ml in 100 μl 95% ethanol and 900 μl sunflower oil and sonicated. Animals were injected intraperitoneally with 10 mg/kg tamoxifen or vehicle (95% ethanol and sunflower oil only) daily for 5 days, unless otherwise noted.

D.   Myocardial Infarction:

NTG mice were subjected to *in vivo* permanent myocardial infarction for 6h,

16h, 1d, 3d, 4d, 7d, or 14d. After each time point, mice were sacrificed and heart

sections were prepared for immunocytofluoescence confocal microscopy. Tissue

extracts were also prepared for qRT-PCR or western blot analysis. All of these

procedures have been previously described.[35,58] An antibody, which recognizes

cleaved, 50KD ATF6 was used (ATF6 H-280, Santa Cruz, catalog #22799).

E.   Cardiac RNA Extracts:

Frozen mouse tissues were pulverized and RNA was extracted using RNAzol

(Tel-Test, Friendswood, Tex) and cDNA was generated by reverse transcriptase

reaction using Superscript III (Invitrogen, Carlsbad, Calif) according to manufacturer

instructions.

F.   Cardiac Protein Extracts:

Frozen mouse tissues were pulverized and sonicated in SDS lysis buffer (50

mM Tris pH 7.5, 20 mM B-glycerophosphate, 250 mM NaCl, 2 mM DTT, 1 mM

PMSF, 10 μg/ml leupeptin, 3 mM EDTA, 3 mM EGTA, 0.1 mM sodium

orthovanidate, 1 mM PNPP, 10 ug/ml aprotinin, 0.5% SDS). Lysates were centrifuged

at 14,000 x g for 10 minutes. The total protein concentration was determined using the

DC Protein Assay kit according to the manufacturer's recommendations (BioRad,

Hercules, CA).

G.   Immunoblotting:

Tissue extracts were separated on Criterion XT Precast Gels (BioRad,

Hercules, CA) and transferred onto PVDF membrane paper (Perkin Elmer, Boston,

MA). Protein levels were compared by standard Western blotting. Primary antibodies used for immunoblotting include anti-Flag (Sigma, St. Louis, MO at 1:10,000); anti-KDEL (Stressgen, Victoria, BC at 1:20,000); anti-ATF6 annd anti-CHOP (Santa Cruz Biotechnology, Santa Cruz, CA at 1:500 and 1:1,000 respectively); anti GAPDH (Research Diagnostics, Concord, MA at 1:1,500,000), anti-A1AT (Dako, Denmark A/S at 1:8,000), and Derl3 (LifeSpan Biosciences, Seattle, WA at 1:1,000). Secondary antibodies used were horseradish peroxidase conjugated (Jackson Immunoresearch, West Grove, PA), all at 1:2,000. Membranes were incubated with ECL (Amersham, Piscataway, NJ), and chemifluorescence was assessed on a film developer.

H.   ATF6 Immunoprecipitation:

HeLa cells were treated with tunicamycin (10 µg/ml in 10%FCS), and grown to confluency on 100 mm plates, approximately 2×10^7 per dish. Media was removed, 10 mls of 10% FCS containing 625 µl of 16% paraformaldehyde were added to the plate, and plates were incubated at RT for 10 minutes, and then 1 ml of 1M glycine was added to each plate to quench the formaldehyde cross-linking. Cells were then lysed according to the EZ-ChIP protocol (Upstate, catalog # 17-371). Lysates were separated into 250 µl aliquots and then 4 rounds of sonication for 10s, followed by cooling on ice for 10s, were performed on a Fisher Sonic Dismembrator Model 100 at a setting of 5. Following sonication, 5 µl was removed and added to 90 µl H_2O and 4 µl of 5N NaCl, and incubated overnight at 65C. Then 5 µl of each sample was run on a 2 % agarose gel to test for the extent of DNA fragmentation. Appropriate fragmentation was assessed by the presence of a smeared band on the agarose gel from

~100 to 1000 kb. PCR reactions were then set up using ~100 ng of DNA, and 3 μl of primers designed to overlap the canonical ERSE in the human GRP78 promoter, at a concentration of 10 μM.

I.   In Vivo Quantitative ChIP:

Hearts from NTG and TG mice treated with tamoxifen were flash-frozen, and 25 μg of tissue were weighed and removed for processing. Tissues were minced on ice, transferred to 15 ml conicles, 750 μl of 1% paraformaldehyde were added, and rocked at RT for 15 minutes. Then 83 μl of 10X stop buffer (SA Biosciences, Frederick, MD, catalog #GA-101) were added, and conicles were centrifuged at 2,500g for 5 minutes at 4°C. The supernatants were discarded, the tissues were washed twice with 10 mls of 1x PBS, then transferred to a small 500 μl round-bottom douncer (Radnotti, part #440614), and dounced 100x. Samples were transferred to 2 ml conical tubes, and centrifuged at 5,000 rpm for 5 minutes at 4°C. The supernatant was removed, and the pellet was resuspended in 350 μl lysis buffer + protease inhibitor cocktail (SA Biosciences). Samples were incubated on ice for 15 minutes and vortexed briefly every 5 minutes. Samples were then sonicated as described in **Section H** for 5 cycles of sonication per sample, and stored overnight at -80°C. Approximately 200 μg was used for pre-clearing and IP. For pre-clearing, samples were incubated with 2.7 mls of buffer A, 15μl of inhibitor cocktail (SA Biosciences), rocked at 4°C for 45 minutes, and centrifuged at 4 000g for 1 minute at 4°C. Then 30 μl of the supernatant (pre-cleared fraction) was transferred to tubes and incubated with 8 μg of Flag antibody (Sigma, catalog # F1804), or non-immune IgG beads serving as the non-

immune control, and rocked overnight at 4°C. Samples were then centrifuged at 4,000g for 1 minute at 4°C, and washed according to the manufacturer's protocol (SA Biosciences ChampionChIP One-Day kit). For each condition, two parallel IPs were performed and pooled at the final elution step to obtain sufficient material for qRT-PCR.

The following primer sets were designed to overlap ER stress response elements present within the promoter regions of genes tested, or in the case of GAPDH, which does not contain elements, primers were designed to overlap a random portion of the promoter.

Control (no elements):

GAPDH 5': ATGCGGTTTCTAGGTTCACG,

GAPDH 3': ATGTTTTCTGGGGTGCAAAG

Genes Containing ERSEs:

GRP94 5': TGATTGGAGGAAAGCCGC

GRP94 3': CCGAAGCGTGGCTCCTT

GRP78 5': GTGGCATGGACCAATCAGC

GFP78 3': TCCGATTGGTGAAGTCGCTAC

DNAJC3 5': GACCAGCGGACGCAGC

DNAJC3 3': CGCCTCTGATAGGATAACGTGG

XBP1 5': GGACCAATAAGTGATGAATATACCCG

XBP1 3': CGATTGGCCGGTGCTC

Genes Containing ERSEIIs:

MANF 5': AATGAGGATGCAGCATATGGGT

MANF 3': GCTTCCCATTGGTGTGCG

DNAJB11 5': CGTTTTCTCTTCCCATTGGC

DNAJB11 3': TCAGACAGCAGAACAGCCGT

Herpud 5': GGCCACGTTGGACACTGAC

Herpud 3': GCTCTCTGTGGCTGCCATC

Hyou1 5': GACTTCGCAATCCACGAGAG

Hyou1 3': CCCATTGGTCCACGTAGAAG

Genes Containing UPREs:

Fra-2 5': ATGACCATCTTTGGCAACGTG

Fra2 3': GCGCAGCGCCCTTG

Stat3 5': TGCCCATAATCACGCAGAACT

Stat3 3': AACATGGGCAACTCCTGGC

Timp 5': AGGAGGGAGTATCTTTGGGTTTATC

Timp 3': CGCTGGAGTCAAAGCCTAGG

Nmor 5': GCTTACCGTGACGTGGACACT

Nmor 3': TTGAAGGATGCATTCTTTGCC

J.   RNA Analysis:

Total RNA was prepared from hearts using RNAzol (Tel-Test, Friendswood, TX). Total RNA was prepared from NRVMCs using the Zymo RNA Isolation Kit (Orange County, CA). cDNA was generated by incubating 5 μg of RNA with reverse transcriptase using Superscript III (Invitrogen, Carlsbad, CA). Quantitative real-time PCR (qRT-PCR) was performed on 1:100 dilutions of cDNAs.

K.   Whole-Genome Microarray Analysis

NTG and TG mice were treated with vehicle or tamoxifen, n=3 mice per treatment group, as described previously.[20] RNA was extracted from mouse heart ventricles, as described above. Each mouse heart mRNA sample was analyzed on a single microarray chip. Gene expression analysis was performed by the Veterans Medical Research Foundation (VMRF) GeneChip Core at UCSD, in accordance with the Affymetrix GeneChip Expression Analysis Technical Manual (Affymetrix, Inc., Santa Clara, CA). Briefly, cRNA was fragmented for target preparation, then hybridized onto Affymetrix mouse 430 2.0 whole genome arrays (Affymetrix, Inc., part number 900496), which allow for analysis of roughly 40,000 transcripts. Array chips were scanned on an Affymetrix GeneChip Scanner 3000 using Affymetrix GeneChip Operating Software (GCOS) version 1.1.1.

L.   Microarray Statistics and Data Analysis:

Statistical analyses were performed using the BioConductor packages in R.

The ".CEL" files were input directly into R, and mRNA expression values were

obtained using the RMA algorithm (1.10.0).[59] Statistical pairwise comparisons

between treatment groups were carried out in R, using the local pooled error method.[59]

Genes that exhibited significant changes in expression (*i.e.* $p \leq 0.01$) were included for

further study. Genes that were differentially expressed in vehicle *versus* tamoxifen-

treated TG mouse hearts by 2-fold, or more, were selected for further study. Because

tamoxifen may affect gene expression independently of its ability to activate ATF6-

MER, genes that were differentially expressed in vehicle vs tamoxifen-treated NTG

mouse hearts were excluded from further study.

M.   ATF6 Whole-Genome miRNA Array:

NTG and TG mice were treated with vehicle or tamoxifen, n=3 mice per

treatment group, and RNA was extracted from mouse heart ventricles, as described

previously.[41] Each mouse heart RNA sample was analyzed on a single microarray

chip. miRNA expression analysis was performed by LC Sciences (Houston, TX) in

accordance with their specifications. RNA was hybridized onto mouse miRNA chips

(LC Sciences, part #MRA-1002), which were current with Sanger miRBase version

14.0 and contained roughly 700 unique mature miRNA probes.

N.   miRNA Array Statistics and Data Analysis:

Statistics and data analysis were carried out essentially as previously

described.[41] miRNAs that exhibited significant changes in expression ($p \leq 0.05$) were

included for further study. Given the modest range of induction in this array study,

miRNAs that were differentially expressed in vehicle vs. tamoxifen-treated TG mouse hearts by 1.5-fold, or more, were selected for further study. Since tamoxifen may affect miRNA independently of its ability to activate ATF6-MER, miRNAs that were differentially expressed in vehicle vs. tamoxifen-treated NTG mouse hearts were excluded from further study.

O.   miRNA Target Prediction:

Bioinformatic prediction of target sites and miRNA binding sites was performed by first searching for the miRNA of interest on Sanger miRBase (http://www.mirbase.org) and then identifying potential targets using TargetScan Version 5.1 (http://www.targetscan.org). Hypothetical proteins were not considered for further analysis. Predicted targets of each ATF6-regulated miRNA were then compared to the 607 genes listed in the ATF6 array to determine if ATF6-regulated miRNA targets were differentially regulated at the transcript level by ATF6.

P.   Gene Ontology and Pathway Analysis:

Gene Ontology (GO) classifications were assigned to the predicted targets of the differentially expressed miRNAs using Ensembl Biomart (http://www.ensembl.org/biomart/martview).

Q.   miRNA and mRNA Extraction and Quantification:

For tissue samples, total RNA was extracted using TRIzol (Invitrogen, Carlsbad, CA) as previously described.[41] For cultured NRVMCs, both total and small RNA-enriched RNA fractions were obtained using the miRNeasy and miRNA cleanup kits (Qiagen, Valencia, CA) according to the manufacturer's specifications. miRNA

levels were analyzed using the TaqMan quantitative real-time PCR (qRT-PCR)

method (10 ng/assay), and quantified with an ABI 7000 Real-Time PCR System

(Applied Biosystems, Foster City, CA). Primers for miRNAs and the reagents for

reverse transcriptase and qRT-PCR reactions were all obtained from Applied

Biosystems. Relative expression was calculated using the comparative cycle threshold

(Ct) method ($2^{-\Delta\Delta Ct}$). miRNA levels were normalized to U6 RNA expression. mRNA

levels were measured as previously described[41] using custom primers and normalizing

to GAPDH mRNA expression.

R.   Primary Neonatal Rat Ventricular Myocyte Cultures:

Hearts were excised from 1-4 day-old Harlan Sprague-Dawley rats. The atrias

were removed and ventricles were washed in DMEM. Cells were dissociated with

multiple rounds of incubation in 0.001% trypsin. After each incubation, supernatant

was removed and added to an equal volume of 20% fetal bovine serum. Cells were

pelleted by centrifugation, and resuspended in 10% fetal bovine serum. Myocytes

were enriched by pre-plating for 1-2 hours, which allows fibroblasts to attach to the

plastic while myocytes remain in suspension. Myocytes were then plated onto 6 or 12-

well plates pre-coated with 5 μg/ml fibronectin in DMEM/F-12 (1:1) at a density

ranging from 0.5 to 1.5 x 10^6 cells per well, depending on the experimental conditions.

S.   Adenovirus:

The AdEasy system was used for preparing recombinant adenovirus encoding

the genes of interest, including ATF6 and a dominant-negative form of ATF6 lacking

the transactivtion domain, as well as XBP1, Derl3, A1AT and mutant A1AT. The

gene of interest was PCR-amplified from the parent templates to create restriction sites

that would facilitate cloning into pAdTrack-CMV, an adenoviral shuttle vector that harbors CMV-driven green fluorescent protein (GFP), and a CMV-flanked multiple cloning site for the insertion of the gene of interest. A control adenovirus was also constructed which only encodes GFP. PCR-amplified genes were cloned into the *Eco*RI and *Not*I sites of pGEX-6P-1 (Amersham Pharmacia Biotech), which served as a shuttle cloning vector. Shuttle vectors were then digested with *Bam*HI and *Not*I, and the resulting products of interest were cloned into the *Bgl*II and *Not*I sites of pAdTrack-CMV to create pAdTrack-CMV-gene of interest, which was linearized and then co-transformed with the adenoviral vector, pAdEasy-1, into *Escherichia coli* strain BM5183. This strain allows for homologous recombination of pAdEasy-1 and the pAdTrack-CMV shuttle vector containing the gene of interest. Recombinants were selected on kanamycin and screened by restriction digestion with *Pac*I. Recombinant plasmids were then retransformed into *E.coli* DH5 for propagation. Recombinant adenoviral plasmids were linearized with *Pac*I and then transfected into 293 human embryonic kidney cells using LipofectAMINE (Life Technologies, Inc.). The recombinant viruses were then harvested 7-10 days post-infection after comet formation had appeared. Adenoviral lysates were amplified by a second round of infection. The second infection lysates or later were used for experiments; viral titers were determined by observing GFP fluorescence in NRVMCs, the volume required for a 50% infection was used to calculate a multiplicity of infection (MOI) of one by doubling the volume. An MOI of 2 was used in experimental designs, as this guaranteed a 100% infection rate.

T.   Promoter Element Searches:

The 2kb promoter sequences lying 5' of the start sites for each of the ATF6-regulated transcripts identified in our previous array study[41] were retrieved using Ensembl Biomart (http://www.ensembl.org/biomart/martview). The same regions of each of the roughly 40,000 transcripts on the Affymetrix mouse 430 2.0 whole genome array chips (Affymetrix, Inc., part #900496) used in this previous study were also acquired. These sequences were then searched for ERSEs, ERSE-IIs and UPREs using a custom Perl script and the following sequences:

ERSE- CCAAT-N9-CCACG[9]

ERSE 1bp mismatch- Allows for 1bp mismatch in any nucleotide in either of the 5bp flanking regions of the consensus ERSE

ERSE-II- ATTGG-N-CCACG[23]

ERSE-II 1bp mismatch- Allows for 1bp mismatch in any nucleotide in either of the 5bp flanking regions of the consensus ERSEII

UPRE: TGACGTGGA[22]

UPRE 1bp mismatch: Allows for 1bp mismatch in any nucleotide of the consensus UPRE

U.   Determination of Element Enrichment in ATF6 Array:

To determine whether the genes previously identified in the mouse heart as ATF6-regulated[41] were enriched for ERSEs, ERSE-IIs and UPREs, a bootstrapping analysis was performed, essentially as previously described.[59,60] Briefly, 1,000 promoter sets, each of which contained 607 promoters, were generated from genes either from the mouse whole-genome Affymetrix GeneChip array, or from the ATF6-

regulated gene cluster, using Ensembl Biomart

(http://www.ensembl.org/biomart/martview). Bootstrapped promoter sets were

generated using a custom Perl script.   The number of times these elements were found

in each bootstrapped promoter set, i.e. the frequency of appearance in the whole

genome and in the ATF6-regulated genes, is shown in **Figure 10**.

V.   Promoter Luciferase Assays

RCAN1-Luciferase and RCAN1-Mutant Luciferase Constructs:

A region of the 5'-flanking sequence preceding exon 4 of the human RCAN1

gene from -984 to +30 was isolated by PCR and cloned into a pGL2 luciferase

reporter vector (Clontech). The nucleotides from -329 to+311 in the

humanRCAN1gene are CCATT-$(N)_9$CAAAG, which exhibits about 73% homology

to a consensus ERSE, CCAAT-$(N)_9$CCACG. The same region of the mouse RCAN1

promoter has the following ERSE-like sequence CCACC-$(N)_9$CAGAG, which also

exhibits about 73% homology to a consensus ERSE. Using PCR-based mutagenesis,

the region from -329 to +311 of human RCAN1-luciferase was changed to AACGG-

$(N)_9$CCCTT, creating the mutated RCAN1-M-luciferase, which has a mutated ERSE.

Derl3-Luciferasse and Derl3-mut-luciferase constructs:

The mouse Derl3 gene from -1359 to +26 was amplified by PCR and cloned

into a pGL2 luciferase reporter vector (Clontech, Inc.) and designated Construct 1.

Two consensus ERSE sequences, CCAAT-$(N)_9$CCACG, located between nt -183 to -

165 and nt -285 to -267 were designated ERSE1 and ERSE2, respectively. Using

PCR-based mutagenesis, ERSE1 of Derl3-luciferase Construct 1 was mutated to

AACCG-(N)$_9$-AACAT, creating Construct 2. ERSE2 of Derl3-luciferase Construct 1

was also mutated to AACCG-(N)$_9$-AACAT, creating Construct 3.

W.   Simulated Ischemia/Reperfusion:

NRVMCs were subjected to simulated ischemia (sI) and/or simulated ischemia

followed by reperfusion (sI/R) to mimic physiological ischemia/reperfusion (I/R).

NRVMCs were plated on fibronectin-coated 6-well plates at 0.5M cells per well, for at

least 24h in DMEM/F-12 with 10% serum, and then incubated with the adenoviral

strain of interest for 6h in 2% serum, followed by 18h of 2% serum alone. For sI, the

medium was replaced with glucose-free DMEM/F12 containing 2% dialyzed fetal

bovine serum, and cultures were placed in a chamber (PROOX model 110, Sensor Part

#E702, BioSpherix, Ltd Redfield, NY), filled with N_2/CO_2 (95% N_2/ 5% CO_2)for 20h.

For experiments investigating cell viability, induction of KDEL-containing proteins,

and induction of apoptotic markers, sI media was supplemented with 3 mM 2-

deoxyglucose (Sigma, catalog #D6134), For all experiments, sI/R consisted of the

following approach. After sI, the medium was replaced with glucose-containing

DMEM/F-12 supplemented with 2% bovine serum albumin, and cultures were

incubated in O_2/CO_2 (18% O_2) for 24h.

X.   Immunocytofluorescence:

NRVMCs were fixed in 4% paraformaldehyde in PBS, and if immediate

staining was not carried out, stored in 0.4% paraformaldehyde. Slides were washed 3x

with PBS prior to permeabilization in 0.1% BSA/0.2% Triton X-100 in PBS for 30

minutes at 37°C. Permeabilized cells were washed in PBS and blocked for 1 hour

with 5% goat serum in PBS prior to primary antibody application, 1h RT, which was

diluted in blocking buffer. Immunocytofluorescence was carried out using a rabbit

anti-GRP78 (Stressgen, 1:200), Derl3 (Sigma, 1:50) or α-actinin (Sigma, 1:500). The

samples were then washed 3x with PBS and then incubated with Texas-red or Fitc-

conjugated secondary antibody (Jackson, 1:1000). The secondary antibody was

removed by serial PBS washing and slides were subsequently visualized on a Leica

DM IRE2 confocal microscope.

Y. Small Interfering RNA Treatment of Cultured Cardiac Myocytes:

NRVMCs were transfected with a combination of 3 different Stealth small

interfering (si) RNA oligoribonucleotides targeted to rat RCAN1 (Invitrogen, catalog

number 130003), or a validated Stealth RNA interference negative control (Invitrogen,

catalog number 12935300), as they were plating down on 12-well plates at $1x10^6$ cells

per well Each well was transfected with a total of 10 ρmols of Stealth siRNA using

TransMessenger Transfection Reagent (Qiagen, Valencia, CA). siRNA mixes were

prepared before plating cells onto fibronectin-coated 12-well plates. Control and

RCAN1-directed siRNA mixes were prepared as follows, with the volumes listed

multiplied by the number of wells necessary for the experiment: 3.2 μl buffer E-R,

95.2 μl buffer EC-R (Transmessenger), and 1.6 μl of siRNA totaling 10 ρmols.

siRNAs were mixed gently and incubated at RT for 5 minutes. Then 6 μl of

Transmessenger reagent per well was added to each siRNA mix, and incubated at RT

for 10 minutes. The appropriate number of cells for the experiment were then

centrifuged at ~500 rpm, the media was removed, and the pellet was then resuspended

in DMEM-F12 media without antibiotics, at 400 μl times the number of wells for the

experiment. Cells were then plated at 400 μl per well onto fibronectin-coated plates,

and 100 μl of the appropriate siRNA mix was immediately applied to each well, adding the mix slowly and distributing it throughout the well. Cells were incubated for 4h at 37°C. siRNA mixes were then aspirated off, and 1 ml of 10% FCS was immediately added per well, without any wash steps. After 20h, cells were infected with control adenovirus, or an adenovirus encoding ATF6 for 5h in minimal media. Twenty-four hours after infection, cells were then treated ± phenylephrine (50 μM) in minimal medium for 48h. RNA was extracted, and transcript levels were then assessed using qRT-PCR, or cell size was analyzed using ImageJ; as described in **Section Z**.

Z.   Cell Size Assay:

NRVMCs were plated on fibronectin-coated 6-well plates at $1x10^6$ cells/well in 10% FCS. Twenty-four hours after plating, cells were infected with adenovirus encoding GFP (control) or ATF6 in minimal media for 6h at an MOI of 2, and then the media was replaced with minimal media. Sixteen hours later, cells were treated with 50 μM phenylephrine in minimal media, or minimal media alone (control), for 48h. Cells were then visualized on a fluorescent microscope at 10X, and 3-5 images were acquired per well. Images were then analyzed with NIH ImageJ software to obtain the average cell area. At least 250 cells were quantified per condition.

AA. ^{3}H Leucine Incorporation Assay:

NRVMCs were plated and treated as in **Section Z**, and then minimal media containing ^{3}H Leucine ± 50 μM phenylephrine was added, and cells were incubated and processed as previously described.[61]

BB.   Calcineurin Activity Assay:

Calcineurin phosphatase activity was measured according to the

manufacturer's protocol using a calcineurin cellular assay kit (BIOMOL, Plymouth

Meeting, PA). Briefly, NRVMCs were collected in 400 μl of lysis buffer (50 mM Tris,

pH 7.5, 0.1mM EDTA, 0.1mM EGTA, 1 mM dithiothreitol, 0.2% Nonidet P-40). Free

phosphate was removed by passing the lysates through a desalting column (BIOMOL

assay kit) before assaying. Calcineurin phosphatase activity was measured

spectrophotometrically by detecting free phosphate released from the synthetic RII

phosphopeptide.

CC.   Caspase-3 Activity Assay:

NRVMCs were infected with AdVCon, AdVDerl3, AdVmiCon, or

AdVmiDerl3, in 2% FCS-containing medium for 6 hours, after which, cells were

washed and fed with the same medium, but without the AdV. After 24h, cells were

treated +/- sI or sI/R, as described above. Cultures were extracted in caspase assay

buffer containing 50 mM Hepes, pH 7.4, 0.1% CHAPS, 0.1 mM EDTA. Protein

concentrations were determined as described in **Section F**. A total of 50 μL of the

lysate and 10 μL of the assay buffer were then combined with 45 μL of reaction buffer

(40 μL caspase assay buffer, 1 mM DTT, 40 μM DEVD-AFC in DMSO (Sigma,

catalog no. A0466). After 1 hour at 37°C, fluorescence was measured at an excitation

wavelength of 400 nm and an emission wavelength of 505 nm. Caspase activity was

defined as fluorescence/protein.

DD.   Live/Dead Assay:

Assessment of cell death in NRVMCs was performed using Hoescht (catalog no. H21486; Invitrogen) and propidium iodide (PI, Invitrogen, catalog no. P1304MP), as previously described.[58]

EE.   FACS Cell Viability Assay:

NRVMCs were electroporated with plasmids encoding GFP alone or Derl3-DN, which encodes a Derl3-GFP fusion protein, and plated onto 6-well dishes. Cultures were subjected to sI or sI/R, as described above. Cells were then collected using TripLE (Gibco, catalog #12605), washed with PBS, resuspended in PBS, and analyzed by flow cytometry on a BD FACSAria cell sorter. Approximately 150,000 events were recorded for each condition. Cells were first gated to eliminate debris and aggregates. Transfected cells were identified by gating for GFP expression, and the percentage of these transfected cells that were also PI-positive was determined. This percentage was normalized to the percent of overall PI-positive cells for each condition. Data were presented as fold-of-control. Shown is the average of three independent experiments.

FF.   A1AT Clearance Assay:

HeLa cells were co-transfected with a plasmid encoding A1ATmut and varying concentrations of a plasmid encoding Derl3, or co-transfected with A1ATmut and GFP or Derl3-DN. After 24h, cultures were scraped in protein lysis buffer, then analyzed by SDS-PAGE followed by immunoblotting with anti-A1AT antibody at a concentration of 1:8,000 (Dako, Denmark A/S, Catalog #A 0012).

GG. **Statistical Analysis:**

All data are reported as mean ± S.E. and analyzed via one-way analysis of variance with Newman-Keuls post hoc analysis, or two-way Student's T-Test, using SPSS version 11.0. Unless otherwise stated in the figure legends, *, #, or § = $p \leq 0.05$ different from all other values.

III. Results

A. Identification of ATF6-Regulated Genes

Upon ER stress, ATF6 is activated, leading to cleavage and translocation of the N-terminal portion of the protein to the nucleus, where it acts as a robust transcription factor, mediating the induction of several well-known ER stress response genes. These genes function to resolve the stress and restore ER homeostasis, promoting proper protein folding to ensue.

The hearts of transgenic mice possessing a novel, tamoxifen-regulated form of N-terminal ATF6 display improved recovery from *ex vivo* ischemia/reperfusion injury, and decreased apoptosis and necrosis following the injury.[20] The mechanism of action of the tamoxifen-regulated form of ATF6 was shown in **Fig. 4**. While ATF6 is known to induce a handful of ER stress response genes,[20] the effect of ATF6 activation on a genome-wide level has never been studied.

1. Validation of Tamoxifen-Mediated Activation of ATF6:

In initial studies of tamoxifen-dependent ATF6 activation *in vivo*, the expression of the well-known ATF6-target gene, GRP78, was examined in ATF6-MER TG mouse hearts by confocal immunofluorescence microscopy. Sections from vehicle-treated TG mouse hearts showed that GRP78 expression in cardiomyocytes was relatively low under these conditions **(Fig. 8A, panels 1 and 4 [green])**.
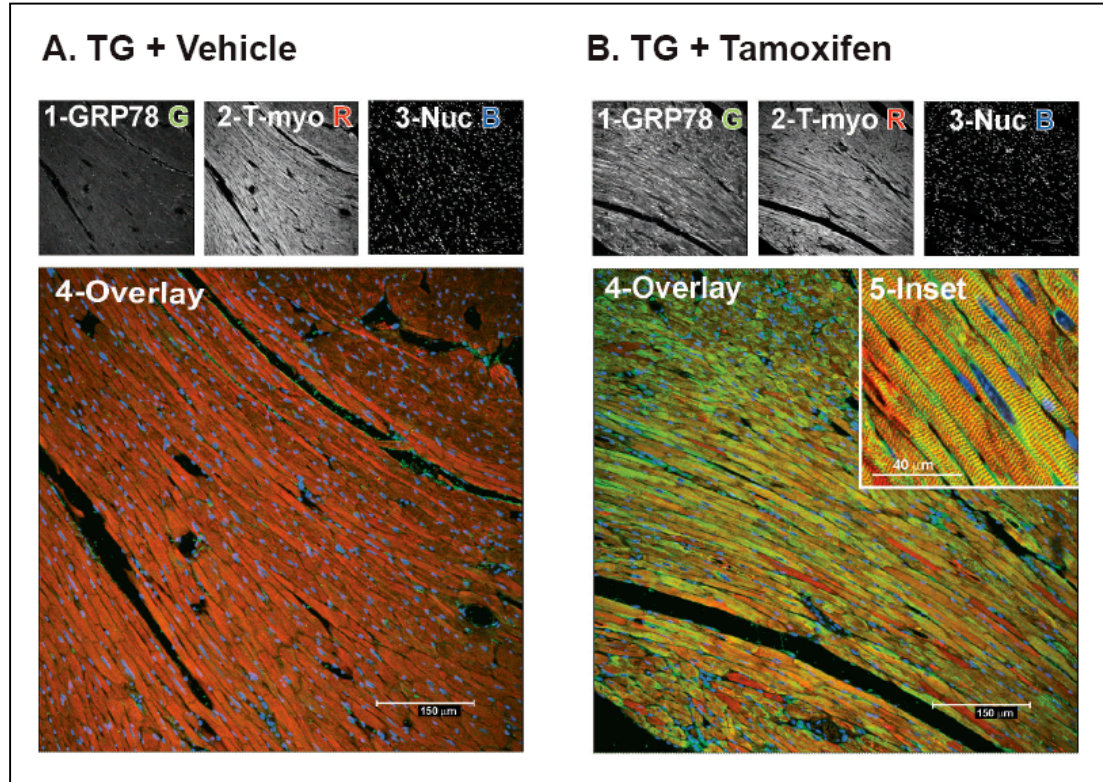
Figure 8. Effect of tamoxifen on the ATF6-inducible gene, GRP78, in ATF6-MER transgenic mouse hearts.

TG mice treated with vehicle **(A)** or tamoxifen **(B)**, n=3 hearts per treatment, one heart per treatment shown. Heart sections were stained for GRP78 protein (1, green), tropomyosin (2, red) or TOPRO-3 (blue).

Similar results were found in sections from tamoxifen-treated NTG mouse hearts (not shown). In contrast, sections from tamoxifen-treated TG mouse hearts exhibited robust GRP78 expression **(Fig. 8B, panel 1)**, which was localized to most of the cardiomyocytes, as indicated by co-staining for GRP78 and tropomyosin **(Fig. 8B, panel 4)**. For the most part, GRP78 exhibited a perinuclear staining pattern in cardiomyocytes, which is typical of ER-localized proteins **(Fig. 8B, panel 5 [green])**. In addition, GRP78 was expressed in other regions of cardiomyoyctes, exhibiting a sarcomeric staining pattern, which has been previously observed.[35] These results demonstrated that tamoxifen effectively up-regulated this ATF6-target gene in the majority of the myocytes in ATF6-MER TG mouse hearts, supporting the utility of this model for analyses of the effects of ATF6 on the induction of other genes, *in vivo*.

2.   ATF6 Whole-Genome Microarray:

To identify ATF6-regulated genes in the heart, a full-genome microarray study was carried out. Both TG and NTG mice were treated with vehicle or tamoxifen, hearts were harvested, and RNA was extracted for analysis on Affymetrix whole-genome 430 2.0 microarray chips, which contain probes for roughly 40,000 transcripts. To ensure the inclusion of genes that were induced as a result of tamoxifen-mediated activation of ATF6, genes that were differentially expressed in untreated NTG vs tamoxifen-treated NTG mice were excluded. After these exclusions, 607 genes exhibited differential expression of at least 2-fold ($p \leq 0.01$), with 381, or about 63% of the genes exhibiting increased expression.

3. Analysis of Differentially Expressed Genes:

The differentially expressed genes were analyzed using the Gene Ontology (GO) classification system, which organizes genes on the basis of the molecular and biological function.[62] Using these approaches, as well as other data analysis techniques, 23 known and 14 putative ERSR genes were identified **(Table 1)**, the latter of which were defined as genes with published characteristics similar to known ERSR genes, but not previously shown to be ATF6-inducible. 36 of the 37 known and putative ERSR genes were up-regulated by levels ranging from 2- to 46-fold.

Table 1. Known and Putative ERSR Genes Induced by ATF6 Activation in the Heart.

	MGI symbol	Alias or protein names	NCBI RefSeq	-Fold up	Valid
Known ERSR genes					
1	Derl3	Degraded in ER protein 3	NM_024440	18.50	X
2	Pdia4	Cai	NM_009787	16.37	
3	DNAJC3	P58; P58IPK	NM_008929	12.75	X
4	DNAJB11	ERdj3; HEDJ; HSP40	NM_026400	12.39	X
5	Socs3	STAT Induced STAT inhibitor	NM_007707	9.68	
6	Asns	Asparagine synthetase	NM_012055	9.26	
7	P4hB	PDI associated 1; ERp59; Thbp	NM_011032	9.17	
8	Armet	Arginine-rich, mutated early stage tumors	NM_029103	8.21	X
9	Hsp90b1	Tra1; GRP94	NM_011631	7.07	X
10	Trib3	Nip kinase; Ifld2	NM_144554	6.66	
11	Edem1	EDEM	NM_138677	5.36	X
12	Calr	Calreticulin	NM_007591	5.29	X
13	Atf4	ATF4	NM_009716	4.93	
14	Pdia3	Protein-disulfide isomerase 3, GRP8; ERp61	NM_007952	4.72	
15	Hspa5	GRP78	NM_022310	4.71	X
16	Syvn1	Synoviolin 1	NM_028769	4.60	
17	Eif2Ak3	PERK	NM_010121	4.18	
18	Pin1	DOD; UBL5; Rotamase	NM_023371	4.12	
19	Hyou1	GRP170; ORP150	NM_021395	3.86	X
20	Ugcgl1	UDP-glucose ceramide glucosyltransferase-like 1	NM_198899	3.70	
21	XBP1	X-box binding protein 1	NM_13842	2.95	X
22	Herpud1	HERP; Mif1; SUP	NM_022331	2.43	X
23	Herpud2	HERPUD family member 2	NM_020586	0.23	
Putative ERSR genes					
24	Ptx3	Pentaxin-related gene	NM_008987	46.31	X
25	IL6	Interleukin-6	NM_031168	38.45	
26	Sdf2l1	Stromal cell derived factor 1	NM_022324	17.41	
27	GADD45g	Growth arrest DNA damage-inducible protein 45	NM_011817	10.52	
28	Rtn4	Reticulon 4	NM_024226	9.28	
29	Azin1	Ornithine decarboxylase; Oazin	NM_018745	5.96	
30	Gas5	Growth arrest specific 5	AK206770	5.90	
31	Snord22	Small nucleolar RNA, C/D box 22	AK051045	4.48	
32	Txnrd1	Thioredoxin reductase	NM_015762	4.32	
33	RCAN1	Regulator of calcineurin 1	NM_019466	4.29	X
34	Serpinh1	Serpin peptidase inhibitor, HSP47	NM_009825	3.10	
35	Gsk3β	Glycogen synthase kinase-3β	NM_019827	3.00	
36	Sec11a	Signal peptidase complex	NM_019951	2.53	
37	H47	VCP-interacting membrane protein; Vimp	NM_024439	2.53	

All differentially expressed genes are sorted by fold change. Also shown is the gene symbol, alias or protein name, and NCBI Reference Sequence ID. The X in the "Valid" column indicates that the microarray results for these genes have been validated by RT-qPCR using the same RNA that was used in the microarray.

4.   Validation of ATF6-Regulated Genes:

Quantitative real time quantitative PCR (qRT-PCR) was used to validate the

microarray results for 13 of the known and putative ERSR genes. All 13 genes

examined were found to be up-regulated in RNA prepared from tamoxifen-treated TG

mouse hearts, but not in RNA from any of the other treatment groups (see "X" in

Table 1). An example of this validation for 6 of the genes shows induction of 5

known ERSR genes (*GRP78, Erp72, DnajB11, Hyou1* and *XBP1*) and one putative

ERSR gene (*RCAN1*) **(Fig. 9A)**.
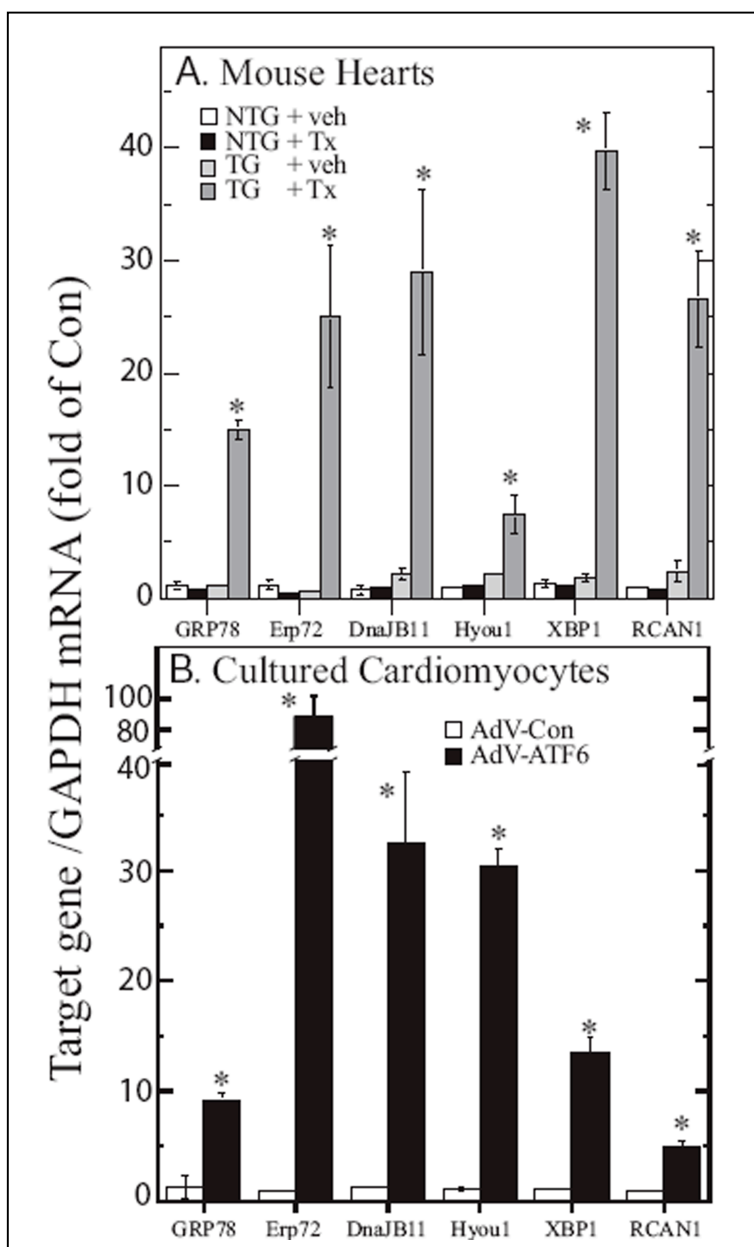
Figure 9. Validation of Microarray Results with qRT-PCR.

Panel A: The RNA samples that were used for the microarray analysis were subjected to RT-qPCR to examine the levels of the mRNAs encoded by the GRP78, Erp72, DnaJB11, Hyou1, XBP1, and RCAN1 genes. Shown are the mean -/+ S.E. for each target gene (n=3 mouse hearts per treatment). Veh, vehicle; Tx, tamoxifen. **Panel B:** NRVMCs were infected with either AdV-Con or AdV-ATF6 (n=3 cultures per treatment). 48 h after infection, cultures were extracted and the RNA was subjected to RT-qPCR to examine the levels of mRNA for the same target genes described in Panel A. Shown are the mean -/+ S.E. for each target gene (n=3 cultures per treatment). * = $p < 0.05$ different from all other values for each target gene.

5.   ATF6 Overexpression in NRVMCs:

We also determined whether these 6 genes were induced upon overexpression

of activated ATF6 in primary neonatal rat ventricular myocyte cultures (NRVMCs).

All 6 of the genes examined were up-regulated in cells infected with an adenovirus

that encodes activated ATF6 (AdV-ATF6) **(Fig. 9B)**. These findings provided further

validation of the microarray results, and demonstrated that these 6 genes could be

induced, *in vivo,* and in cultured cells using two different approaches for

overexpressing activated ATF6. This also established a cell culture model for

examining the functional characteristics of known and putative ATF6-inducible ERSR

genes.

6.   ER Stress Response Element Promoter Search:

To determine which of the 607 genes from the microarray analyses of ATF6-

MER TG mouse hearts might be direct targets of ATF6, we retrieved 2kb of the 5'

flanking regulatory regions of each gene using Ensembl Biomart

(http://www.ensembl.org/biomart/martview), and searched these regions for known

canonical ER stress response cis-acting binding sites, including the ER stress response

element (ERSE), ER stress response element-II (ERSE-II), and the unfolded protein

response element (UPRE).[22,23,63] To determine the full set of genes containing each of

these elements throughout the genome, we also retrieved the 2kb 5' flanking

regulatory regions of each gene in the entire mouse genome. The identities of the

genes containing these elements, both from our ATF6-regulated list, and the whole

genome, can be found in **Tables 2 through 7.** Among the 607 ATF6-regulated genes

in the heart, 16 have canonical ERSEs, ERSEIIs and/or UPREs **(Tables 2, 3, and 4**

respectively), while 211 have elements with 1 base pair mis-matched **(Tables 5, 6, and 7 respectively)**; mismatches of 1bp have been shown in other studies to be potential ATF6-binding elements.[22,24] Thus, 227 genes are likely to be direct targets of ATF6.

Table 2. Genes containing consensus ERSE elements within 2KB promoter regions.

ATF6-Regulated Genes

Number	MGI symbol	Alias or Protein Name	NCBI RefSeq	Start	End	Strand	Fold Change
1	Derlin-3	Degraded in ER protein 3	NM_024440	257	239	-	18.5
1	Derlin-3	Degraded in ER protein 3	NM_024440	155	137	-	18.5
2	DNAJC3	P58; P58IPK	NM_008929	146	128	+	12.75
3	Hsp90b1	Tra1; GRP94	NM_011631	41	23	-	7.07
3	Hsp90b1	Tra1; GRP94	NM_011631	64	46	+	7.07
4	Calr	Calreticulin	NM_007591	161	143	-	5.29
5	Hspa5	GRP78	NM_022310	148	130	+	4.71
6	Syvn1	Synoviolin 1	NM_028769	129	111	+	4.6
7	XBP1	X-box binding protein 1	NM_013842	60	42	+	2.95

Full Genome

Number	MGI symbol	Alias or Protein Name	NCBI RefSeq	Start	End	Strand
1	Adamtsl5	ADAMTS-like 5	NM_001024139	591	573	-
2	Adcy3	adenylate cyclase 3	NM_027857	216	198	+
3	Alg12	asparagine-linked glycosylation 12 homolog	NM_145477	219	201	+
4	Calr	Calreticulin	NM_007591	161	143	-
5	Cd209d	CD209d antigen	NM_130904	666	648	+
6	Clec12a	C-type lectin domain family 12, member a	NM_177686	1919	1901	+
7	CNX	calnexin	NM_001110499	161	143	+
8	Creld2	cysteine-rich with EGF-like domains 2	NM_029720	125	107	-
9	Ddefl1	development and differentiation enhancing factor-like 1	NM_001008232	1504	1486	+
10	Derlin-3	Degraded in ER protein 3	NM_024440	257	239	-
10	Derlin-3	Degraded in ER protein 3	NM_024440	155	137	-
11	Dnajb14	DnaJ (Hsp40) homolog, subfamily B, member 14	XM_001473173	1784	1766	-
12	DNAJC3	P58; P58IPK	NM_008929	146	128	+
13	Ero1lb	ERO1-like beta	NM_026184	200	182	-
14	Foxk1	forkhead box K1	NM_010812	1227	1209	-
15	Grp45	G protein-coupled receptor 44	NM_009962	173	155	-
16	Hnrpa3	heterogeneous nuclear ribonucleoprotein A3	NM_053263	243	225	-
17	Hsp90b1	Tra1; GRP94	NM_011631	41	23	-
17	Hsp90b1	Tra1; GRP94	NM_011631	64	46	+
18	Hspa5	GRP78	NM_022310	64	46	+
19	Kbtbd8	kelch repeat and BTB (POZ) domain containing 8	NM_001008785	1165	1147	+
20	Kcna6	potassium voltage-gated channel, shaker-related, subfamily, member 6	NM_013568	1668	1650	+
21	Kcnmb2	potassium large conductance calcium-activated channel, subfamily M, beta member 2	NM_028231	1920	1902	-
22	Klk1b8	kallikrein 1-related peptidase b8	NM_008457	321	303	+
23	Klk1b22	kallikrein 1-related peptidase b22	NM_010114	318	300	+
24	Mfsd11	major facilitator superfamily domain containing 11	NM_178620	579	561	+
25	Nox3	NADPH oxidase 3	NM_198958	1045	1027	-
26	Nt5dc3	5'-nucleotidase domain containing 3	NM_175331	338	320	+
26	Nt5dc3	5'-nucleotidase domain containing 3	NM_175331	233	215	-
27	Pdia6	protein disulfide isomerase associated 6	NM_022959	103	85	+
28	Setbp1	SET binding protein 1	NM_053099	322	304	-
29	Sfrs2	splicing factor, arginine/serine-rich 2 (SC-35)	NM_011358	358	340	-
30	Syvn1	Synoviolin 1	NM_028769	129	111	+
31	Tmprss11e	transmembrane protease, serine 11e	NM_172880	1554	1536	+
32	Tmprss12	transmembrane protease, serine 12	NM_183109	1003	985	+
33	Usp52	ubiquitin specific peptidase 52	NM_133992	47	29	-
34	XBP1	X-box binding protein 1	NM_013842	60	42	+
35	Xlr3a	X-linked lymphocyte-regulated 3A	NM_001110784	171	153	+
36	Xlr3b	X-linked lymphocyte-regulated 3B	NM_001081643	148	130	+
37	Xlr3c	X-linked lymphocyte-regulated 3C	NM_011727	168	150	+
38	Zfp57	zinc finger protein 57	NM_001013745	49	31	-
39	Zfp777	zinc finger protein 777	NM_001081382	1948	1930	-

Each unique gene containing a consensus ERSE (CCAAT-N9-CCACG) is numbered once. All ATF6-regulated genes are sorted by the fold change from the ATF6 microarray. All genes from the full genome are sorted alphabetically. The MGI symbol, alias or common name, and NCBI Reference Sequence ID, or accession number, is shown for each gene. More information about each gene can be obtained by entering the MGI symbol into the Mouse Genome Informatics (MGI 3.54) website. Also shown is the Start and End location for each ERSE identified, as determined by retrieving the 2000bp 5' flanking promoter sequence using Ensembl Biomart and searching for each element with our custom Perl script.

Table 3. Genes containing consensus ERSEII elements within 2KB promoter regions.

Genes containing consensus ERSEII elements within 2KB promoter regions

ATF6-Regulated Genes

Number	MGI symbol	Alias or Protein Name	NCBI RefSeq	Start	End	Strand	Fold Change
1	Dnajb11	DnaJ (Hsp40) homolog, subfamily B, member 11	NM_026400	11	1	+	12.39
2	Armet	arginine-rich, mutated in early stage tumors	NM_029103	110	100	-	8.21
3	Hyou1	hypoxia up-regulated 1	NM_021395	178	168	-	3.864
3	Hyou1	hypoxia up-regulated 1	NM_021395	77	67	-	3.864
4	Herpud1	homocysteine-inducible, endoplasmic reticulum stress-inducible, ubiquitin-like domain member 1	NM_022331	117	107	+	2.43

Full Genome

Number	MGI symbol	Alias or Protein Name	NCBI RefSeq	Start	End	Strand
1	1110067D22Rik	Grpa	NM_173752	80	70	-
2	4933421E11Rik	Rif1	NM_001039478	67	57	+
3	1500005K14Rik	Fam101b	XM_893392	1067	1057	+
4	Apon	apolipoprotein N	NM_133996	1464	1454	-
5	Armet	arginine-rich, mutated in early stage tumors	NM_029103	110	100	-
6	Cxcl12	chemokine (C-X-C motif) ligand 12	NM_001012477	479	469	+
7	D430018E03Rik	RIKEN cDNA D430018E03 gene	NM_001002769	1449	1439	-
8	Dnajb11	DnaJ (Hsp40) homolog, subfamily B, member 11	NM_026400	11	1	+
9	Efhc1	EF-hand domain-containing protein 1	XM_129694	349	339	-
10	EG665305	LOC665305	XM_975981	123	113	-
11	Gal3st4	galactose-3-O-sulfotransferase 4	NM_001033416	865	855	+
12	Herpud1	homocysteine-inducible, endoplasmic reticulum stress-inducible, ubiquitin-like domain member 1	NM_022331	117	107	+
13	Hyou1	hypoxia up-regulated 1	NM_021395	178	168	-
13	Hyou1	hypoxia up-regulated 1	NM_021395	77	67	-
14	Iqcf5	IQ motif containing F5	XM_356185	740	730	-
15	Mcm9	minichromosome maintenance complex component 9	NM_027830	867	857	-
16	Ninj1	Ninjurin-1	NM_013610	781	771	+
17	Nrxn2	Neurexin II	XM_978630	100	90	-
18	Nucb1	nucleobindin 1	NM_008749	40	30	-
19	Rasd1	Dexras1	NM_009026	768	758	
20	Rbm39	RNA binding motif protein 39	NM_133242	80	70	+
21	Rcl1	RNA terminal phosphate cyclase-like 1	NM_021525	81	71	-
22	Rnf151	ring finger protein 151	NM_026205	33	23	+
23	Tbccd1	TBCC domain containing 1	NM_001081368	323	313	-
24	Tbx2	T-box 2	NM_009324	1913	1903	-
25	Tmed2	transmembrane emp24 domain trafficking protein 2	NM_019770	202	192	+
26	Tmem119	transmembrane protein 119	NM_146162	380	370	+
27	Trim46	tripartite motif-containing 46	NM_183037	1300	1290	-
28	Ufd1	ubiquitin fusion degradation 1 like	NM_011672	657	647	+
29	Ung	UDG	NM_001040691	1152	1142	-

Each unique gene containing a consensus ERSEII (ATTGG-N-CCACG) is numbered once. All genes are sorted as in Table 2, and all information is presented as in Table 2.

Table 4. Genes containing consensus UPRE elements within 2KB promoter regions.

Genes containing consensus UPRE elements within 2KB promoter regions

ATF6-Regulated Genes

Number	MGI symbol	Alias or Protein Name	NCBI RefSeq	Start	End	Strand	Fold Change
1	Timp1	tissue inhibitor of metalloproteinase 1	NM_001044384	83	75	+	7.78
2	Stat3	signal transducer and activator of transcription 3	NM_011486	563	555	-	2.777
3	Fra-2	fos-like antigen 2	NM_008037	1118	1110	-	2.477
4	Nmor2	NAD(P)H dehydrogenase, quinone 2	NM_020282	539	531	+	0.3413
5	Kcnv2	potassium channel, subfamily V, member 2	NM_183179	124	116	-	0.179

Full Genome

Number	MGI symbol	Alias or Protein Name	NCBI RefSeq	Start	End	Strand
1	1110049F12Rik	RIKEN cDNA 1110049F12 gene	NM_025411	62	54	-
2	1810007P19Rik	RIKEN cDNA 1810007P19 gene	NM_172701	827	819	+
3	2010203O07Rik	DnaJ (Hsp40) homolog, subfamily C , member 25	NM_001033165	48	40	+
4	4921507L20Rik	RIKEN cDNA 4921507L20 gene	AK014837	1959	1951	+
5	4921530L21Rik	RIKEN cDNA 4921530L21 gene	NM_025733	1067	1059	+
6	4930579K19Rik	RIKEN cDNA 4930579K19 gene	NM_175227	138	130	+
7	9230112E08Rik	RIKEN cDNA 9230112E08 gene	NM_177264	197	189	+
8	9930038B18Rik	RIKEN cDNA 9930038B18 gene	NM_176929	1502	1494	-
9	Adam32	a disintegrin and metallopeptidase domain 32	NM_153397	1850	1842	+
10	Adamts17	a disintegrin-like and metallopeptidase (reprolysin type) with thrombospondin type 1 motif, 17	NM_001033877	660	652	-
11	Adrp	adipose differentiation related protein	NM_007408	1062	1054	+
12	Aff4	AF4/FMR2 family, member 4	NM_033565	470	462	-
13	Afg3l1	AFG3(ATPase family gene 3)-like 1 (yeast)	NM_054070	466	458	+
14	Alx3	aristaless-like homeobox 3	XM_973424	37	29	+
15	Aox3	aldehyde oxidase 3	NM_023617	228	220	-
16	Apbb1	amyloid beta (A4) precursor protein-binding, family B, member 1	NM_009685	778	770	-
17	Apc2	adenomatosis polyposis coli 2	NM_011789	1732	1724	-
18	Apobec3	apolipoprotein B editing complex 3	NM_030255	372	364	+
18	Apobec3	apolipoprotein B editing complex 3	NM_030255	1851	1843	+
19	App	amyloid beta (A4) precursor protein	NM_007471	638	630	-
20	Azi1	5-azacytidine induced gene 1	NM_001109658	698	690	-
21	B530045E10Rik	RIKEN cDNA B530045E10 gene	NM_177302	881	873	+
22	BC022687	cDNA sequence BC022687	NM_145450	1466	1458	+
23	BC031781	cDNA sequence BC031781	NM_145943	1503	1495	+
24	Brd9	bromodomain containing 9	NM_001024508	1813	1805	-
25	C130021I20Rik	Riken cDNA C130021I20 gene	NM_177842	110	102	-
26	C230094A16Rik	RIKEN cDNA C230094A16 gene	NM_146016	332	324	-
27	C330006K01Rik	RIKEN cDNA C330006K01 gene	NM_172725	186	178	+
28	Camta2	calmodulin binding transcription activator 2	NM_178116	1116	1108	+
29	Ccdc126	coiled-coil domain containing 126	NM_175098	1514	1506	+
30	CCS	copper chaperone for superoxide dismutase	NM_016892	1998	1990	+
31	Cd101	immunoglobulin superfamily, member 3	NM_207205	507	499	+
32	Cd3e	CD3 antigen, epsilon polypeptide	NM_007648	73	65	+
33	Cdk2ap1	CDK2 (cyclin-dependent kinase 2)-associated protein 1	NM_013812	1981	1973	+
34	Cenpp	centromere protein P	NM_025495	1690	1682	-
35	Chchd4	coiled-coil-helix-coiled-coil-helix domain containing 4	NM_133028	888	880	-
36	CHLFH1a	CKLF-like MARVEL transmembrane domain containing 1	NM_181990	599	591	-
37	Chrnb2	cholinergic receptor, nicotinic, beta polypeptide 2 (neuronal)	NM_009602	198	190	-
38	Clcn6	chloride channel 6	NM_011929	1740	1732	+
39	Clstn3	calsyntenin 3	NM_153508	367	359	+
40	Cmkbr6	chemokine (C-C motif) receptor 6	NM_009835	634	626	-
41	Col20a1	collagen, type XX, alpha 1	XM_001473208	664	656	-
42	Crtap	cartilage associated protein	NM_019922	1145	1137	+
43	Ctbs	chitobiase, di-N-acetyl-	NM_028836	1853	1845	+
44	Cul4a	cullin 4A	NM_146207	703	695	+
45	Cyb561	cytochrome b-561	NM_007805	236	228	+
46	Dchs1	dachsous 1	XM_993405	660	652	+
47	Dcun1d1	DCN1, defective in cullin neddylation 1, domain containing 1	NM_033623	320	312	+
48	Defb38	defensin beta 38	NM_183036	1399	1391	+
49	Dkk3	dickkopf homolog 3	NM_015814	1414	1406	-
50	Dscaml1	Down syndrome cell adhesion molecule-like 1	NM_001081270	787	779	-
51	Ebf4	early B-cell factor 4	NM_001110513	951	943	+
52	EG245174	predicted gene, EG245174	XM_001480860	403	395	-
53	Eif2a	eukaryotic translation initiation factor 2a	NM_001005509	823	815	-
54	Fank1	fibronectin type 3 and ankyrin repeat domains 1	NM_025850	71	63	-
55	Fbxo9	f-box protein 9	NM_001081490	188	180	+
56	Fer1l4	fer-1-like 4	XM_001481335	417	409	+
57	Fgfbp1	fibroblast growth factor binding protein 1	NM_008009	1931	1923	-
58	Fpgt	fucose-1-phosphate guanylyltransferase	NM_029330	69	61	-
59	Fra-2	fos-like antigen 2	NM_008037	1118	1110	-
60	Fscn3	fascin homolog 3, actin-bundling protein, testicular (Strongylocentrotus purpuratus)	NM_019569	1230	1222	+
61	Gabarap	gamma-aminobutyric acid receptor associated protein	NM_019749	464	456	+
62	Gabpb1	GA repeat binding protein, beta 1	NM_207669	568	560	-
63	Gcg	glucagon	NM_008100	1175	1167	+
64	Gfra1	glial cell line derived neurotrophic factor family receptor alpha 1	NM_010279	696	688	+
65	Glut4	solute carrier family 2 (facilitated glucose transporter), member 4	NM_009204	1890	1882	-
66	Gnai3	guanine nucleotide binding protein (G protein), alpha inhibiting 3	NM_010306	1028	1020	+

Each unique gene containing a consensus ERSEII (ATTGG-N-CCACG) is numbered once. All genes are sorted as in Table 2, and all information is presented as in Table 2.

Table 5. Genes containing 1bp-mismatched ERSE elements within 2KB promoter regions.

Genes containing consensus UPRE elements within 2KB promoter regions

Full Genome (Continued)

Number	MGI symbol	Alias or Protein Name	NCBI RefSeq	Start	End	Strand
67	Gosr2	golgi SNAP receptor complex member 2	NM_019650	471	463	-
68	Gria3	glutamate receptor, ionotropic, AMPA3 (alpha 3)	NM_016886	668	660	-
69	Gtf2h2	general transcription factor II H, polypeptide 2	NM_022011	805	797	-
70	Gtf2h4	general transcription factor II H, polypeptide 4	NM_010364	632	624	-
71	H1fx	H1 histone family, member X	XM_981507	1795	1787	-
72	Hbs1l	Hbs1-like (S. cerevisiae)	NM_001042593	122	114	-
73	Hk2	hexokinase 2	XM_00147807	48	40	-
74	Hoxa11	homeo box A11	NM_010450	20	12	-
75	Igf2r	insulin-like growth factor 2 receptor	NM_010515	1719	1711	-
76	IL-10	interleukin 10	NM_010548	355	347	-
77	Isg20	interferon-stimulated protein	NM_001113527	95	87	-
78	Kbtbd11	kelch repeat and BTB (POZ) domain containing 11	XM_921147	710	702	+
79	Kcnk6	potassium inwardly-rectifying channel, subfamily K, member 6	NM_001033525	1305	1297	-
80	Kcnv2	potassium channel, subfamily V, member 2	NM_183179	124	116	-
81	Lcat	lecithin cholesterol acyltransferase	NM_008490	1211	1203	+
82	Lmx1b	LIM homeobox transcription factor 1 beta	NM_010725	619	611	+
83	Lrrc58	leucine rich repeat containing 58	XM_915566	793	785	+
84	Maoa	monoamine oxidase A	NM_173740	1228	1220	+
85	Menkes	ATPase, Cu++ transporting, alpha polypeptide	NM_001109757	175	167	+
86	Mga	MAX gene associated	NM_013720	9	1	+
87	MGBmper	BMP-binding endothelial regulator	NM_028472	1178	1170	-
88	Mpzl3	myelin protein zero-like 3	NM_001093749	560	552	-
89	Mthfr	5,10-methylenetetrahydrofolate reductase	NM_010840	644	636	-
90	Mycbpap	Mycbp associated protein	NM_170671	496	488	+
91	Ncstn	nicastrin	NM_021607	92	84	-
92	Necab2	N-terminal EF-hand calcium binding protein 2	XM_001001292	966	958	+
93	Neurl2	Neurl2	NM_001081656	1675	1667	+
94	Nfe2l1	nuclear factor, erythroid derived 2,-like 1	NM_001130453	171	163	-
95	Nmor2	NAD(P)H dehydrogenase, quinone 2	NM_020282	572	564	+
96	Nod1	nucleotide-binding oligomerization domain containing 1	NM_172729	1495	1487	-
97	Olfr837	olfactory receptor 837	NM_146565	1960	1952	+
98	Ormdl3	ORM1-like 3	NM_025661	980	972	+
99	Paqr9	progestin and adipoQ receptor family member IX	NM_198414	740	732	+
100	Park7	Parkinson disease (autosomal recessive, early onset)	NM_020569	413	405	+
101	Pax-1	paired box gene 1	NM_008780	48	40	+
102	Pdgfd	platelet-derived growth factor, D polypeptide	NM_027924	65	57	-
103	Rbks	ribokinase	NM_153196	866	858	-
104	Rlbp1l1	retinaldehyde binding protein 1-like 1	NM_028940	809	801	+
105	Rnf213	ring finger protein 213	NM_001040005	1754	1746	+
106	Serpini1	serine (or cysteine) peptidase inhibitor, clade I, member 1	NM_009250	1609	1601	-
107	Sez6l2	seizure related 6 homolog like 2	NM_144926	1974	1966	-
108	Sgk2	serum/glucocorticoid regulated kinase 2	XM_984112	1712	1704	+
109	Sgk3	serum/glucocorticoid regulated kinase 3	NM_177547	619	611	+
110	Slc16a8	solute carrier family 16 (monocarboxylic acid transporters), member 8	NM_020516	1740	1732	-
111	Slc19a3	solute carrier family 19 (sodium/hydrogen exchanger), member 3	NM_030556	189	181	+
112	Sncaip	synuclein, alpha interacting protein (synphilin)	NM_026408	1118	1110	-
113	Sohlh2	spermatogenesis and oogenesis specific basic helix-loop-helix 2	NM_028937	87	79	-
114	Sp4	trans-acting transcription factor 4	NM_009239	1571	1563	-
115	Stat3	signal transducer and activator of transcription 3	NM_011486	563	555	-
116	Ston1	stonin 1	NM_029858	589	581	+
117	Tas1r1	taste receptor, type 1, member 1	NM_031867	1538	1530	-
118	Thnsl1	threonine synthase-like 1	NM_177588	1665	1657	-
119	Timp1	tissue inhibitor of metalloproteinase 1	NM_001044384	83	75	+
120	Tmem102	transmembrane protein 102	NM_001033433	1389	1381	-
121	Tmem104	transmembrane protein 104	NM_001033393	360	352	-
122	Tpbpa	trophoblast specific protein alpha	NM_009411	338	330	-
123	Trog1	taste receptor protein 1	NM_001014398	1899	1891	+
124	Trim8	tripartite motif protein 8	NM_053100	208	200	-
125	Tsc22d3	TSC22 domain family, member 3	NM_001077364	1897	1889	+
126	Tsfm	Ts translation elongation factor, mitochondrial	NM_025537	1054	1046	-
127	Ttc27	tetratricopeptide repeat domain 27	NM_152817	901	893	-
128	Txdc11	thioredoxin domain containing 11	NM_029582	60	52	+
129	Ubqln3	ubiquilin 3	NM_198623	1073	1065	+
129	Ubqln3	ubiquilin 3	NM_198623	1919	1911	-
130	Wfikkn2	WAP, follistatin/kazal, immunoglobulin, kunitz and netrin domain containing 2	NM_181819	561	553	-
131	Zfhx3	zinc finger homeobox 3	NM_007496	265	257	+
132	Zfp653	zinc finger protein 653	NM_177318	1649	1641	+

Each unique gene containing an ERSE (CCAAT-N9-CCACG) with 1bp-mismatched anywhere on either flanking region, is numbered once. All ATF6-regulated genes are sorted by the fold change from the ATF6 microarray. The MGI symbol, alias or common name, and NCBI Reference Sequence ID, or accession number, is shown for each gene. More information about each gene can be obtained by entering the MGI symbol into the Mouse Genome Informatics (MGI 3.54) web site. Also shown is the Start and End location for each 1bp-mismatched ERSE identified, as determined by retrieving the 2000bp 5' flanking promoter sequence using Ensembl Biomart and searching for each element with our custom Perl script.

Table 5: Genes containing 1bp-mismatched ERSE elements within 2KB promoter regions. (continued)

Genes containing 1bp-mismatched ERSE elements within 2KB promoter regions

ATF6-Regulated Genes

Number	MGI symbol	Alias or Protein Name	NCBI RefSeq	Start	End	Strand	Fold Change
1	Alkbh2	alkB, alkylation repair homolog 2	NM_175016	534	516	+	47.45
2	Il-6	interleukin 6	NM_031168	134	116	+	38.45
3	Pdia4	protein disulfide isomerase associated 4	NM_009787	107	89	-	16.37
4	Ears2	glutamyl-tRNA synthetase 2 (mitochondrial)(putative)	NM_026140	91	73	-	7.841
5	Eda2r	ectodysplasin A2 isoform receptor	NM_175540	1590	1572	+	7.464
6	Hsp90b1	heat shock protein 90, beta (Grp94), member 1	NM_011631	1287	1269	-	7.071
6	Hsp90b1	heat shock protein 90, beta (Grp94), member 1	NM_011631	185	167	-	7.071
7	Kpnb1	karyopherin (importin) beta 1	NM_008379	1328	1310	+	6.42
8	Sel1h	sel-1 suppressor of lin-12-like	NM_001039089	190	172	-	6.297
9	Tubb3	tubulin, beta 3	NM_023279	777	759	+	5.795
10	Edem1	ER degradation enhancer, mannosidase alpha-like 1	NM_138677	299	281	-	5.36
11	G530011O06Rik	RIKEN cDNA G530011O06 gene	NM_001039559	595	577	+	5.216
12	Trim37	tripartite motif-containing 37	NM_197987	239	221	-	5.208
12	Trim37	tripartite motif-containing 37	NM_197987	228	210	+	5.208
13	Kcnq1	potassium voltage-gated channel, subfamily Q, member 1	NM_008434	1891	1873	+	5.136
14	Ubfd1	ubiquitin family domain containing 1	NM_138589	79	61	+	5.048
15	Pdia3	protein disulfide isomerase associated 3	NM_007952	28	10	+	4.718
16	Arntl	aryl hydrocarbon receptor nuclear translocator-like	NM_007489	291	273	+	4.267
17	Tbcb	tubulin folding cofactor B	NM_025548	35	17	-	4.188
18	Pin1	protein (peptidyl-prolyl cis/trans isomerase) NIMA-interacting 1	NM_023371	100	82	-	4.119
19	2610036L11Rik	RIKEN cDNA 2610036L11 gene	NM_001109747	47	29	+	4.106
20	Hyou1	hypoxia up-regulated 1	NM_021395	513	495	+	3.864
21	p97/VCP	valosin containing protein	NM_009503	263	245	+	3.288
22	Rabepk	Rab9 effector protein with kelch motifs	NM_145522	168	150	-	3.066
23	Ptpn14	protein tyrosine phosphatase, non-receptor type 14	NM_001033287	1377	1359	+	3.045
24	Gsk3b	glycogen synthase kinase 3 beta	NM_019827	217	199	+	2.998
24	Gsk3b	glycogen synthase kinase 3 beta	NM_019827	1441	1423	-	2.998
25	Sfpq	splicing factor proline/glutamine rich (polypyrimidine tract binding protein associated)	XM_994784	1725	1707	-	2.906
26	Nmt1	N-myristoyltransferase 1	NM_008707	29	11	+	2.832
27	Fkbp11	FK506 binding protein 11	NM_024169	1089	1071	+	2.814
28	Ormdl2	ORM1-like 2	NM_024180	1673	1655	-	2.785
29	Tmem45a	transmembrane protein 45a	NM_019631	961	943	+	2.756
30	Rasl11b	RAS-like, family 11, member B	NM_026878	760	742	-	2.54
30	Rasl11b	RAS-like, family 11, member B	NM_026878	87	69	-	2.54
31	Nip7	nuclear import 7 homolog	NM_025391	32	14	-	2.513
32	Herpud1	homocysteine-inducible, endoplasmic reticulum stress-inducible, ubiquitin-like domain member 1	NM_022331	83	65	+	2.4315
33	Ngdn	neuroguidin, EIF4E binding protein	NM_026890	1844	1826	+	2.379
34	Mrps18b	mitochondrial ribosomal protein S18B	NM_025878	499	481	-	2.228
35	Lip1	lysosomal acid lipase A	NM_001111100	91	73	-	2.21
36	Ddx54	DEAD (Asp-Glu-Ala-Asp) box polypeptide 54	NM_028041	1142	1124	+	2.189
36	Ddx54	DEAD (Asp-Glu-Ala-Asp) box polypeptide 54	NM_028041	1204	1186	+	2.189
37	Stmn1	stathmin 1	NM_019641	1034	1016	-	2.143
38	Dnaja4	DnaJ (Hsp40) homolog, subfamily A, member 4	NM_021422	1834	1816	+	2.107
38	Dnaja4	DnaJ (Hsp40) homolog, subfamily A, member 4	NM_021422	350	332	+	2.107
39	Tubb5	tubulin, beta 5	NM_011655	158	140	+	2.084
40	Popdc3	popeye domain containing 3	NM_024286	1592	1574	+	2.043
41	Crls1	cardiolipin synthase 1	NM_025646	662	644	-	2.037
42	Enpp5	ectonucleotide pyrophosphatase/phosphodiesterase 5	NM_032003	741	723	-	0.495
43	Jam2	junction adhesion molecule 2	NM_023844	470	452	+	0.487
44	Auh	AU RNA binding protein/enoyl-coenzyme A hydratase	NM_016709	1410	1392	+	0.475
45	Ppil1	Cypl1	NM_025646	913	895	-	0.47
46	B3gnt6	UDP-GlcNAc:betaGal beta-1,3-N-acetylglucosaminyltransferase 6 (core 3 synthase)	NM_001081167	1138	1120	+	0.46
47	2410012H22Rik	zinc finger, SWIM-type containing 7	XM_001473892	575	557	+	0.45
48	Egflam	EGF-like, fibronectin type III and laminin G domains	NM_178748	189	171	+	0.435
49	Hrasls	HRAS-like suppressor	NM_013751	141	123	-	0.428
50	Myh6	myosin, heavy polypeptide 6, cardiac muscle, alpha	NM_010856	773	755	-	0.398
51	Cog8	component of oligomeric golgi complex 8	NM_139229	188	170	+	0.384
52	Siae	sialic acid acetylesterase	NM_011734	1525	1507	+	0.365
53	Nit2	nitrilase family, member 2	NM_023175	1041	1023	+	0.36
54	Asb14	ankyrin repeat and SOCS box-containing 14	NM_080856	1045	1027	+	0.187
55	Fbp2	fructose bisphosphatase 2	NM_007994	1068	1050	+	0.159
56	Acsm5	acyl-CoA synthetase medium-chain family member 5	NM_178758	287	269	-	0.0961
57	Ogdh	oxoglutarate dehydrogenase (lipoamide)	NM_010956	133	115	+	0.0828
58	Apba3	amyloid beta (A4) precursor protein binding, family A, member 1	NM_177034	600	582	-	0.0753

Table 6. Genes containing 1bp-mismatched ERSEII elements within 2KB promoter regions.

Genes containing 1bp-mismatched ERSEII elements within 2KB promoter regions

ATF6-Regulated Genes

Number	MGI symbol	Alias or Protein Name	NCBI RefSeq	Start	End	Strand	Fold Change
1	Sdf2l1	stromal cell-derived factor 2-like 1	NM_022324	166	156	-	17.41
2	Tspyl2	TSPY-like 2	NM_029836	1326	1316	+	9.294
3	Ears2	glutamyl-tRNA synthetase 2 (mitochondrial)(putative)	NM_026140	351	341	+	7.841
4	Sel1h	sel-1 suppressor of lin-12-like	NM_001039089	161	151	-	6.297
5	D16Ertd472e	DNA segment, Chr 16, ERATO Doi 472, expressed	NM_025967	315	305	-	6.255
6	Edem1	ER degradation enhancer, mannosidase alpha-like 1	NM_138677	201	191	-	5.36
7	Ebp	phenylalkylamine Ca2+ antagonist (emopamil) binding protein	NM_007898	460	450	+	5.287
8	Atf4	activating transcription factor 4	NM_009716	81	71	-	4.928
9	Hspa5	heat shock protein 5, GRP78	NM_022310	103	93	-	4.706
10	Syvn1	synovial apoptosis inhibitor 1, synoviolin	NM_028769	154	144	+	4.5995
11	Arntl	aryl hydrocarbon receptor nuclear translocator-like	NM_007489	288	278	+	4.267
12	Egr-1	early growth response 1	NM_007913	342	332	-	3.667
13	Junb	Jun-B oncogene	NM_008416	360	350	-	2.639
14	Fra-2	fos-like antigen 2	NM_008037	1051	1041	-	2.477
15	3110050N22Rik	RIKEN cDNA 3110050N22 gene	NM_173181	23	13	-	2.396
16	Stt3b	STT3, subunit of the oligosaccharyltransferase complex, homolog B	NM_024222	191	181	+	2.228
17	Rpl14	ribosomal protein L14	NM_025974	80	70	-	2.087
18	Pank1	pantothenate kinase 1	NM_001114339	81	71	-	0.401
19	Slc22a5	solute carrier family 22 (organic cation transporter), member 5	NM_011396	246	236	-	0.3895
20	Acot11	acyl-CoA thioesterase 11	NM_025590	160	150	+	0.34
21	Tfdp2	transcription factor Dp 2	XM_001481271	110	100	-	0.335
22	Tfdp2	transcription factor Dp 2	XM_001481271	557	547	+	0.335
23	Asb10	ankyrin repeat and SOCS box-containing 10	NM_080444	516	506	-	0.231
24	ACH2	acyl-CoA thioesterase 1	NM_012006	1238	1228	-	0.225
25	Acot1	acyl-CoA thioesterase 1	NM_012006	686	676	-	0.225

Each unique gene containing an ERSEII (ATTGG-N-CCACG) with 1bp-mismatched anywhere on either flanking region, is numbered once. All genes are sorted as in Table 2, and all information is presented as in Table 2.

Table 7. Genes containing 1bp-mismatched UPRE elements within 2KB promoter regions.

Genes containing 1bp-mismatched UPRE elements within 2KB promoter regions

ATF6-Regulated Genes

Number	MGI symbol	Alias or Protein Name	NCBI RefSeq	Start	End	Strand	Fold Change
1	Far1	fatty acyl CoA reductase 1	NM_027379	131	123	+	120.9
2	Spp1	secreted phosphoprotein 1	NM_009263	1645	1637	+	91.47
3	Il-6	interleukin 6	NM_031168	886	878	+	38.45
4	Tk-1	thymidine kinase 1	NM_009387	745	737	+	20.57
5	Sdf2l1	stromal cell-derived factor 2-like 1	NM_022324	1539	1531	-	17.41
5	Sdf2l1	stromal cell-derived factor 2-like 1	NM_022324	1456	1448	-	17.41
6	Pdia4	protein disulfide isomerase associated 4	NM_009787	838	830	-	16.37
7	Dnajc3	DnaJ (Hsp40) homolog, subfamily C, member 3	NM_008929	194	186	-	12.75
8	Pgp	phosphoglycolate phosphatase	NM_025954	1099	1091	-	10.09
8	Pgp	phosphoglycolate phosphatase	NM_025954	386	378	+	10.09
9	eIF-1A	eukaryotic translation initiation factor 1A	NM_010120	81	73	+	9.657
10	P4hb	prolyl 4-hydroxylase, beta polypeptide	NM_011032	924	916	-	9.173
11	Chac1	ChaC, cation transport regulator-like 1	NM_026929	1603	1595	-	8.065
11	Chac1	ChaC, cation transport regulator-like 1	NM_026929	979	971	-	8.065
12	Hsp90b1	heat shock protein 90, beta (Grp94), member 1	NM_011631	823	815	+	7.071
12	Hsp90b1	heat shock protein 90, beta (Grp94), member 1	NM_011631	665	657	+	7.071
13	Itgam	integrin alpha M	NM_001082960	590	582	+	6.878
14	Hn1l	hematological and neurological expressed 1-like	NM_198937	1061	1053	+	6.772
15	Dbf4	DBF4 homolog	NM_013726	1383	1375	-	6.442
16	Sel1h	sel-1 suppressor of lin-12-like	NM_001039089	1652	1644	-	6.297
17	D16Ertd472e	DNA segment, Chr 16, ERATO Doi 472, expressed	NM_025987	1986	1978	+	6.255
18	2810474O19Rik	RIKEN cDNA 2810474O19 gene	NM_026054	1509	1501	+	6.0485
19	M(beta)2	tubulin, beta 2a	NM_009450	1604	1596	+	5.579
19	M(beta)2	tubulin, beta 2a	NM_009450	1222	1214	-	5.579
20	Tubb2b	tubulin, beta 2b	NM_023716	1957	1949	-	5.579
21	Fem1b	feminization 1 homolog b	NM_010193	881	873	+	5.325
22	Morf4l2	mortality factor 4 like 2	NM_019768	902	894	-	5.32
22	Morf4l2	mortality factor 4 like 2	NM_019768	1105	1097	+	5.32
23	G530011O06Rik	RIKEN cDNA G530011O06 gene	NM_001039559	1815	1807	-	5.216
24	Kcnq9	potassium voltage-gated channel, subfamily Q, member 1	NM_008434	1928	1920	-	5.136
25	TSA903	uridine-cytidine kinase 2	NM_030724	423	415	+	5.0273
26	Rbm15b	RNA binding motif protein 15B	NM_175402	1302	1294	-	4.989
27	Rras2	related RAS viral (r-ras) oncogene homolog 2	NM_025846	1075	1067	-	4.947
27	Rras2	related RAS viral (r-ras) oncogene homolog 2	NM_025846	224	216	-	4.947
28	Aldh18a1	aldehyde dehydrogenase 18 family, member A1	NM_019698	1768	1760	+	4.8045
29	Grp58	protein disulfide isomerase associated 3	NM_007952	484	476	+	4.718
30	Ms4a4c	membrane-spanning 4-domains, subfamily A, member 4C	NM_029499	694	686	+	4.565
31	Plac8	placenta-specific 8	NM_139198	721	713	-	4.559
31	Plac8	placenta-specific 8	NM_139198	1433	1425	+	4.559
32	Kif5b	kinesin family member 5B	NM_008448	119	111	+	4.55
33	Nans	N-acetylneuraminic acid synthase (sialic acid synthase)	NM_053179	42	34	+	4.5345
34	Nola2	nucleolar protein family A, member 2	NM_026631	1215	1207	-	4.441
35	Map3k3	mitogen-activated protein kinase kinase kinase 3	NM_011947	13	5	+	4.287
36	Bmal1	aryl hydrocarbon receptor nuclear translocator-like	NM_007489	1388	1380	-	4.267
37	Tbcb	tubulin folding cofactor B	NM_025548	1014	1006	+	4.188
38	2610036L11Rik	RIKEN cDNA 2610036L11 gene	NM_001109747	1175	1167	+	4.106
39	Hmgb1	high mobility group box 1	NM_010439	962	970	+	4.083
40	Hagh	hydroxyacyl glutathione hydrolase	NM_024284	1761	1753	+	3.1413
40	Hagh	hydroxyacyl glutathione hydrolase	NM_024284	1504	1496	+	3.1413
40	Hagh	hydroxyacyl glutathione hydrolase	NM_024284	794	786	-	3.1413
41	Mesdc2	mesoderm development candidate 2	NM_023403	306	298	+	3.139
42	Serpinh1	serine (or cysteine) peptidase inhibitor, clade H, member 1	NM_001111044	315	307	-	3.097
43	Gsk3b	glycogen synthase kinase 3 beta	NM_019827	1288	1280	-	2.998
44	2700049P18Rik	RIKEN cDNA 2700049P18 gene	NM_175382	570	562	+	2.984
45	Flnc	filamin C, gamma (actin binding protein 280)	NM_001081185	1973	1965	-	2.9105
46	Dlgap4	discs, large homolog-associated protein 4	NM_001042488	407	399	+	2.907
46	Dlgap4	discs, large homolog-associated protein 4	NM_001042488	1591	1583	-	2.907
47	Nol12	nucleolar protein 12	NM_133800	1268	1260	+	2.888
48	Mettl1	methyltransferase-like 1	NM_010792	1029	1021	-	2.873
49	Srm	spermidine synthase	NM_009272	905	897	-	2.812
50	H2-Ke6	H2-K region expressed gene 6	NM_013543	934	926	+	2.719
51	Os9	amplified in osteosarcoma	NM_177614	1935	1927	-	2.672
52	Med19	mediator of RNA polymerase II transcription, subunit 19 homolog	NM_025885	989	981	-	2.66
53	Apex1	apurinic/apyrimidinic endonuclease 1	NM_009687	569	561	-	2.632

Each unique gene containing an UPRE (TGACGTGGA) with 1bp-mismatched anywhere on the element, is numbered once. All genes are sorted as in Table 2, and all information is presented as in Table 2.

Table 7- Genes containing 1bp-mismatched UPRE elements within 2KB promoter regions. (continued)

Genes containing 1bp-mismatched UPRE elements within 2KB promoter regions

Full Genome (Continued)

Number	MGI symbol	Alias or Protein Name	NCBI RefSeq	Start	End	Strand	Fold Change
54	Cyb5r1	cytochrome b5 reductase 1	NM_028057	220	212	-	2.597
55	Pja2	praja 2, RING-H2 motif containing	NM_001025309	968	960	+	2.568
55	Pja2	praja 2, RING-H2 motif containing	NM_001025309	706	698	+	2.568
55	Pja2	praja 2, RING-H2 motif containing	NM_001025309	676	668	+	2.568
55	Pja2	praja 2, RING-H2 motif containing	NM_001025309	646	638	+	2.568
55	Pja2	praja 2, RING-H2 motif containing	NM_001025309	616	608	+	2.568
55	Pja2	praja 2, RING-H2 motif containing	NM_001025309	586	578	+	2.568
55	Pja2	praja 2, RING-H2 motif containing	NM_001025309	556	548	+	2.568
55	Pja2	praja 2, RING-H2 motif containing	NM_001025309	526	518	+	2.568
55	Pja2	praja 2, RING-H2 motif containing	NM_001025309	496	488	+	2.568
55	Pja2	praja 2, RING-H2 motif containing	NM_001025309	466	458	+	2.568
55	Pja2	praja 2, RING-H2 motif containing	NM_001025309	436	428	+	2.568
55	Pja2	praja 2, RING-H2 motif containing	NM_001025309	939	931	+	2.568
55	Pja2	praja 2, RING-H2 motif containing	NM_001025309	406	398	+	2.568
55	Pja2	praja 2, RING-H2 motif containing	NM_001025309	376	368	+	2.568
55	Pja2	praja 2, RING-H2 motif containing	NM_001025309	346	338	+	2.568
55	Pja2	praja 2, RING-H2 motif containing	NM_001025309	316	308	+	2.568
55	Pja2	praja 2, RING-H2 motif containing	NM_001025309	286	278	+	2.568
55	Pja2	praja 2, RING-H2 motif containing	NM_001025309	256	248	+	2.568
55	Pja2	praja 2, RING-H2 motif containing	NM_001025309	226	218	+	2.568
55	Pja2	praja 2, RING-H2 motif containing	NM_001025309	196	188	+	2.568
55	Pja2	praja 2, RING-H2 motif containing	NM_001025309	910	902	+	2.568
55	Pja2	praja 2, RING-H2 motif containing	NM_001025309	881	873	+	2.568
55	Pja2	praja 2, RING-H2 motif containing	NM_001025309	852	844	+	2.568
55	Pja2	praja 2, RING-H2 motif containing	NM_001025309	823	815	+	2.568
55	Pja2	praja 2, RING-H2 motif containing	NM_001025309	794	786	+	2.568
55	Pja2	praja 2, RING-H2 motif containing	NM_001025309	765	757	+	2.568
55	Pja2	praja 2, RING-H2 motif containing	NM_001025309	736	728	+	2.568
56	Sec11a	SEC11 homolog A	NM_019951	1759	1751	-	2.528
57	Trove2	TROVE domain family, member 2	NM_013835	236	228	-	2.5145
58	Nip7	nuclear import 7 homolog	NM_025391	561	553	-	2.513
59	Heatr5a	HEAT repeat containing 5A	NM_177171	1031	1023	+	2.512
60	Rap2b	RAP2B, member of RAS oncogene family	NM_028712	1437	1429	+	2.454
61	Ywhaz	tyrosine 3-monooxygenase/tryptophan 5-monooxygenase activation protein, zeta polypeptide	NM_011740	92	84	-	2.446
62	Gmppb	GDP-mannose pyrophosphorylase B	NM_177910	1739	1731	-	2.437
63	Ehd4	EH-domain containing 4	NM_133838	353	345	-	2.403
64	3110050N22Rik	RIKEN cDNA 3110050N22 gene	NM_173181	191	183	+	2.396
65	Ngd	neuroguidin, EIF4E binding protein	NM_026890	1576	1568	-	2.379
65	Ngd	neuroguidin, EIF4E binding protein	NM_026890	743	735	+	2.379
66	LOC217431	nucleolar protein 10	NM_001008421	282	274	+	2.373
67	Ing1	inhibitor of growth family, member 1	XM_976943	518	510	+	2.369
67	Ing1	inhibitor of growth family, member 1	XM_976943	1333	1325	+	2.369
68	Cldnd1	claudin domain containing 1	NM_171826	809	801	-	2.338
69	Pdap1	PDGFA associated protein 1	NM_001033313	931	923	+	2.336
70	Nucks1	nuclear casein kinase and cyclin-dependent kinase substrate 1	NM_175294	1921	1913	+	2.326
70	Nucks1	nuclear casein kinase and cyclin-dependent kinase substrate 1	NM_175294	274	266	+	2.326
71	Gcs1	glucosidase 1	NM_020619	33	25	+	2.323
72	1700025G04Rik	RIKEN cDNA 1700025G04 gene	NM_197990	1978	1970	-	2.2625
73	Pde4b	phosphodiesterase 4B, cAMP specific	NM_019840	253	245	-	2.216
73	Pde4b	phosphodiesterase 4B, cAMP specific	NM_019840	1062	1054	-	2.216
74	Fads3	fatty acid desaturase 3	NM_021890	1516	1508	-	2.21
75	Slc6a6	solute carrier family 6 (neurotransmitter transporter, taurine), member 6	NM_009320	1768	1760	+	2.207
75	Slc6a6	solute carrier family 6 (neurotransmitter transporter, taurine), member 6	NM_009320	480	472	-	2.207
76	Adamts15	a disintegrin-like and metallopeptidase (reprolysin type) with thrombospondin type 1 motif, 15	NM_001024139	52	44	-	2.182
77	Tln1	talin 1	NM_011602	1444	1436	+	2.137
77	Tln1	talin 1	NM_011602	1060	1052	+	2.137

Table 7- Genes containing 1bp-mismatched UPRE elements within 2KB promoter regions. (continued)
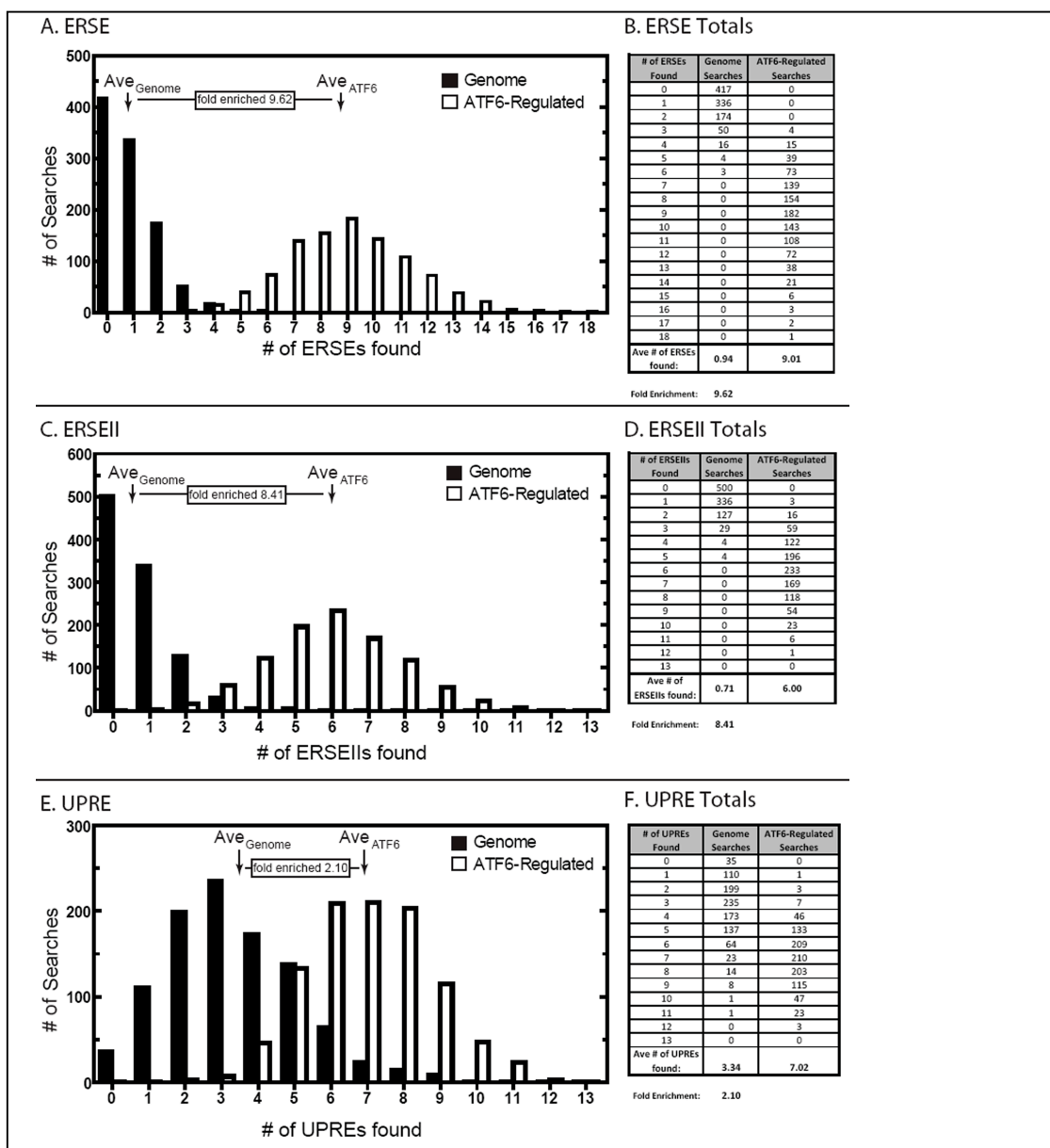
Genes containing 1bp-mismatched UPRE elements within 2KB promoter regions

Full Genome (Continued)

Number	MGI symbol	Alias or Protein Name	NCBI RefSeq	Start	End	Strand	Fold Change
78	Tmem57	transmembrane protein 57	NM_025382	735	727	+	2.136
79	Rrbp1	ribosome binding protein 1	NM_024281	626	618	-	2.114
80	Rrbp1	ribosome binding protein 1	NM_024281	311	303	+	2.114
81	Ralb	v-ral simian leukemia viral oncogene homolog B (ras related)	NM_022327	1719	1711	+	2.109
82	tTGas	transglutaminase 2, C polypeptide	NM_009373	1498	1490	-	2.106
83	Srxn1	sulfiredoxin 1 homolog	NM_029688	750	742	+	2.084
84	Stip1	stress-induced phosphoprotein 1	NM_016737	1476	1468	+	2.051
85	Rps27l	ribosomal protein S27-like	NM_026467	1848	1840	-	2.05
86	Crls1	cardiolipin synthase 1	NM_025646	1192	1184	+	2.037
87	B3galtl	beta 1,3-galactosyltransferase-like	NM_194318	586	578	-	0.494
88	Rhobtb1	Rho-related BTB domain containing 1	NM_001081347	624	616	-	0.478
89	Lmod2	leiomodin 2 (cardiac)	NM_053098	615	607	+	0.473
90	Clip4	CAP-GLY domain containing linker protein family, member 4	NM_175378	1672	1664	-	0.472
91	3110002H16Rik	RIKEN cDNA 3110002H16 gene	NM_029623	1093	1085	+	0.461
91	3110002H16Rik	RIKEN cDNA 3110002H16 gene	NM_029623	23	15	+	0.461
92	Lpl	lipoprotein lipase	NM_008509	1987	1979	+	0.459
93	Cbr1	carbonyl reductase 1	NM_007620	1061	1053	+	0.451
94	Ccni	cyclin I	NM_017367	519	511	-	0.445
95	Grb14	growth factor receptor bound protein 14	NM_016719	1187	1179	+	0.44
96	Neo1	neogenin	NM_001042752	1193	1185	-	0.427
97	Atp6v0e2	ATPase, H+ transporting, lysosomal V0 subunit E2	NM_133764	1191	1183	+	0.42
97	Atp6v0e2	ATPase, H+ transporting, lysosomal V0 subunit E2	NM_133764	542	534	+	0.42
98	Sirt5	sirtuin 5 (silent mating type information regulation 2 homolog) 5	NM_178848	20	12	+	0.403
98	Sirt5	sirtuin 5 (silent mating type information regulation 2 homolog)	NM_178848	1344	1336	-	0.403
99	Gramd1b	GRAM domain containing 1B	NM_172768	1577	1569	+	0.396
100	Mrpl49	mitochondrial ribosomal protein L49	NM_026246	1216	1208	-	0.395
100	Mrpl49	mitochondrial ribosomal protein L49	NM_026246	1230	1222	-	0.395
101	Asb11	ankyrin repeat and SOCS box-containing 11	NM_026853	90	82	-	0.383
102	Mfsd4	major facilitator superfamily domain containing 4	NM_001114662	973	965	-	0.361
102	Mfsd4	major facilitator superfamily domain containing 4	NM_001114662	235	227	+	0.361
103	D930001I22Rik	RIKEN cDNA D930001I22 gene	NM_173397	427	419	-	0.357
104	Ak3	adenylate kinase 3	NM_021299	454	446	-	0.3505
105	Gdc1	glycerol-3-phosphate dehydrogenase 1 (soluble)	NM_010271	1384	1376	+	0.342
106	Retsat	retinol saturase (all trans retinol 13,14 reductase)	NM_026159	1863	1855	-	0.34
106	Ccdc69	coiled-coil domain containing 69	NM_177471	82	74	+	0.331
107	gamma-SG	sarcoglycan, gamma (dystrophin-associated glycoprotein)	NM_011892	1227	1219	+	0.317
108	Gpcr10	endothelin receptor type A	NM_010332	1954	1946	-	0.3167
109	Cutc	cutC copper transporter homolog	NM_001113562	128	120	-	0.307
110	ORF28	DnaJ (Hsp40) homolog, subfamily C, member 28	NM_001099738	1820	1812	+	0.302
111	Sord	sorbitol dehydrogenase	NM_146126	218	210	-	0.295
112	Ucp3	uncoupling protein 3 (mitochondrial, proton carrier)	NM_009464	1723	1715	-	0.27
112	Ucp3	uncoupling protein 3 (mitochondrial, proton carrier)	NM_009464	925	917	-	0.27
113	Asb2	ankyrin repeat and SOCS box-containing 2	XM_977692	51	43	-	0.249
114	Fndc5	fibronectin type III domain containing 5	NM_027402	166	158	+	0.243
115	Acy3	aspartoacylase (aminoacylase) 3	NM_027857	306	298	-	0.239
116	Asb-10	ankyrin repeat and SOCS box-containing 10	NM_080444	1338	1330	-	0.231
117	Wdr21	WD repeat domain 21	NM_030246	412	404	+	0.19
118	Pdlim4	PDZ and LIM domain 4	NM_019417	1371	1363	-	0.102
119	Acsm5	acyl-CoA synthetase medium-chain family member 5	NM_178758	1356	1348	+	0.0961
120	Apba3	amyloid beta (A4) precursor protein-binding, family A, member 3	NM_018758	844	836	+	0.0753

7. ATF6-Regulated Genes are Enriched in ER Stress Elements:

Since ATF6 has been shown to bind to ER stress response elements in the promoter regions of target genes, it was expected that the list of ATF6-regulated genes would contain a significant number of genes that possess ER stress response elements within their regulatory regions. To determine whether the list of ATF6-regulated genes was significantly enriched in genes containing ER stress elements, as compared to a list of randomly-generated genes, a bootstrapping analysis was performed as previously described.[59,60] The ERSE, ERSE-II and UPRE sequences were found 9.6-, 8.4- and 2.1-fold more frequently, respectively, than in random searches from the whole mouse genome **(Fig. 10)**. This confirms that the list of ATF6-regulated genes is indeed enriched in genes containing ER stress elements, and validates ATF6 as a critical activator of ER stress response genes.

A. ERSE

Ave$_{Genome}$ fold enriched 9.62 Ave$_{ATF6}$

■ Genome   □ ATF6-Regulated

# of Searches vs # of ERSEs found

B. ERSE Totals

# of ERSEs Found	Genome Searches	ATF6-Regulated Searches
0	417	0
1	336	0
2	174	0
3	50	4
4	16	15
5	4	39
6	3	73
7	0	139
8	0	154
9	0	182
10	0	143
11	0	108
12	0	72
13	0	38
14	0	21
15	0	6
16	0	3
17	0	2
18	0	1
Ave # of ERSEs found:	0.94	9.01

Fold Enrichment: 9.62

C. ERSEII

Ave$_{Genome}$ fold enriched 8.41 Ave$_{ATF6}$

■ Genome   □ ATF6-Regulated

# of Searches vs # of ERSEIIs found

D. ERSEII Totals

# of ERSEIIs Found	Genome Searches	ATF6-Regulated Searches
0	500	0
1	336	3
2	127	16
3	29	59
4	4	122
5	4	196
6	0	233
7	0	169
8	0	118
9	0	54
10	0	23
11	0	6
12	0	1
13	0	0
Ave # of ERSEIIs found:	0.71	6.00

Fold Enrichment: 8.41

E. UPRE

Ave$_{Genome}$ fold enriched 2.10 Ave$_{ATF6}$

■ Genome   □ ATF6-Regulated

# of Searches vs # of UPREs found

F. UPRE Totals

# of UPREs Found	Genome Searches	ATF6-Regulated Searches
0	35	0
1	110	1
2	199	3
3	235	7
4	173	46
5	137	133
6	64	209
7	23	210
8	14	203
9	8	115
10	1	47
11	1	23
12	0	3
13	0	0
Ave # of UPREs found:	3.34	7.02

Fold Enrichment: 2.10

Figure 10. ATF6-MER TG Mouse Microarray is Enriched in Genes with ERSEs, ERSEIIs and/or UPREs.

To determine the enrichment of the numbers of ERSEs in the ATF6-regulated gene list, a bootstrapping analysis was performed, as described in the Methods. The number of times these elements were found in each search was plotted as a function of the number of searches, resulting in a representation of the frequency with which each was found in the whole genome **(Panels A, C and E, black bars)** and in the ATF6-regulated gene list **(Panels A, C and E, white bars)**. The data used to generate each bar graph are shown in the tables in **Panels B, D and F**. For example, 417 of 1,000 searches of the whole genome resulted in the identification of zero ERSEs **(row 1, Panel B)**. The average number of times each element was found per search (i.e. average frequency) is shown as Ave$_{Genome}$ and Ave$_{ATF6}$. The average frequency with which each element was found in the ATF6-regulated gene list was divided by the average in whole genome, and defined as the fold-enrichment of the array.

8.   ATF6 Immunoprecipitations:

We wished to further investigate the dynamics of the 3xflag-ATF6-MER fusion protein activation upon tamoxifen treatment. First, we assessed the presence of the ATF6 fusion protein by immunoprecipitating cardiac tissue extracts from NTG and TG mice. NTG and TG mice were treated with tamoxifen, hearts were extracted, and protein lysates were generated. Lysates were immunoprecipitated with an anti-flag antibody, which should detect the flag-tagged ATF6-MER fusion protein only from the hearts of TG mice. Immunoprecipitates were subjected to SDS-PAGE and then probed with an anti-flag antibody to detect the presence of the fusion protein. As shown in **Fig. 11A**, there is no band detected in the NTG sample from the input, non-immune IP, or flag IP fractions, while a band corresponding to 3xflag-ATF6-MER was detected in the input and flag IP fractions from the TG mice (unpublished data, manuscript in preparation).

To confirm that the endogenous, active N-terminal form of the ATF6 protein could be successfully immunoprecipitated and probed for binding to a promoter regulatory region of interest, HeLa cells were treated with the typical ER stressor, tunicamycin, which stimulates cleavage and mobilization of the N-terminal form of ATF6 to act as a transcription factor. Cells were then subjected to paraformaldehyde crosslinking and chromatin immunoprecipitation using an anti-ATF6 antibody, which recognizes the active, N-terminal portion of ATF6 (Santa Cruz, catalog # SC-22799). Crosslinking was reversed, and DNA was purified and analyzed by standard polymerase chain reaction (PCR) using primers which overlap the canonical ERSE in the human GRP78 5' regulatory region, proximal to the ATG start site. ATF6 has been

shown to bind to this ERSE region of the GRP78 promoter.[64] As shown in **Fig. 11B**,

there was no PCR band detected in control cells, while cells subjected to TM

displayed a band corresponding to the ERSE region of the GRP78 promoter

(unpublished data, manuscript in preparation).
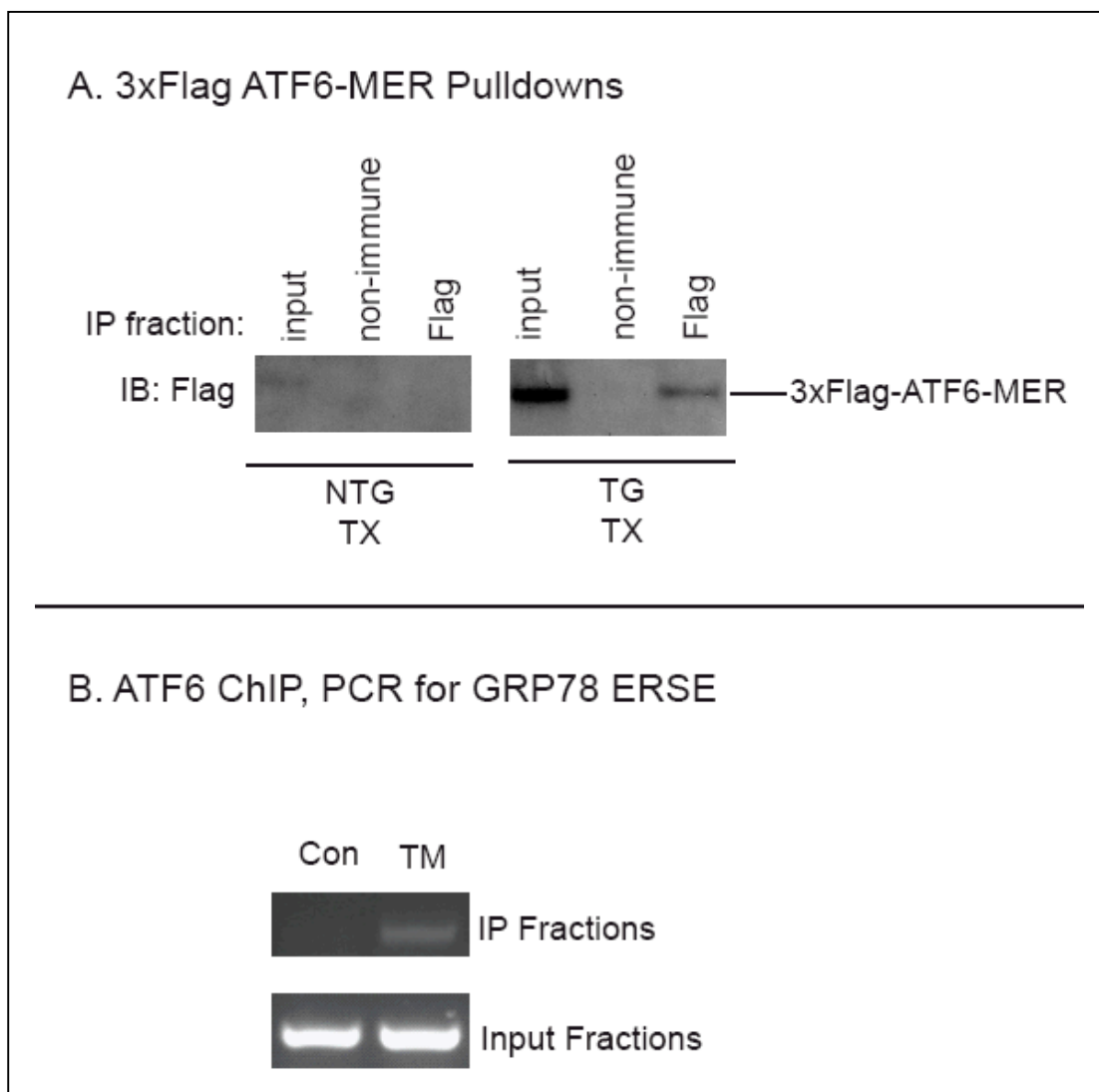
Figure 11. 3xFlag ATF6-MER Pulldowns and Chromatin Immunoprecipitations.

Panel A: NTG and TG mice were treated with tamoxifen, which activates the 3xflag-ATF6-MER protein as a transcription factor only in TG mice. Hearts were extracted, and cardiac protein lysates were immunoprecipitated with anti-flag antibody. Immunoprecipitates were analyzed by SDS-PAGE followed by immunoblotting for Flag. Shown is the band which corresponds to the 3xflag-ATF6-MER protein. **Panel B:** HeLa cells were subjected to control conditions (10% FCS) or 10 μg/μl TM in 10% FCS for 16h. Cells were cross-linked with paraformaldehyde and lysed. Lysates were subjected to a chromatin immunoprecipitation protocol, and immunoprecipitated with an anti-ATF6 antibody, which detects endogenous, active ATF6. Crosslinking was reversed, and DNA was purified and analyzed by PCR using primers which overlap the proximal ERSE in the GRP78 5' flanking promoter region.

9.   Confirmation of ATF6 Binding to Promoter Element Regions, *In Vivo:*

To query whether activated ATF6-MER can bind in the vicinity of putative ER stress response elements in the promoter regions of target genes *in vivo*, we utilized chromatin immunoprecipitation (ChIP), followed by qRT-PCR, also known as quantitative ChIP (qChIP). NTG or TG mice were treated with tamoxifen, which activates the transcriptional activity of ATF6-MER, only in TG mice. Hearts were then extracted, flash-frozen, and cardiac tissue was used for chromatin immunoprecipitations. Briefly, ~30 µg of cardiac tissue was minced, incubated with paraformaldehyde to cross-link proteins and DNA, and then sonicated to fragment any large pieces of DNA stuck to protein. Samples were then immunoprecipitated for the flag-tagged ATF6-MER protein, using an anti-flag antibody. Cross-linking was reversed, and DNA was purified and then analyzed for the presence of specific promoter regions of genes of interest using qRT-PCR primers designed to overlap specific regions in these promoters which contain ER stress elements. It was then determined whether TG samples exhibited a significant increase in signal for each of the promoter regions tested over NTG samples, which do not contain the flag-tagged ATF6-MER protein, and thus represent a level of non-specific, background binding inherent in the chromatin immunoprecipitation process.

Since ATF6 has been shown to bind with high affinity to ERSEs and ERSEIIs, and relatively little to UPREs,[24] it was expected that ATF6 would display high relative binding to ERSEs and ERSEIIs, compared to UPREs, as determined by qChIP. As shown in **Fig. 12**, ATF6 does indeed show elevation of relative binding in TG vs NTG samples, for ERSE- and ERSEII-containing regions, and displays little if any elevation

of binding to regions containing UPREs. In addition, as a control, ATF6 binding to the

GAPDH gene, which does not contain any ER stress response elements, was assessed,

and enriched binding was not seen **(Fig 12A, GAPDH)** (unpublished data, manuscript

in preparation). Thus, this qChIP technique confirms enriched binding of ATF6 to the

promoter regions of known or putative ER stress genes, and provides a powerful tool

for assessing the level of ATF6 binding to promoter regions of genes of interest.
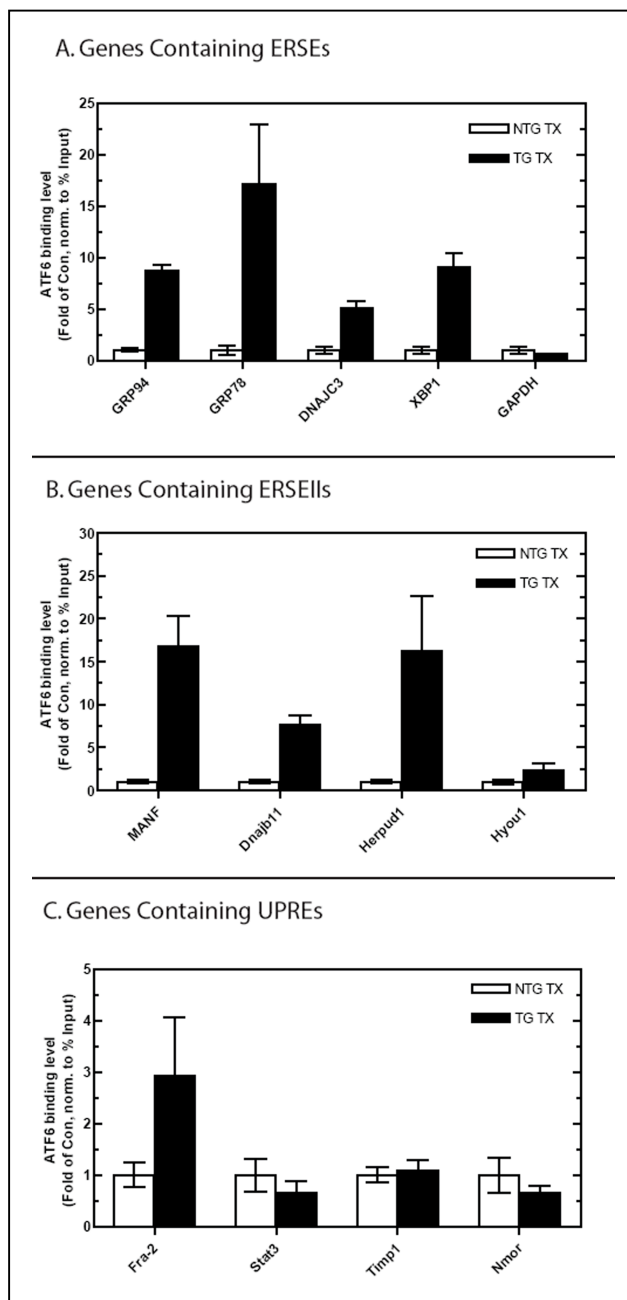
Figure 12. Quantitative ChIP assays: ATF6 binds to ER stress response element regions.

NTG and TG mice were treated with tamoxifen, which activates the 3xflag-ATF6-MER protein as a transcription factor only in TG mice. ChIP assays were performed with flag antibody, and immunoprecipitated DNA was purified. Primers used for qRT-PCR were designed to amplify regions containing the ERSE **(Panel A)**, ERSEII **(Panel B)** or UPRE **(Panel C)** within the promoter regions of the genes analyzed. Shown are the mean -/+ S.E. for each target gene (n=2 mice per treatment). *_p<0.05 different from all other values for each target gene.

10.   Identification of Potential Protective ATF6-Regulated Genes:

To identify potentially novel, protective ATF6-regulated genes from our array for further study, we considered two possible sets of genes. The first set contains genes which have been well-characterized in the cardiac context, but have not been characterized as ER stress response genes. From this set, we decided to focus on regulator of calcineurin 1 (RCAN1), also known as *modulatory calcineurin-interacting protein 1* (*MCIP1*) **(entry 33 in Table 1)**. This gene is of particular interest, because it regulates calcium/calcineurin A-mediated growth and development in numerous tissue types.[65] When activated by calcium, the cytosolic phosphatase, calcineurin A, dephosphorylates nuclear factor of activated T cells (NFAT), which translocates to the nucleus and activates genes that contribute to growth [42]. RCAN1 binds to and inhibits calcineurin A, thus modulating NFAT-mediated growth under certain conditions [66,67]; however, little is known regarding RCAN1 and ER stress response signaling. A detailed description of RCAN1 and its role in the integration of hypertrophic and ER stress response signaling is included as **Part B** of the Results.

The second group of genes considered was those that have known ER stress response properties, but are not well-known in the cardiac context. From this list, we chose degradation in endoplasmic reticulum protein 3 (Derl3) for further analysis, because while it has been characterized as a potential mediator of ER-associated degradation, its role in the heart is unknown. A detailed description of Derl3 and its role in enhancing ERAD and in turn providing cardioprotection is included as **Part C** of the Results.

B.   Characterization of RCAN1 as an ATF6-Regulated ER Stress Response Gene

As shown in **Part A** of the Results, RCAN1 was upregulated in our ATF6 whole-genome microarray (see **Table 1 entry 33**). While RCAN1 is known to play a role in modulating NFAT-mediated growth, the role of RCAN1 in ER stress response signaling had not been studied, and RCAN1 had not been previously identified as an ATF6-regulated gene. Because of its wide range of effects in many different cell types, we used cultured cardiac myocytes as a cell model to determine whether RCAN1 is an ATF6-inducible ERSR gene and whether it modulates growth when induced by ATF6.

1.   Induction of RCAN1 mRNA by ER Stressors:

When NRVMCs were treated with the prototypical ER stressor, tunicamycin, which inhibits ER protein glycosylation, RCAN1 mRNA increased by about 8-fold **(Fig. 13A, bars 1 and 2)**, similar to previous findings for GRP78 induction in NRVMCs.[35] Simulated ischemia (sI), which activates ER stress and induces GRP78 in the heart and in NRVMCs,[20,35,68] increased RCAN1 mRNA in NRVMC by about 3-fold **(Fig. 13, bar 3)**. However, when sI was followed by simulated reperfusion (sI/R), RCAN1 mRNA levels returned to control values **(Fig. 13A, bar 4)**, which was also previously observed for GRP78.[35]. These results demonstrated that RCAN1 is induced by ER stress in NRVMCs.

2.   Induction of RCAN1 Promoter by ATF6:

Since ATF6 is activated by tunicamycin and is a transcriptional inducer of ERSR genes, the effect of overexpressing the constitutively active, N-terminal

fragment of ATF6 on the RCAN1 promoter was examined. Infecting NRVMC with
recombinant adenovirus encoding activated ATF6 (AdV-ATF6) activated the RCAN1
promoter by about 5-fold, compared to a control strain of adenovirus (AdV-Con) **(Fig.
13B, bars 1 and 2)**. However, when a putative ERSE, located between positions -329
to -311 of the RCAN1 promoter, was mutated, promoter activation by ATF6 was lost
(Fig. 13B, bar 3). Tunicamycin also induced the native RCAN1 promoter by about 2-
fold; this induction was also lost when the putative ERSE was mutated, or when cells
were infected with recombinant adenovirus encoding a dominant-negative form of
ATF6 (AdV-DN-ATF6) **(Fig. 13B, bars 4-6)**. Thus, the RCAN1 promoter is
activated in cultured cardiac myocytes by ATF6 or tunicamycin through an ERSE
similar to that observed in previously characterized ERSR genes, including *GRP78* [69].
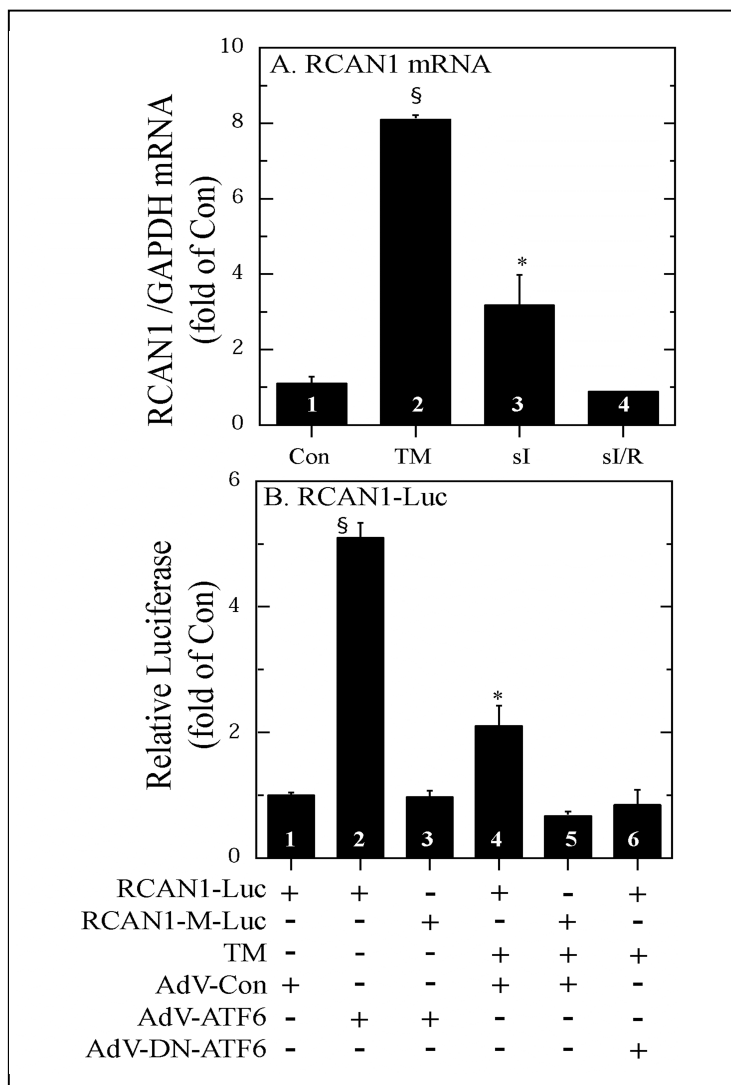
Figure 13. Effect of various treatments on RCAN1 mRNA and RCAN1 promoter activity in cultured cardiac myocytes.
Panel A: NRVMCs were treated -/+ tunicamycin (TM, 10 μg/ml, bar 2) for 16 h, or subjected to sI for 24 h (bar 3), or sI for 20 h followed by simulated reperfusion for 20 h (sI/R, bar 4); RNA was isolated from culture extracts and subjected to RT-qPCR to determine the levels of RCAN1 and RCAN1 mRNAs. The primers used for RCAN1 were designed to amplify a region of exon 4. Shown are the mean values of RCAN1/GAPDH mRNA, expressed as the fold of control. **Panel B:** The human RCAN1 gene promoter (-984 to+30 of the region located to the 5' of exon 4) and a version harboring a mutation in a putative ERSR element located at -329 to -311 (RCAN1-M), were cloned into a luciferase expression construct. NRVMC were transfected with RCAN1-luciferase or RCAN1-M-luciferase and CMV-β-galactosidase and then infected with AdV-Con, AdV-ATF6, or AdV-DN-ATF6. 24 h after infection, cultures were treated -/+ TM, as shown and as described in panel A. 16 h later, cultures were extracted and luciferase and β-galactosidase reporter enzyme activities were determined. AdV-DN-ATF6 alone had no effect on RCAN1- luciferase, or RCAN1-M-luciferase activation (not shown). Shown are the mean relative luciferase (luciferase /β-galactosidase), expressed as the fold of control.

3. Effect of ATF6 on Calcineurin Activity and Genetic Markers of Myocyte Growth:

The α1-adrenergic receptor agonist, phenylephrine (PE), activates the calcineurin/NFAT signaling in NRVMCs (30), but is not known to activate ER stress (31). Accordingly, we examined the effects of ATF6 on the activation of calcineurin by PE. PE conferred an approximate 3-fold increase in calcineurin activation, as expected; however, calcineurin activation was completely blocked by AdV-ATF6 **(Fig. 14A)**. We also examined the effects of activated ATF6 on two well characterized, NFAT-inducible genes, *atrial natriuretic peptide* (*ANP*) and *B-type natriuretic peptide* (*BNP*). PE treatment of AdV-Con-infected cells increased ANP and BNP and RCAN1 mRNA by 8- and 4-fold, respectively **(Fig. 14B and C, bars 1 and *2*)**. In contrast, AdV-ATF6 decreased the effects of PE on *ANP* and *BNP* gene expression **(Fig. 14B and C, bar 3)**. These results are consistent with the hypothesis that ATF6 induces *RCAN1*, which in turn, inhibits calcineurin phosphatase activity, as well as calcineurin/NFAT-mediated *ANP* and *BNP* gene induction.

Since RCAN1 can inhibit calcineurin-mediated NFAT gene induction, we examined the effects of activated ATF6 on two well characterized, NFAT-inducible genes, *atrial natriuretic peptide* (*ANP*) and *B-type natriuretic peptide* (*BNP*). Accordingly, NRVMC were treated with the α$_1$-adrenergic agonist, phenylephrine (PE), which activates calcinuerin/NFAT signaling in NRVMC [70], but is not known to activate ER stress [71]. PE treatment of AdV-Con-infected cells increased ANP, BNP and RCAN1 mRNA by 8-, 4-, and 3-fold, respectively **(Fig. 14A-C, bars 1 and 2)**. In contrast, AdV-ATF6 decreased the effects of PE on ANP and BNP mRNA, while augmenting the effects of PE on RCAN1 mRNA **(Fig. 14A-C, bar 3)**. These results

are consistent with the hypothesis that ATF6 induces RCAN1, which in turn inhibits

calcineurin/NFAT-mediated *ANP* and *BNP* gene induction.
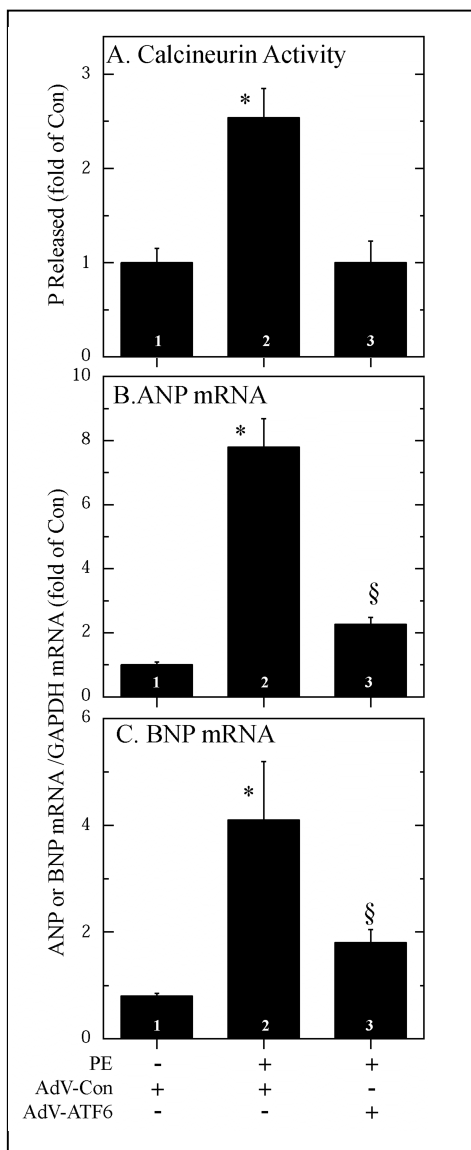
Figure 14. Effect of phenylephrine on calcineurin phosphatase activity, and on ANP and BNP induction.

NRVMC were infected with AdV-Con or AdV-ATF6, and 24 h later, cultures were treated ± PE (50 μM) for 48 h. Cultures were then examined for calcineurin activity (*panel A*), *ANP* mRNA (*panel B*), or *BNP* mRNA (*panel C*). Shown are the mean values of calcineurin phosphatase activity, or for *ANP* or *BNP* mRNA/GAPDH mRNA expressed as the -fold of control (*bar 1*) ± S.E. for each treatment (n = 3 cultures per treatment). * and §, $p \leq 0.05$ different from all other values.

4. Effect of RCAN1 siRNA on Hypertrophic Markers in Response to Growth Stimuli:

To determine whether RCAN1 was responsible for the effects of ATF6 on

ANP and *BNP* induction, NRVMC were treated with RCAN1 siRNA. In preliminary

experiments, we showed that RCAN1 mRNA/GAPDH mRNA decreased significantly

($p < 0.01$) from $100 \pm 7\%$ to $39 \pm 8\%$ (ave $\pm$ SE) in cells treated with control siRNA,

or RCAN1 siRNA, respectively. As expected, the control siRNA had no effect PE-

mediated *ANP* and *BNP* induction, or the ability of ATF6 to modulate this induction

(Fig. 15A and B, bars 1-3). However, the modulating effect of ATF6 on *ANP* and

BNP induction was attenuated significantly, albeit, not completely, in cells transfected

with RCAN1 siRNA **(Fig.15A and B, bar 4)**. These results are consistent with the

hypothesis that ATF6-mediated modulation of *ANP* and *BNP* gene induction is

mediated partly by RCAN1.
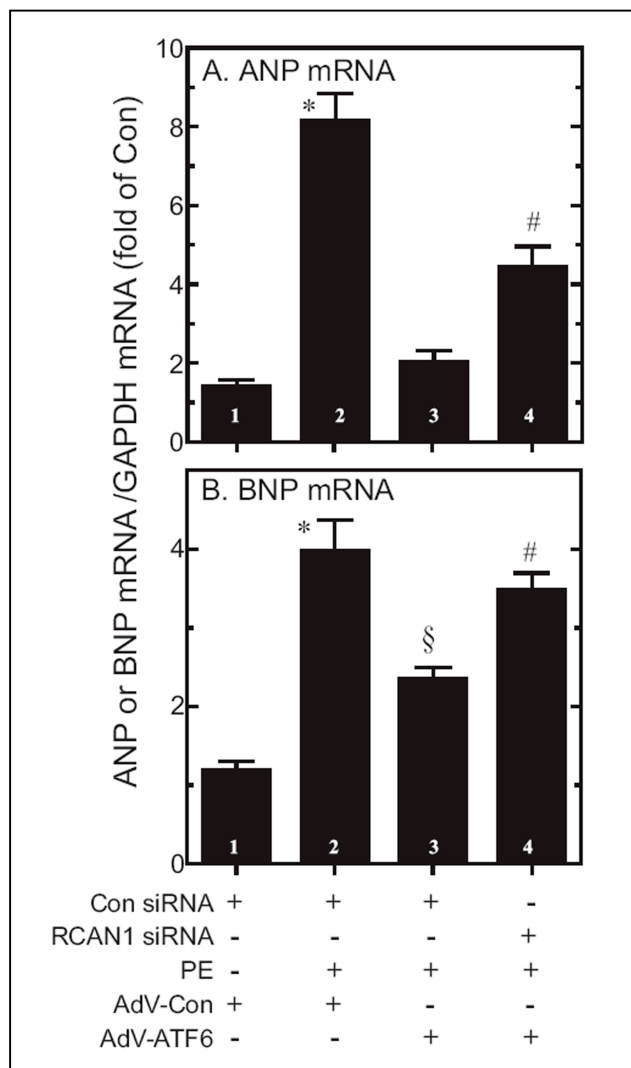
Figure 15. Effect of RCAN1 siRNA and activated ATF6 on ANP and BNP gene induction by phenylephrine.

NRVMCs were transfected with either control siRNA (*Con siRNA*) or *RCAN1* siRNA, and then infected with AdV-Con or AdV-ATF6. 24 h later, cultures were treated ± phenylephrine (50 μM) for 24 h. Cultures were then extracted and *ANP* **(Panel A)**, or *BNP* **(Panel B)** mRNA levels were determined by RT-qPCR. Shown are mean values of each target geneGAPDH mRNA, expressed as the -fold of control (*bar 1*) ± S.E. for each treatment (*n*=3 cultures per treatment). * and §, *p*<0.05 different from all other values.

5.   Effect of ATF6 on Cell Size and Protein Synthesis in Response to Growth Simuli:

NRVMC do not divide in culture, and in this way, they mimic cardiac myocytes in the adult myocardium. Growth factors, such as PE, induce increased cell size, which mimics hypertrohic growth, and increased protein synthesis, both of which are known to be mediated in large part by calcineurin/NFAT signaling [72,73]. Accordingly, the effects of ATF6 on myocyte size and protein synthesis were examined in NRVMC. As expected, in AdV-Con-infected cells, PE increased myocyte area, which serves as a measure of hypertrophic growth **(Fig. 16A, B and E, bars 1 and 2)**. PE also increased the incorporation of ^{3}H-leucine into cellular protein, which serves as an indirect estimate of protein synthesis **(Fig. 16F bars 1 and 2)**. The effects of PE on cell size **(Fig. 16C and E, bar 3)** and ^{3}H-leucine incorporation **(Fig. 16F, bar 3)** were reduced by AdV-ATF6. However, RCAN1 siRNA relieved these effects of ATF6, suggesting that RCAN1 was responsible for ATF6-mediated growth modulation in cultured cardiac myocytes.
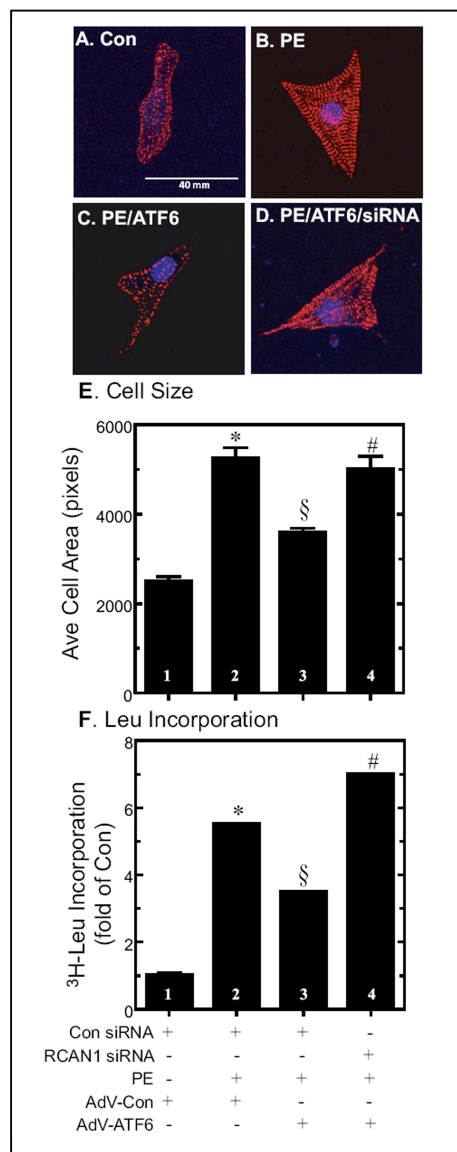
Figure 16. Effect of activated ATF6, RCAN1 siRNA, and phenylephrine on cardiomyocyte area and [³H]leucine incorporation into protein.

Panels A-D: NRVMC were transfected with control siRNA or RCAN1 siRNA, infected with AdV-Con or AdV-ATF6, and treated_PE. Cultures were then fixed and immunostained for α-actinin protein (*red*) and the nuclei were identified using TOPRO-3 (*blue*). Fluorescence confocal micrographs show samples of cells after exposure to each treatment. **Panel E:** cell images obtained from micrographs similar to those shown in A–C were quantified densitometrically for area, $n > 250$ cells counted for each treatment; each treatment was carried out on 3 different cultures. Shown is the mean of the relative cell area -/+S.E., normalized to the control, which was set at 100% (*n*=3 cultures per treatment). **Panel F:** cells were cultured and treated as described in A–D, except they were incubated with [³H]leucine and the amount of radiolabel incorporated into trichloroacetic acid-precipitable protein was examined, Shown is the mean -/+ S.E. of labeled protein, normalized to the control. $n = 3$ cultures/treatment/experiment. *, §, and #, $p < 0.05$ different from all other values.

6.   Conclusions:

Because of the widespread importance of NFAT as a regulator of growth and development in essentially all tissue types,[65] we focused on RCAN1 as one of the genes through which ATF6 might exert its growth-regulating effects. We found that activated ATF6 induced RCAN1 in cultured cardiac myocytes in a manner that required a putative ERSE located in the regulatory region of the RCAN1 gene. Moreover, ATF6 modulated NFAT-mediated gene expression and cell growth, both of which were shown to be partially dependent upon RCAN1. Taken together, these results show that ATF6 exerts growth modulating effects in cardiac myocytes, and the ATF6-inducible, ERSR gene, RCAN1, is responsible for a portion of this growth modulation. Therefore, RCAN1 may contribute to the protective effects of ATF6 by modulating NFAT-regulated growth and reducing the protein synthesis load in the ER during ER stress.

C. Characterization of Derl3 as an ATF6-Regulated ER Stress Response Gene

As shown in **Part A** of the Results, Derl3 was among the genes with the most robust up-regulation in our ATF6 whole-genome microarray. While Derl3 has been show to play a role in ER stress and specifically ER-associated degradation in other cell types[74], both the mechanism of Derl3 induction, and its role in the heart, are completely unknown.

Currently, relatively little is known about the effects of misfolded protein aggregation in cardiac myocytes; however, the effects of misfolded or aggregated proteins in other post-mitotic cells, such as neurons and cells of the brain, has been widely studied.[75,76] Like neurons, myocytes are for the most part, post-mitotic cells which are required to undergo repeated cycles of contraction and relaxation throughout the life of the organism, and which depend on a highly ordered sarcomeric structure. Therefore, we hypothesized that myocytes require a strict protein quality control mechanism, which can recognize and target terminally misfolded proteins for degradation. Given the role of Derl3 in ERAD in other cell types, we wished to determine whether Derl3 induction in myocytes could increase protein clearance, and provide protection to myocytes subjected to stress.

1. Promoter Analysis of ATF6-Regulated Genes in the Heart Identifies Derl3:

We previously identified ATF6-regulated genes in ATF6-MER TG mouse hearts.[41] To determine which of the genes from the microarray analyses of ATF6-MER TG mouse hearts might be direct targets of ATF6, the regulatory regions of

each were analyzed for the ATF6 binding sites, ERSE, ERSE-II and UPRE,[22,23,63] as described in **Chapter A** above.

As shown in **Table 2** ("full genome" entries 10 and 17), there are only two genes in the mouse genome with two canonical ERSEs within their 2kb 5' promoter regions, and both of these genes appears on the list of ATF6-regulated genes with ERSEs (**Table 2**, "ATF6-regulated" entries 1and 3). One gene is glucose-regulated protein 94 (GRP94), the well-known ER stress responsive chaperone, and the other is Derlin-3 (Derl3), a member of the Derlin family of proteins, which are thought to play a role in ER-associated degradation (ERAD). Relatively little is known about the regulation of Derl3 or its specific role in the ERAD pathway, and nothing is known about its function in the heart, or whether it could potentially provide protection during cardiac stress due to its role in ERAD. Since it may play a role in ERAD, we investigated the mechanism of induction and the function of Derl3 in the heart and cultured cardiac myocytes.

2.　　Regulation of the Derl3 Promoter by ATF6 and ER Stressors:

To examine transcriptional regulation cultured cardiac myocytes were transfected with several luciferase reporter constructs $\pm$ subsequent infection with either a control (AdVCon) or an adenovirus that encodes activated ATF6 (AdVATF6) **(Fig. 17A-B)**. Luciferase activation in cultures infected with AdVATF6 and transfected with reporter Construct 1 was 200-fold of control **(Fig. 7B, Bar 4)**. ATF6-mediated luciferase induction was reduced by 75 to 80% in Constructs 2 and 3, which each contain one mutated ERSE **(Fig. 17B, Bars 5, 6)**. The ERSR activator,

tunicamycin (TM), conferred robust induction of Construct 1 **(Fig. 17B, Bar 7)**;

however, Constructs 2 and 3 exhibited decreased induction **(Fig. 17B, Bars 8, 9)**.

Thus, maximal ATF6- or TM-mediated induction of the Derl3 promoter was

dependent upon both ERSE1 and ERSE2.
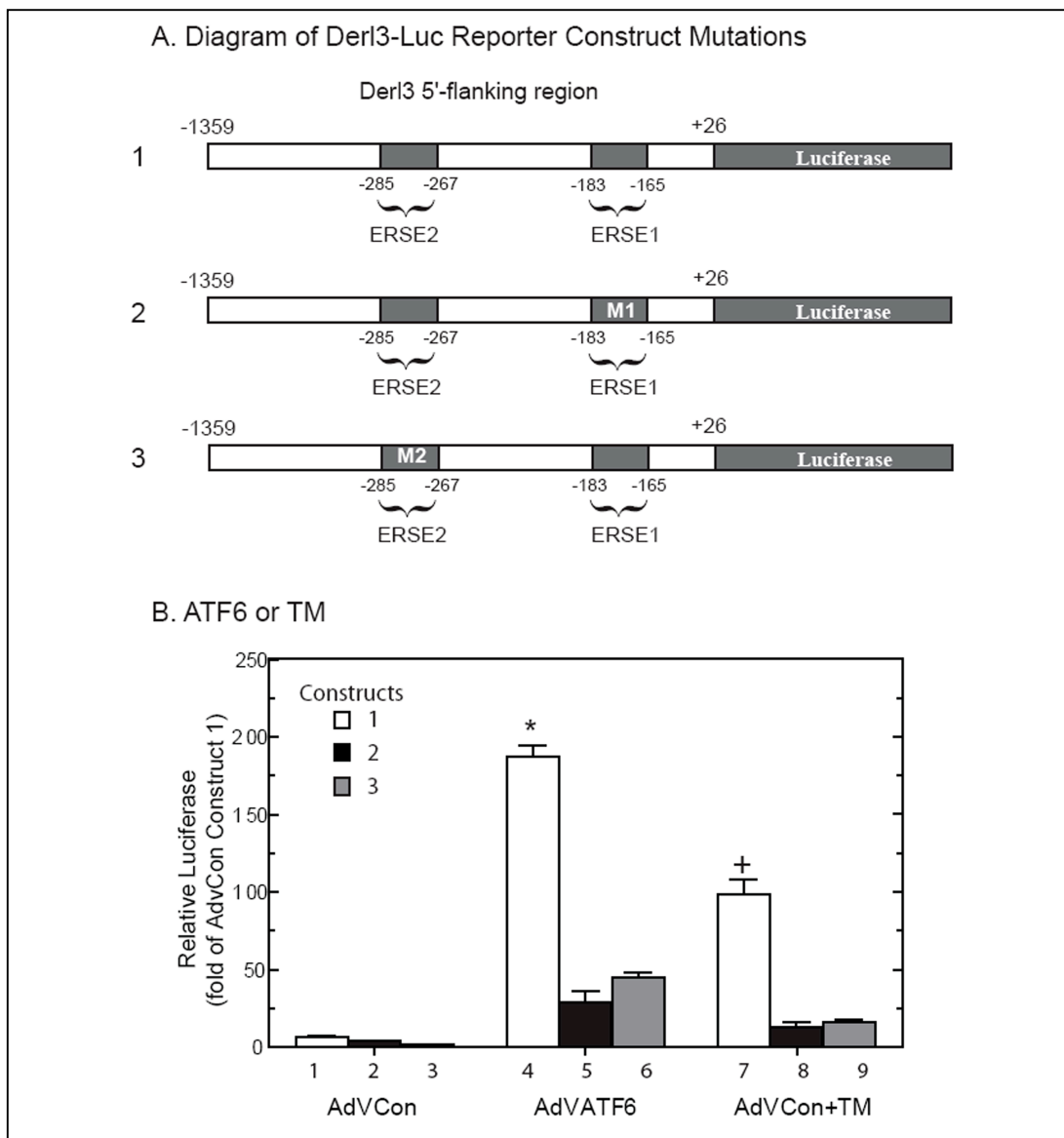
Figure 17. Effect of ATF6 Overexpression and Tunicamycin on Derl3 Promoter Activity in Cultured Cardiac Myocytes.
Panel A: The mouse Derl3 promoter (-1359 to +26, Construct 1) and versions harboring mutations in putative ERSE elements located at either -183 to -165 (Construct 2) or –285 to –267 (Construct 3), were cloned into a luciferase expression construct. **Panel B:** NRVMCs were transfected with luciferase constructs 1, 2, or 3, and CMV-β-gal and then infected with AdV-Con or AdV-ATF6, as previously described [35]. Twenty-four hours after infection, cultures were treated ± TM; 16h later, cultures were extracted and luciferase and β-galactosidase reporter enzyme activities were determined, as previously described [35]. Shown are the mean relative luciferase activities (luciferase/β-galactosidase), expressed as the fold of construct 1 treated with AdVCon (bar 1) ± SE for each treatment (n = 3 cultures per treatment, sum of 3 separate experiments). *, + = $p \leq 0.05$ from all other values by ANOVA.

3.   ATF6 Induces Derl3 in Mouse Hearts:

While neither Derl1 nor Derl2 were induced by tamoxifen in the ATF6 TG mouse hearts **(Fig. 18A, Bars 1-8)**, Derl3 was induced by 400-fold by tamoxifen, but only in the TG mouse hearts **(Fig. 18A, Bars 9-12)**; thus, only Derl3 was ATF6-inducible in the heart, consistent with the lack of ERSEs in the Derl1 and Derl2 genes **(Table 2)**.

Derlin levels were relatively low in sections from vehicle-treated ATF6-MER TG hearts **(Fig. 18B, Derl3)** and tamoxifen-treated NTG mouse hearts (not shown). In contrast, tamoxifen-treated ATF6-MER TG mouse hearts exhibited robust Derl3 expression that co-localized primarily with actin-postive cardiomyocytes **(Fig. 18C, overlay)**. Thus, ATF6 induces Derl3 expression in cardiac myocytes, *in vivo*.
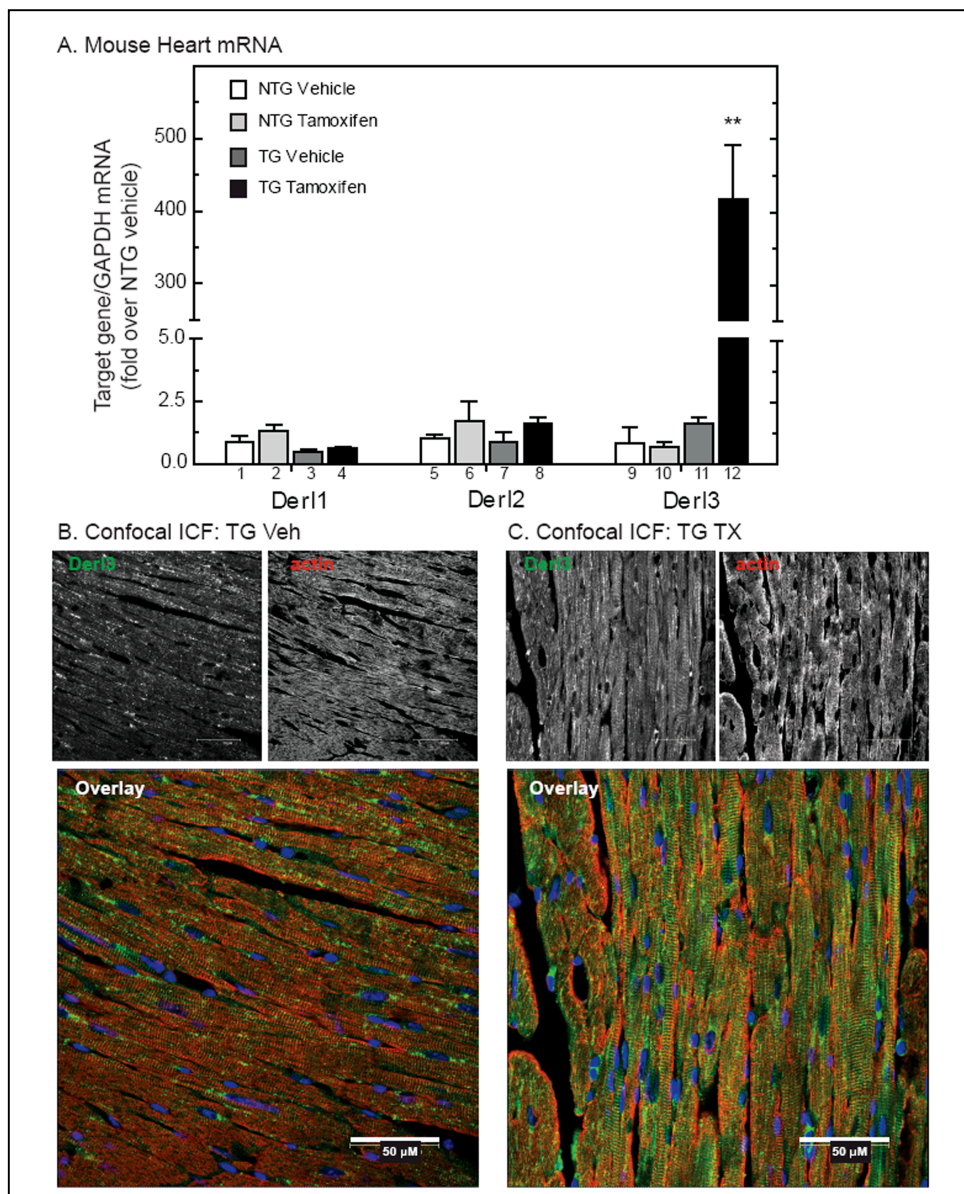
Figure 18. Effect of Activated ATF6 on Derlin Family Member Induction in ATF6-MER TG Mouse Hearts.

Panel A: NTG and ATF6- MER TG mice were treated ± vehicle or tamoxifen, and RNA was extracted from hearts, as previously described [20]. RNA samples were subjected to RT-qPCR to examine the levels of mRNAs for Derl1, Derl2, Derl3, and GAPDH. Shown are the mean values of each target gene/GAPDH mRNA, expressed as the fold of NTG vehicle ± SE for each target gene (n = 3 mice per treatment). TG = ATF6-MER transgenic; NTG = non-transgenic; Veh = vehicle; Tx = tamoxifen. ** = $p \leq 0.01$ from all other values by ANOVA.

Panels B and C: TG mice were treated ± Veh (Panel B) or TX (Panel C), and hearts were sectioned for immunofluorescence confocal microscopy. Sections were co-stained with Derl3 and actin.

4. Derl3 is an ATF6-Inducible ER Stress Response Gene:

The effects of ATF6 or ER stress on Derlin mRNA in cultured cardiac myocytes were examined. Derl3 was the only family member that exhibited ATF6-inducibility, in cultured cardiac myocytes **(Fig. 19A, Bars 1-6)**. When cells were treated with TM, Derl1 and Derl2 mRNA levels were 3- and 8-fold of control, respectively **(Fig. 19B, Bars 2, 6)**; however, neither was affected by dominant-negative ATF6 **(Fig. 19B, Bars 4, 8)**. In contrast, upon TM treatment, Derl3 mRNA was 200-fold of control **(Fig. 19B, Bar 10)**, and this induction was attenuated by more than half by dominant-negative ATF6 **(Fig. 19B, Bar 12)**.

Simulating ischemia (sI) activates ER stress in cardiac myocytes[35]; accordingly, the effect of sI on Derlin expression was examined. While Derl1 and Derl2 have been shown to be inducible by TM in XBP1 knockout MEFs[74], in the current study in NRVMCs, sI had no effect on Derl1, and Derl2 was only slightly increased, but this increase did not reach significance **(Fig. 19C, Bars 2, 6)**. In contrast, sI significantly increased Derl3 to ~2.5-fold of control **(Fig. 19C, Bar 10)**; moreover, sI-mediated Derl3 induction was completely blocked by dominant-negative ATF6 **(Fig. 19C, Bar 12)**, which was different than the partial blockage of Derl3 induction following TM treatment. This could be due to the higher dynamic range of induction experienced with TM, or due to other potential mediators of Derl3 induction during TM but not sI. Thus, Derl1 and Derl2 were induced by the prototypical ER stressor, TM, independently of ATF6. Moreover, only Derl3 was induced by the physiological ER stressor, sI, in an ATF6-dependent manner.
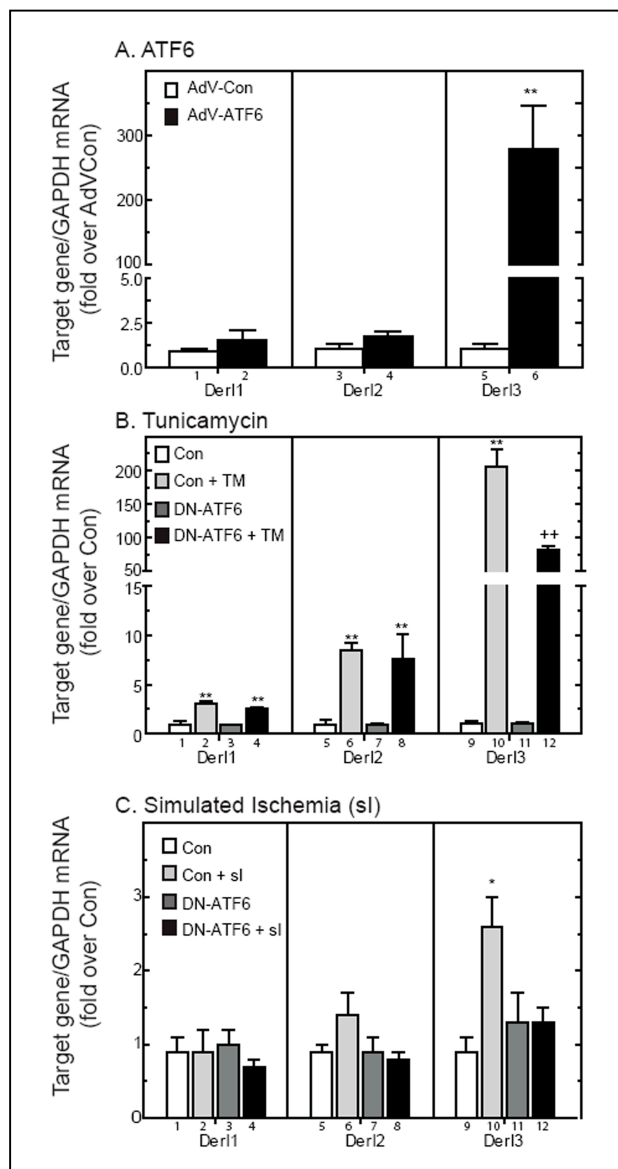
Figure 19. Derl3 mRNA is Induced by ATF6, TM and sI in Cultured Cardiac Myocytes.

Panel A: NRVMCs were infected with either AdV-Con or AdV-ATF6 (n = 3 cultures per treatment). Forty eight hours after infection, cultures were extracted and the RNA was subjected to RT-qPCR to examine the levels of mRNA for the target genes described in Figure 3. Shown are the mean ± SE for each target gene (n = 3 cultures per treatment). * = p≤0.05 different from all other values by ANOVA. **Panels B and C:** NRVMC were infected with either AdV-Con or AdV-DNATF6 (n = 3 cultures per treatment). Twenty four hours after infection, cultures were treated with TM for 16h (10 µg/ml, Panel B) or sI for 20h (Panel C). Cells were extracted and subjected to RT-qPCR to examine the levels of mRNA for the target genes described in Panel A. Shown are the mean ± SE for each target gene (n = 3 cultures per treatment).

5. ATF6 is Activated and Derl3 is Induced in an *In Vivo* Model of Myocardial Infarction:

We previously showed that ER stress is activated in the mouse heart by myocardial infarction (MI).[35] During ER stress, full-length, 90KD ATF6 is converted to 50KD ATF6 which is an active transcription factor.[10,11] Accordingly, the effects of ischemia on ATF6 and Derl3 upon MI were examined, *in vivo*. An MI time course indicated that the 50KD form of ATF6 increased significantly after 16h of MI, remained elevated after 1d and 3d, and decreased at 4d of MI, consistent with activation of ATF6[77] **(Fig. 20 Panels A-B)**. The 50KD band migrated slightly further than a 3xFlag-tagged form of cleaved, N-terminal ATF6, consistent with its identity as cleaved ATF6 **(Figure 21A)**.

Compared to sham, the mRNA levels of all Derl family members increased in 4d MI mouse hearts, , with Derl1 and Derl3 reaching significance, and Derl3 exhibiting the most robust up-regulation of ~6-fold **(Fig. 20C, bars 2, 4, 6).** An MI time course showed that while Derl3 mRNA exhibited a trend of being increased after 1d of MI, it was significantly increased after 4d and 7d of MI **(Fig. 21B)**. The increase in p50 ATF6 by 16h of MI, and the continued elevation after 1 and 3d of MI, were consistent with the possibility that ATF6 could induce Derl3 mRNA as early as 1d after MI. However, since the elevation of p50 ATF6 after 1 and 3d of MI, and the elevated Derl3 mRNA after 1d of MI did not reach statistical significance, it is formally possible that ATF6 activation/inactivation may precede Derl3 induction, suggesting that ATF6 may induce Derl3 expression indirectly. For example, ATF6 is known to induce the ER stress response transcription factor, XBP1, which could induce Derl3. These limitations leave open the question of whether ATF6 directly

induces Derl3 mRNA in the heart, which we intend to investigate in future studies; nonetheless, ATF6 isa potent inducer of Derl3 gene expression in the myocardium.

Derl3 was low in sham mouse hearts **(Fig. 20D, Panel 1)**, but elevated in surviving myocytes in the infarct zone **(Fig. 20E, Panels 1 and 3, Arrow 1)**, as well as other tropomyosin-negative cells, which were most likely non-myocytes **(Fig 20E, Panels 1 and 3, Arrow 2)**. Derl3 staining was perinuclear in the myocytes, consistent with expression in the ER.
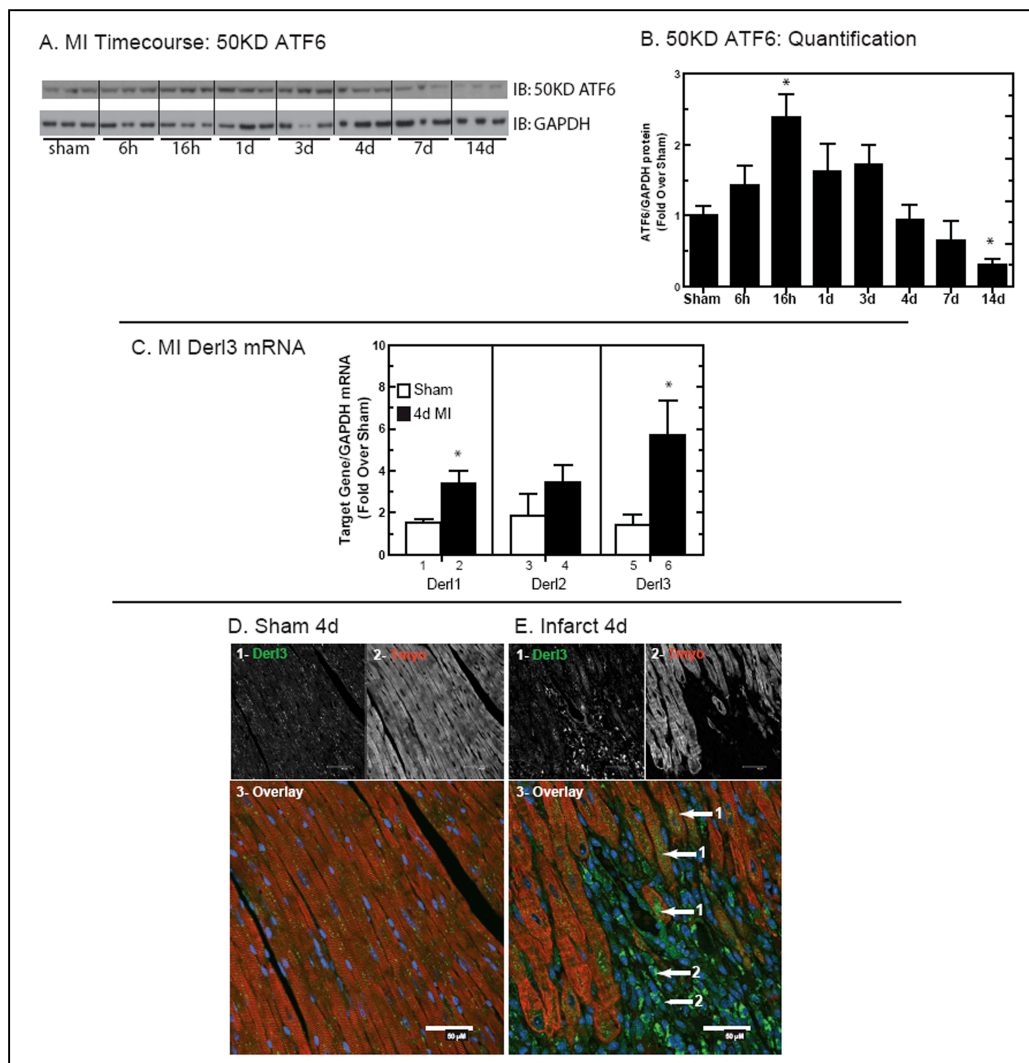
Figure 20. Derl3 is Up-Regulated by Myocardial Infarction in Mouse Hearts.
Panels A-B: NTG mice were subjected to sham infarct surgery or to permanent occlusion myocardial infarction for the indicated times. Animals were sacrificed and hearts were used to prepare tissue extracts for western blot analysis, as previously described,[58] n=3 animals per time point. * = p<0.05 different from sham, determined by two-way T-Test. ***Panel C:*** NTG mice were subjected to sham infarct surgery or to permanent occlusion myocardial infarction for 4d. Animals were then sacrificed and hearts were used to prepare tissue extracts for RT-qPCR, as previously described,[58] sham n = 4; MI n= 7 to 9. * = p≤0.05 different from all other values determined by ANOVA. ***Panels D-E:*** Mice were subjected to surgeries as in Panel C, and then scarified and hearts were sectioned for confocal immunocytofluorescence as previously described,[58] n=3 mice per treatment, one heart/treatment shown in this figure. Heart sections were stained for Derl3 (green) **(1)**, or tropomyosin (red) **(2)**, and an overlay is shown **(3)**. Samples were viewed by laser scanning confocal immunofluorescent microscopy as previously described [35]. Arrows 1 point to Derl3-positive cardiac myocytes in the infarct border zone, and arrows 2 point to Derl3-positive non-myocytes in the infarct zone.
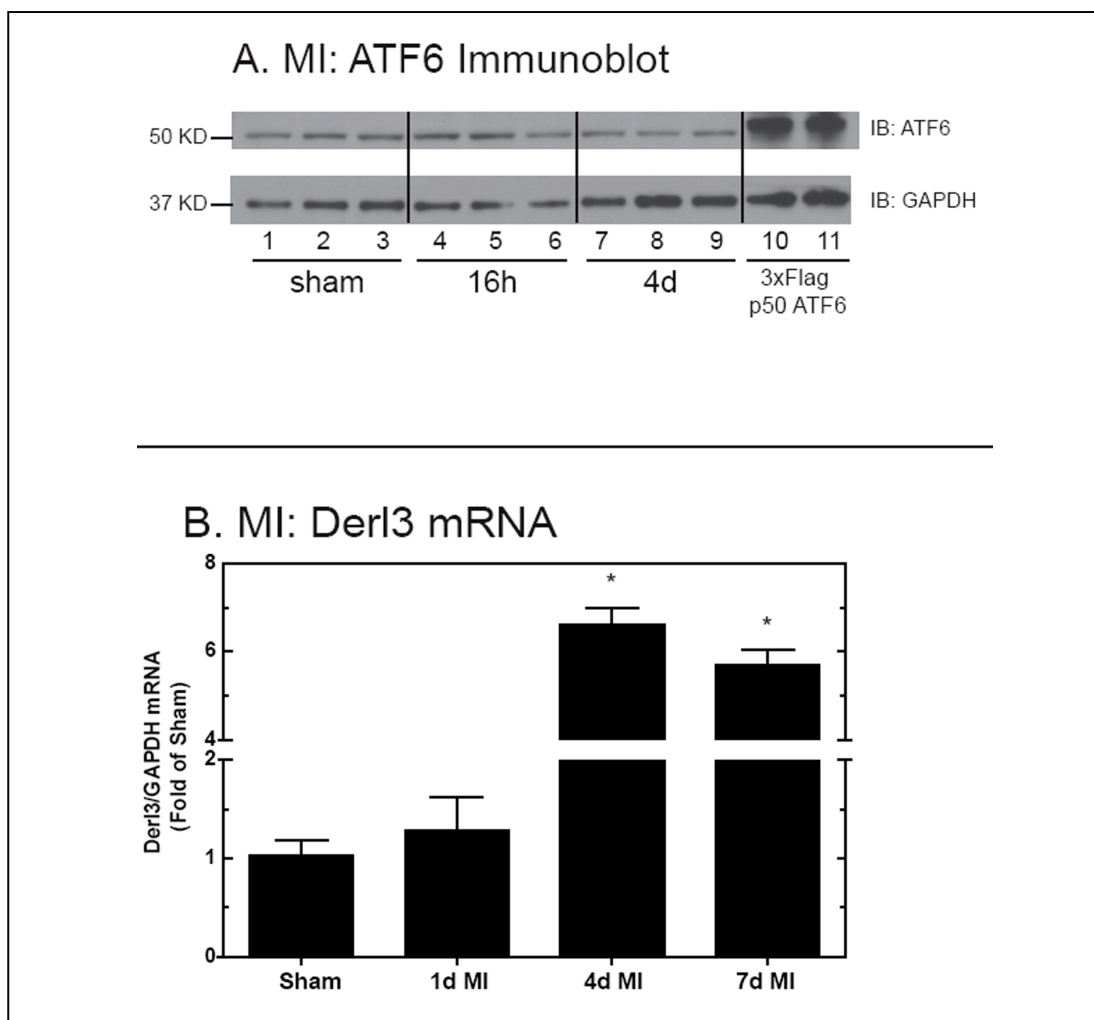
Figure 21. MI Increases 50KD ATF6 and Derl3 mRNA.

Panels A-B: NTG mice were subjected to sham infarct surgery or to permanent occlusion myocardial infarction for the indicated times. Animals were then sacrificed and hearts were used to prepare tissue extracts for western blot analysis, as previously described (lanes 1-9).[58] To confirm the identity of the 50KD band, cell lysates from HeLa cells transfected with a 3xFlag-tagged ATF6 plasmid and subjected to the protease inhibitor ALLN (3mM) in order to preserve the labile, N-terminal form of ATF6, were loaded (lanes 10-11). **Panel C:** NTG mice were subjected to sham infarct surgery or to permanent occlusion myocardial infarction for 1d, 4d, or 7d. Animals were then sacrificed and hearts were used to prepare tissue extracts for RT-qPCR, as previously described.[58] The numbers of animals used for each trial were as follows: sham n = 4; MI n= 7 to 8. * = p≤0.05 different from all other values determined by ANOVA.

6.   Derl3 Protects Cardiac Myocytes from Cell Death:

ERAD reduces ER stress by degrading mis-folded ER proteins; accordingly, the effect of Derl3 on ER stress was examined. Following sI or sI/R, control cells exhibited a significant increase in the prototypical ER stress response proteins, GRP94 and GRP78 **(Fig. 22A Lanes 1-3 vs 7-9 and 11-13; Fig. 22B and 6C, Bars 1, 3, 5)**. In contrast, cells infected withAdV-Derl3 exhibited reduced GRP94 and GRP78 **(Fig. 22A Lanes 4-6, 10-12 and 14-16; Fig. 22B and 6C, Bars 2, 4, 6).** GRP94 and GRP78 mRNA levels were also assessed following sI and sI/R **(Fig. 23, Panels A-B)**. Since neither GRP94 nor GRP78 mRNA levels were elevated following 20h of sI **(Fig. 23 Panels A-B bars 3-4)**, we hypothesized that these mRNAs were increased at shorter times of sI. As indicated in **Figure 23 Panels C and D,** GRP94 and GRP78 mRNAs increased at shorter times of sI, reaching a maximum at 12h, and AdV-Derl3 reduced the induction seen at these sI time points, consistent with the reduced levels of these proteins following sI seen in **Fig. 22A-C**. In addition, sI/R significantly increased GRP78 and GRP94 mRNA in AdVCon infected cells by ~15 and 17 fold, respectively **(Fig. 23A-B bar 5)**. AdVderl3 infected cells exhibited a significant reduction in sI/R mediated GRP78 and GRP94 mRNA **(Fig. 23A-B bar 5 vs 6)**. Together, these results suggest that overexpression of Derl3 attenuated sI- and sI/R-activated ER stress.

Prolonged ER stress activates apoptosis;[10,11,44,78] accordingly, we assessed whether Derl3 overexpression decreased the ER stress-inducible, pro-apoptotic protein, C/EBP homologous protein (CHOP) and caspase-3 activation. AdV-Con cells exhibited ~25- and 5-fold increase in CHOP following sI and sI/R, respectively **(Fig.**

22D Lanes 1-2 vs 5-6 and 9-10; Fig. 22E Bars 1, 3, 5). In contrast, AdV-Derl3 cells

exhibited decreased CHOP induction following sI and sI/R **(Fig. 22D Lanes 3-4, 7-8,**

and 11-12; Fig. 22E Bars 2, 4, 6). sI did not activate caspase-3 in AdV-Con- or

AdV-Derl3-infected cells, which is consistent with the lack of ATP required to

activate caspase during sI **(Fig. 22F Bars 1-2 vs 3-4)**. However, sI/R resulted in a ~2-

fold increase in caspase-3 in AdV-Con-infected cells, which was attenuated in AdV-

Derl3-infected cells **(Fig. 22F Bars 5-6)**. In addition, AdV-Con-infected cells

exhibited a ~2-fold and 3.5-fold increases in cell death following sI and sI/R,

respectively **(Fig. 22G Bars 1 vs 3 and 5)**. In contrast, AdV-Derl3-infected cells

exhibited significantly less cell death in response to sI/R **(Figure 22G Bar 6)**. Thus,

overexpression of Derl3 attenuated ER stress and apoptosis in cardiac myocytes

subjected to these stressors.
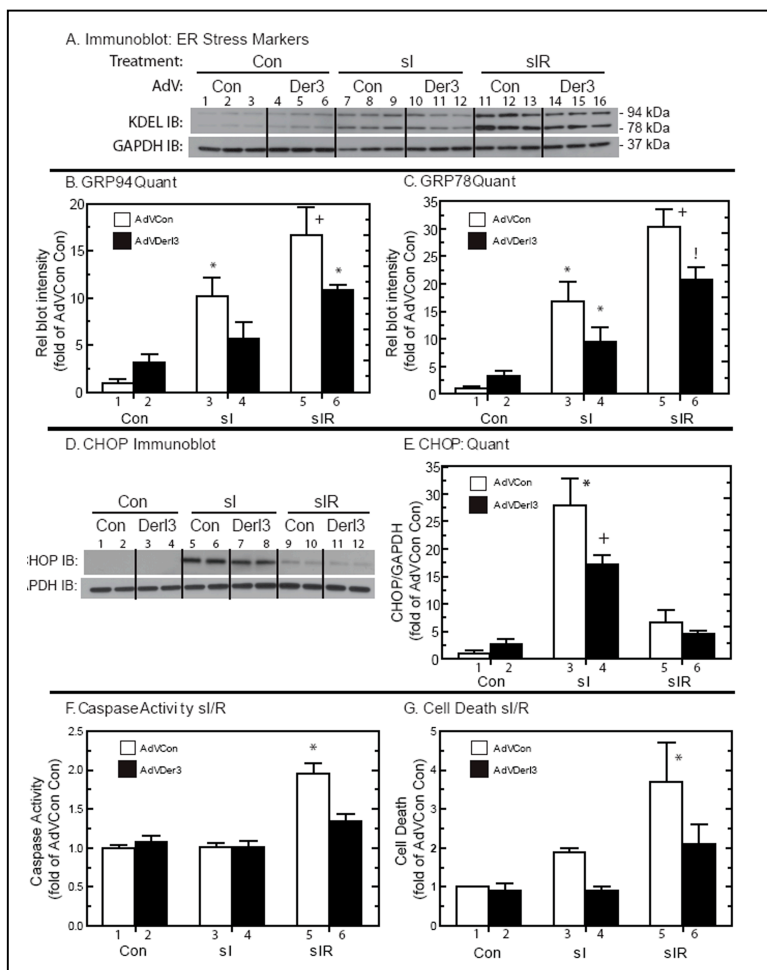
Figure 22. Derl3 Overexpression Attenuates ER Stress Activation, Caspase Activity, and Cell Death Following sI and/or sI/R.

Panels A-C: NRVMCs were infected $\pm$ AdV-Con or AdV-Derl3 and 24h later, cultures were treated $\pm$ sI or sI/R. Cultures were then extracted and cell lysates were analyzed for the levels of the prototypical ERSR proteins, GRP78 and GRP94, using an anti-KDEL antibody (Panel A), as previously described. Panels B and C display the relative blot intensities of each protein/GAPDH, expressed as the fold of control (bar 1) $\pm$ SE for each treatment (n = 3 cultures per treatment). **Panels D and E:** NRVMCs were treated as in Panel A, and cultures were extracted and analyzed for the levels of CHOP using an anti-CHOP antibody in Panel D and quantified in Panel E. **Panel F:** NRVMCs were treated as in Panel A. Cultures were then assayed for caspase-3 activation, as described in the Methods. **Panel G:** NRVMCs were treated as in Panel A. Cultures were then stained with Hoescht and propidium iodide, and images of 5 randomly chosen fields per culture were viewed at 10x magnification on a fluorescent microscope. The numbers of Hoescht-positive (total) cells and propidium iodide-positive (dead) cells were then quantified using NIH ImageJ software (n = 3 cultures per treatment, sum of 3 separate experiments). Shown is the relative amount of cell death, expressed as fold of AdVCon Con, $\pm$ S.E for each treatment. For all panels, *, +, ! = p$\leq$0.05 different from all other values by ANOVA.
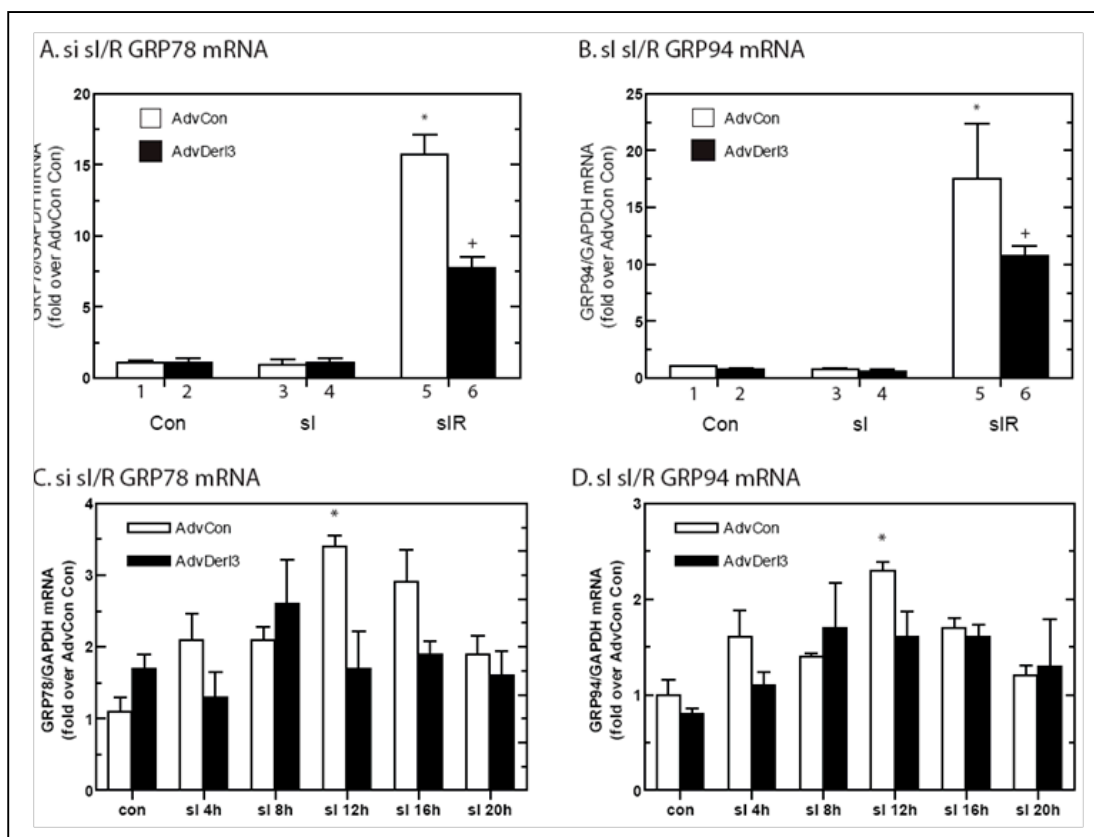
Figure 23. Derl3 Overexpression Attenuates ER Stress mRNA Activation Following sI and sI/R.

NRVMCs were infected $\pm$ AdVCon or AdV-Derl3 and 24h later, cultures were treated $\pm$ sI for 20h followed by sI/R for 24h **(Panels A and B)**, or $\pm$ sI for the indicated times **(Panels C and D)**. Cultures were then extracted and cell lysates were analyzed for the levels of the prototypical ERSR mRNAs, GRP78 and GRP94 (n = 3 cultures per treatment, sum of 2 separate experiments). Shown is the relative amount of each target mRNA/GAPDH, expressed as fold of AdVCon Con, $\pm$ S.E for each treatment. Panels A-B: *,+ = p<0.05 different from all other values by ANOVA, Panels C-D: * = p<0.05 from AdVCon Con by ANOVA.

7.   Derl3 Enhances ERAD and Reduces ER Stress:

The effect of Derl3 on ERAD was examined using a mutant form of the alpha-1 antitrypsin protein (A1ATmut), which is constitutively mis-folded in the ER,[79]. HeLa cells were co-transfected with plasmids expressing A1ATmut and Derl3-encoding plasmid. Derl3 overexpression decreased A1ATmut **(Fig. 24A and B)**, indicating that Derl3 augmented clearance of mis-folded proteins in the ER during ERAD.

The effect of A1ATmut overexpression on ER stress was determined by measuring GRP78 promoter activation. Cells were transfected with plasmids expressing a GRP78-luciferase promoter and A1ATwt, which folds properly or A1ATmut. While A1ATwt had no effect, promoter activity was ~2-fold of control in cells transfected with A1ATmut **(Fig. 24C Bars 2, 3)**. Moreover, co-transfecting Derl3 decreased A1ATmut-mediated GRP78 promoter activation **(Fig. 24C Bars 3 vs 5)**. Thus, Derl3 enhanced the removal of A1ATmut and, in so doing, decreased ER stress.
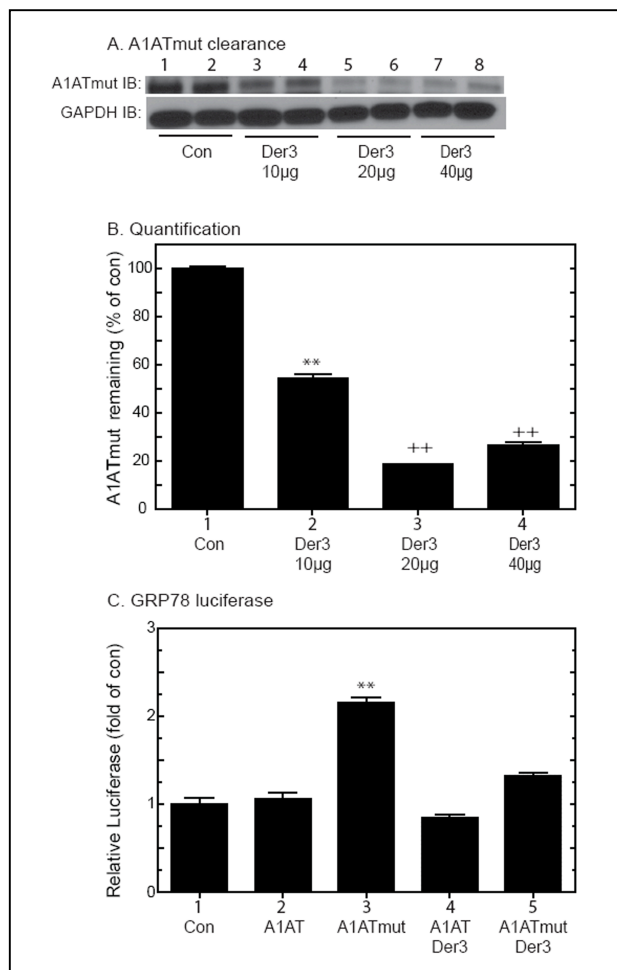
Figure 24. Derl3 Overexpression Enhances Mis-folded Protein Clearance and Attenuates ER Stress Activation.

Panels A-B: HeLa cells were co-transfected with plasmids encoding mutated α-1 antitrypsin (A1ATmut) along with either an empty vector, or increasing concentrations of a plasmid expressing Derl3. Forty eight hours later, cultures were extracted and lysates were analyzed for A1ATmut by immunoblot. Shown are the relative blot intensities of A1ATmut/GAPDH, expressed as the fold of control (bar 1) ± SE for each treatment (n = 3 cultures per treatment). **, ++ = p≤0.01 different from all other values by ANOVA. **Panel C:** NRVMCs were transfected with a GRP78 promoter/luciferase construct and CMV-β-gal as described previously[35], along with plasmids encoding A1ATwt or A1ATmut and Derl3. Forty eight hours later, cells were extracted and luciferase and β-galactosidase reporter enzyme activities were determined, as previously described[35]. Shown are the mean relative luciferase (luciferase/β-galactosidase), expressed as the fold-of-control (bar 1) ± SE for each treatment (n = 3 cultures per treatment, sum of 3 separate experiments). ** = p≤0.01 different from all other values by ANOVA.

8.   Derl3-DN and miDerl3 Enhance sI/R Mediated Cardiac Myocyte Cell Death:

An expression construct encoding an inactive, dominant-negative (DN) form of Derl3 was designed based on previous studies using Derl1 and 2 dominant-negative constructs.[80] HeLa cells were transfected with A1ATmut, and control, Derl3 or Derl3-DN plasmids. Derl3 conferred an approximate 70 percent reduction in the level of A1ATmut, while Derl3-DN did not significantly change the levels of A1ATmut **(Fig. 25A and B)**. Thus, unlike wild-type Derl3, Derl3-DN does not increase the clearance of A1ATmut.

Cultured cardiac myocytes were transfected with Derl3-DN, subjected to sI, or sI/R, then analyzed for cell death by flow cytometry. Compared to control, cells transfected with Derl3-DN exhibited slight increases in cell death under control conditions, although this did not reach significance **(Fig. 25C Bars 1 vs. 2)**. Cells transfected with Derl3-DN exhibited significant increases in cell death upon sI and sI/R (**Fig. 25C Bars 3 vs. 4 and 5 vs 6)**.

To examine roles for Derl3 on cell survival, recombinant adenovirus encoding Derl3-targeted miRNA (AdVmiDerl3) was generated. Compared to control, AdVmiDerl3 decreased basal Derl3 mRNA levels by about 70% **(Fig. 25D)**. To determine whether sI increased Derl3 protein, and whether AdVmiDerl3 could attenuate this increase, NRVMCs were treated with AdVmiDerl3, subjected to sI, and lysates were examined for Derl3 protein. Derl3 was increased with sI **(Fig. 25E bars 1-3 vs 4-6 and Fig. 25F bar 1 vs 2)**. This increase was significantly attenuated by AdVmiDerl3 **(Fig. 25E lanes 4-6 vs 10-12 and Fig. 25F bar 2 vs 4)**. AdVmiDerl3 slightly increased cell death under basal conditions, although this increase did not

reach significance **(Fig. 25G, bars 1 vs. 2)**; however, compared to control,

AdVmiDerl3 significantly increased cell death during sI **(Fig. 25G, bars 3 vs. 4)** and

sI/R **(Fig 25G, bars 5 vs. 6)**.

Thus, Derl3-DN or Derl3 knock-down attenuated clearance of mis-folded ER

proteins, and augmented sI and sI/R-mediated cell death, suggesting that the ability to

clear mis-folded proteins from the ER is especially critical during ischemic stress.
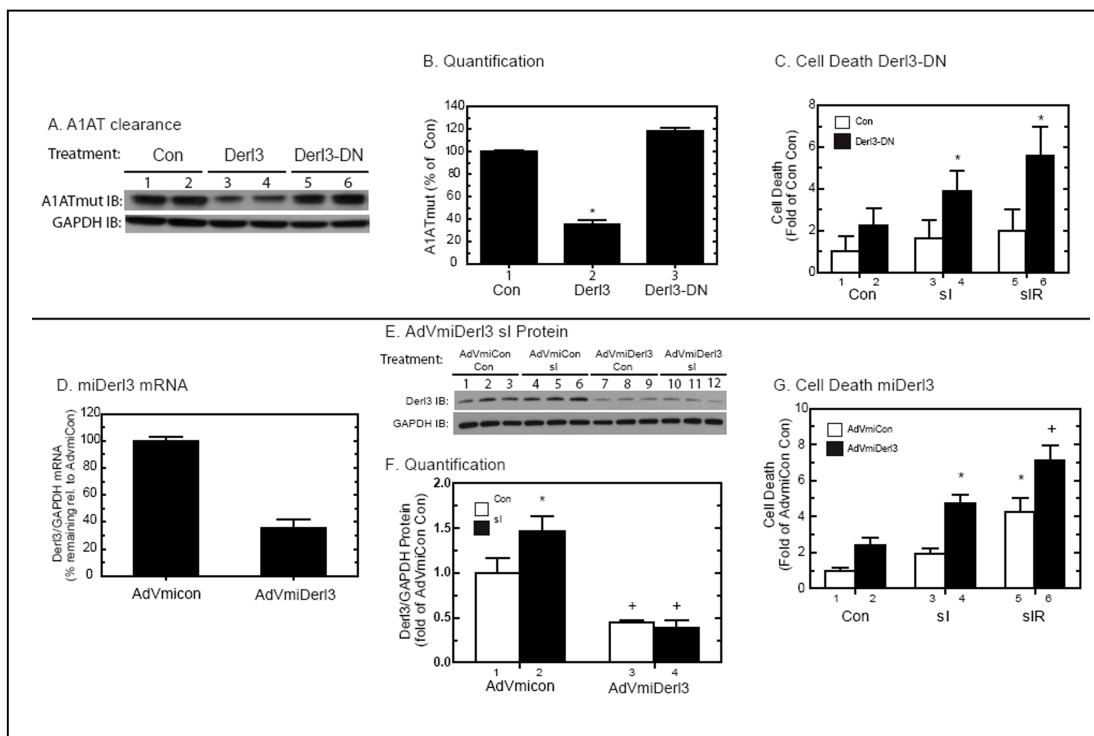
Figure 25. Overexpression of Derl3-DN Attenuates Misfolded Protein Clearance and Enhances Cell Death.

Panels A and B: HeLa cells were transfected with plasmids encoding A1ATmut along with either GFP, Derl3, or Derl3-DN. 48h post-transfection, cells were extracted and analyzed for A1ATmut levels by immunoblot. Shown are the relative blot intensities of A1ATmut/GAPDH, expressed as the fold of control (bar 1) ± SE for each treatment (n = 3 cultures per treatment, sum of 3 separate experiments). **Panel C:** NRVMCs were transfected with plasmids encoding GFP alone or Derl3-DN, which encodes a Derl3-GFP fusion protein. Twenty four hours post-transfection, cultures were subjected to sI or sI/R, after which cells were collected and analyzed by flow cytometry. Cells were gated for GFP expression to identify transfected cells, and then the transfected cells were assessed for cell death by propidium iodide (PI) incorporation, as described in the Methods. Shown are the percentage of GFP-positive cells that are positive for PI, expressed as fold of control (bar 1), (± SE, n = 3 cultures per treatment, sum of 3 separate experiments). * = p≤0.05 different from all other values by ANOVA. **Panel D:** NRVMCs were infected with AdVmiCon or AdVmiDerl3. 48h after infection, cultures were extracted and the RNA was subjected to qRT-PCR to examine the levels of Derl3 mRNA. Shown are the mean ± SE for each target gene (n = 3 cultures per treatment). * = p≤0.05 different from AdVmiCon by two-way T-Test. **Panels E-F:** NRVMCs were infected as in Panel D and 24h later, cultures were treated ± sI. Cells were lysed and analyzed for Derl3 protein levels as Described in the Methods (n = 3 cultures per treatment, sum of 2 separate experiments). Shown is the relative amount of Derl3 protein, expressed as fold of AdVCon Con, ± S.E for each treatment. *, + = p≤0.05 different from all other values by ANOVA. **Panel G:** NRVMCs were infected as in Panel D and 24h later, cultures were treated ± sI or sI/R. Cultures were then stained with Hoescht and propidium iodide, and analyzed for cell death as in Figure 6G (n = 3 cultures per treatment, sum of 3 separate experiments). Shown is the relative amount of cell death, expressed as fold of AdVCon Con, ± S.E for each treatment. *, + = p≤0.05 different from all other values by ANOVA.

9.   Conclusions:

In **Chapter B**, a detailed promoter analysis identified 16 ATF6-regulated

genes which contained canonical ATF6-binding elements **(Tables 2-4)**. Only 2 of

these genes contain two canonical ER stress response elements: GRP94, the well-

known ER stress responsive chaperone, and Derl3, which encodes a protein likely to

be involved in ERAD. Neither Derl3 nor the functional consequences of ERAD have

been previously studied in the cardiac context; therefore, this work focused on this

gene and roles for ERAD in cultured cells and in the mouse heart, *in vivo.*

The Derlins are all ER-transmembrane proteins that associate with other

proteins that participate in the degradation of mis-folded proteins in the ER. Derl1 and

Derl2 associate with the p97 AAA ATPase and VIMP,[80] Derl2 and Derl3 associate

with proteins known to be involved in ERAD, EDEM and p97[74] and the Derl3 yeast

homologue, Der3p/Hrd1p interacts with Hrd3p and the retro-translocon pore complex

protein Sec61p.[81] Overexpression of Derl2 and Derl3 accelerates degradation of

known mis-folded substrates in HEK293 cells, while knockdown blocks degradation.[74]

In addition, the IRE1/XBP1 pathway was implicated to play a role in induction of

Derl1 and Derl2; however, the specific mechanism of Derl3 induction was not

determined.[74]

This work shows that Derl3 was strongly induced by ATF6 *in vivo,* a finding

that was replicated in cultured cardiac myocytes. Derl3 was also induced in the infarct

border zone in an *in vivo* mouse model of myocardial infarction, and by simulated

ischemia in cultured cardiac myocytes. Moreover, since Derl3 enhances ER-associated

degradation of mis-folded proteins in other cell types, we investigated the possibility

that Derl3 may serve a potentially beneficial role during physiologically relevant stresses in cardiac myocytes, such as ischemia and/or reperfusion. We found that overexpressing Derl3 attenuated long-term ER stress response signaling and cell death in response to sI and sI/R, suggesting that enhancing elements of the ERAD machinery in the heart can protect from ischemic injury. In addition, cell death was exacerbated when Derl3 was knocked down prior to sI and sI/R, further indicating a critical role for Derl3 in protecting NRVMCs from stress-induced cell death.

D. Assessment of ATF6 Regulation of microRNAs

Given the role of ATF6 as an active transcription factor and central regulator of ER Stress Response gene expression, we sought to determine whether ATF6 could also influence gene expression through the regulation of microRNAs (miRNAs). miRNAs are small, 20-23 nucleotide non-coding RNA molecules which have been shown to regulate gene expression by targeting and binding to mRNAs. Targeting and binding typically occurs via Watson and Crick binding of a critical 8 nucleotides of the miRNA residing in its stem loop region, termed the "seed sequence," to the 3' untranslated region (3'UTR) of an mRNA, and results in down-regulation of expression of the targeted mRNA, either by inhibiting its translation or enhancing its degradation.[82] Since ATF6 is not known as a repressor of gene expression, and since there were several genes in our ATF6 array which were down-regulated, we hypothesized that part of this down-regulation could be mediated by ATF6-regulated microRNAs.

Gene regulation by miRNAs is very complex, as a given mature miRNA can have several potential mRNA targets, and a single mRNA can be targeted by several miRNAs. The role of miRNAs has been studied in several processes including cell growth, tissue differentiation, cell proliferation, embryonic development, and apoptosis[53] and in several tissue types, including the heart;[83,84] however, the specific role of miRNAs in ER stress response signaling, and the effect of the ATF6 branch on miRNA regulation, remain completely unknown.

1.   ATF6 miRNA Array:

ATF6 activation clearly has a far-reaching effect on gene expression in the heart, as 607 genes were significantly changed as a result of ATF6 activation.[41]Of the 607 ATF6-regulated genes, 227 contained canonical or 1 basepair-mismatched ER stress response elements within their 2kb 5' flanking promoter regions, indicating that the regulatory regions of these genes may be direct targets of ATF6 binding **(see Fig. 7 example 1)**. It is possible that ATF6 may also bind to elements which are less identical to these canonical elements, as evidenced with the apparent regulation of the RCAN1 promoter, which contained a less classical ERSE-like element.[41] It also remains possible that ATF6 could influence gene expression via regulation of miRNAs **(see Fig. 7 examples 2-4)**. To this end, we subjected the RNA used in the ATF6 transcript array to whole-genome microRNA profiling. RNA from each of the four groups used in the initial transcript array study was hybridized to microRNA array chips, which contained probes for roughly 700 mature miRNAs, in accordance with miRBase version 14.0. Statistical analyses were conducted to the ATF6 transcript array study, as those miRNAs which were changed as a non-specific effect of tamoxifen, were removed for further study. In total, 13 miRNAs were significantly changed due to ATF6 activation in these samples. These miRNAs can be found in **Table 8.** Regulation of these miRNAs was rather modest, with fold changes ranging from 0.2 to 2.5.

Table 8. Identification of ATF6-Regulated miRNAs.

#	miRNA Name	Fold	P-Value
1	mmu-miR-721	2.50	0.004
2	mmu-miR-671-5p	2.35	0.003
3	mmu-miR-130b	2.17	0.034
4	mmu-miR-685	2.11	0.026
5	mmu-mir-17	2.00	0.040
6	mmu-miR-202-3p	0.48	0.035
7	mmu-miR-363	0.43	0.030
8	mmu-miR-455	0.40	0.002
9	mmu-miR-467e*	0.40	0.030
10	mmu-miR-299*	0.39	0.046
11	mmu-miR-466g	0.38	0.006
12	mmu-miR-467f	0.31	0.042
13	mmu-miR-466f-3p	0.21	0.032

To identify potential ATF6-regulated miRNAs in the heart, total RNA from cardiac samples used our ATF6 transcript array was subjected to whole-genome miRNA array analysis. Twelve miRNAs were displayed a differential expression as a result of activating ATF6 in our transgenic mice, displaying fold-changes ranging from 0.21 to 2.5 (n=3, $p<0.05$).

2. Identification of Potential Targets for ATF6-Regulated miRNAs:

Since one way that miRNAs can inhibit gene expression is by enhancing the degradation of their target mRNAs, we hypothesized that some of the down-regulated transcripts in the initial ATF6 transcript array could be targets of ATF6-induced miRNAs. Conversely, some of the up-regulated transcripts could be targets of miRNAs which are inhibited by ATF6. To this end, we identified the potential targets of the 12 ATF6-regulated miRNAs using TargetScan Version 5.1 (http://www.targetscan.org). We then cross-checked these targets with the transcripts present in the ATF6 transcript array. As shown in **Table 9**, several of the transcripts which were down-regulated in the ATF6 array are potential targets of miRNAs which were up-regulated by ATF6, and vice versa. This indicates that ATF6 may indeed be modulating gene expression, in part, through miRNAs.

Table 9. Check of ATF6-Regulated miRNA Targets with ATF6-Regulated Transcripts.

Gene Symbol	Gene Name	Transcript Array Fold	miRNA that Targets	miRNA Fold
SYCP2	Synaptonemal complex protein 2	21.1	miR-467f	0.31
SYCP2	Synaptonemal complex protein 2	21.1	miR-466f-3p	0.21
APPL1	DCC-interacting protein 13-alpha	9.3	miR-467f	0.31
RTN4	Reticulon-4	9.3	miR-455	0.40
MLLT3	Myeloid/lymphoid or mixed-lineage	8.7	miR-466f-3p	0.21
THBS1	Thrombospondin-1 Precursor	7.2	miR-202-3p	0.48
MXD1	MAD protein (MAX dimerizer)	6.5	miR-202-3p	0.48
CHKA	Choline kinase alpha	5.5	miR-466f-3p	0.21
EDEM1	ER degradation-enhancing alpha-	5.4	miR-466g	0.38
CALR	Calreticulin	5.3	miR-455	0.40
MORF4L2	Mortality factor 4-like protein 2	5.1	miR-466g	0.38
XPO1	Exportin-1	5.1	miR-467f	0.31
UBFD1	Ubiquitin domain-containing protein	5.0	miR-202-3p	0.48
UBFD1	Ubiquitin domain-containing protein	5.0	miR-455	0.40
UBFD1	Ubiquitin domain-containing protein	5.0	miR-299	0.39
RRAS2	Ras-related protein R-Ras2 Precursor	4.9	miR-466f-3p	0.21
RRAS2	Ras-related protein R-Ras2 Precursor	4.9	miR-467f	0.31
STRBP	Spermatid perinuclear RNA-binding	4.9	miR-202-3p	0.48
TMEM158	Transmembrane protein 158 Precursor	4.8	miR-466f-3p	0.21
COL3A1	Collagen alpha-1(III) chain Precursor	4.6	miR-202-3p	0.48
MAP3K3	Mitogen-activated protein kinase kinase	4.3	miR-202-3p	0.48
SNAP23	Synaptosomal-associated protein 23	4.2	miR-202-3p	0.48
SENP2	Sentrin-specific protease 2	4.2	miR-202-3p	0.48
UGCGL1	UDP-glucose:glycoprotein	3.7	miR-202-3p	0.48
HN1	Hematological and neurological	3.5	miR-455	0.40
UCHL1	Ubiquitin carboxyl-terminal hydrolase	3.4	miR-466g	0.38
WDR68	WD repeat-containing protein 68	3.3	miR-467f	0.31
EIF2S2	Eukaryotic translation initiation factor 2	3.0	miR-466g	0.38
EFNB2	Ephrin-B2 Precursor	3.0	miR-467f	0.31
ENAH	Protein enabled homolog	2.7	miR-467e	0.40
JUNB	Transcription factor jun-B	2.6	miR-466f-3p	0.21
PJA2	E3 ubiquitin-protein ligase Praja2	2.6	miR-466f-3p	0.21
BMPR2	Bone morphogenetic protein receptor	2.6	miR-467f	0.31
PJA2	E3 ubiquitin-protein ligase Praja2	2.6	miR-467f	0.31
SLC39A14	Zinc transporter ZIP14 Precurso	2.5	miR-466g	0.38
INCENP	Inner centromere protein	2.4	miR-466g	0.38
SLC2A1	Solute carrier family 2, facilitated	2.4	miR-466f-3p	0.21
SLC2A1	Solute carrier family 2, facilitated	2.4	miR-467f	0.31
KLHL2	Kelch-like protein 2	2.4	miR-466f-3p	0.21
KLHL2	Kelch-like protein 2	2.4	miR-467f	0.31
ING1	Inhibitor of growth protein 1	2.4	miR-467f	0.31
ARL4C	ADP-ribosylation factor-like protein 4C	2.3	miR-466g	0.38
LRRC59	Leucine-rich repeat-containing protein	2.2	miR-202-3p	0.48
SLC6A6	Sodium- and chloride-dependent taurine	2.2	miR-466f-3p	0.21
CUGBP2	CUG-BP- and ETR-3-like factor 2	2.2	miR-466g	0.38
CUGBP2	CUG-BP- and ETR-3-like factor 2	2.2	miR-467f	0.31
CALM1	Calmodulin	2.2	miR-202-3p	0.48
CDS2	Phosphatidate cytidylyltransferase 2	2.1	miR-466f-3p	0.21
PPAP2A	Lipid phosphate phosphohydrolase 1	2.1	miR-202-3p	0.48
FSTL1	Follistatin-related protein 1 Precursor	2.1	miR-363	0.43
FSTL1	Follistatin-related protein 1 Precursor	2.1	miR-466g	0.38
WDR1	WD repeat-containing protein 1	2.0	miR-467e	0.40
SMAD2	Mothers against decapentaplegic	2.0	miR-455	0.40
A2BP1	Ataxin 2 binding protein 1	0.3	miR-17	2.00
SLC40A1	Solute carrier family 40 (iron-regulated	0.4	miR-17	2.00
HLF	Hepatic leukemia factor	0.4	miR-17	2.00
CLIP4	CAP-GLY domain containing linker	0.5	miR-17	2.00
HLF	Hepatic leukemia factor	0.4	miR-721	2.50
HLF	Hepatic leukemia factor	0.4	miR-130b	2.17
ACSL1	Long-chain-fatty-acid--CoA ligase 1	0.4	miR-721	2.50
ACSL1	Long-chain-fatty-acid--CoA ligase 1	0.4	miR-130b	2.17
UCP3	Mitochondrial uncoupling protein 3	0.3	miR-721	2.50
UCP3	Mitochondrial uncoupling protein 3	0.3	miR-130b	2.17
TBL1XR1	F-box-like/WD repeat-containing protein TBL1XR1	0.2	miR-721	2.50
TBL1XR1	F-box-like/WD repeat-containing protein TBL1XR1	0.2	miR-130b	2.17
FNDC5	Fibronectin type III domain-containing protein 5 Precursor	0.2	miR-671-5	2.35

Potential targets of ATF6-regulated miRNAs were obtained using TargetScan. These potential targets were cross-checked with the 607 ATF6-regulated transcripts in our previous array study.[41] Transcripts which were up-regulated by ATF6 in the transcript array are shown in green, and correspond to miRNAs which were down-regulated in the miRNA array. Transcripts which were down-regulated by ATF6 in the transcript array are shown in red, and correspond to miRNAs which were up-regulated in the miRNA array.

3.   Assessment of ATF6-Regulated miRNA Putative Promoter Regions

Data indicate that miRNAs are encoded by genes containing promoters to which transcriptional elements such as RNA pol II associates,[85] and promoter regulatory elements have been discovered in Arabidosis[86] and other plants.[87] We decided to obtain the nucleotide sequence of 2kb of the 5' regulatory region for each ATF6-regulated miRNA from the mouse genome, and perform searches for ER stress response elements, with the techniques described in **Chapter A**. Such a search revealed that only miR-130b contained an ER stress-like element, in the form of a 1bp-mismatched UPRE. Such an element suggests that miR-130b may be ER stress-responsive.

4.   Conservation of miR-130b Mature Sequence

To determine whether mouse miR-130b is conserved among species, we performed an alignment of the stem-loop sequence and the mature miRNA species across species using the miRBase miRNA alignment program (http://www.mirbase.org). This revealed that the stem loop sequence of mouse miR-130b is well-conserved among species, displaying a 96% identity to rat miR-130b. In addition, the mature mouse miR130b sequence is 100% identical to rat miR-130b **(see Fig. 26A-B)**. This complete homology between mouse and rat miRNA makes miR-130b an attractive target to study in the cardiac context, as it can be studied in transgenic mice and cultured NRVMCs.

B. Alignment of mouse and rat miR-130b

Mature miR-130b
Alignment of mouse and rat

```
mmu-miR-130b       1   cagugcaaugaugaaagggcau   22
                       ||||||||||||||||||||||
rno-miR-130b       1   cagugcaaugaugaaagggcau   22
```

Stem loop miR-130b
Alignment of mouse and rat

```
Mmu-miR-130b 1   ggcuuguuggacacucuuucccuguugcacuacuguggggccucugggaagcagugcaaugaugaaagggcaucugucgggcc   82
                 ||||||| |||||||||||||||||||||||||||||||||||||||||||||||||||||||||||||||||||||||| ||| ||||
rno-mir-130b 1   ggcuugcuggacacucuuucccuguugcacuacuguggggccucugggaagcagugcaaugaugaaagggcauccgucaggcc   82
```

Figure 26. Alignment of mouse and rat miR-130b mature and stem loop sequences.

The mature miRNA sequences of mouse and rat miR-130b display 100% identity, and the stem loop sequences display 96% identity.

5.   Validation of miR-130b Induction by ATF6

To validate the ATF6-mediated induction of miR-130b displayed in the miRNA array, we conducted qRT-PCR analysis of miR-130b using these samples. In addition, we subjected RNA from NRVMCs subjected to adenoviral-mediated ATF6 overexpression. Mature miR-130b was amplified and analyzed by qRT-PCR on an ABI Prism 7000 machine using pre-validated TaqMan miRNA assays. As indicated in **Fig. 27A**, ATF6 displayed a ~2-fold induction of miR-130b in the hearts of transgenic mice treated with tamoxifen, which did not reach significance. In addition, NRVMCs treated with AdV-ATF6 displayed a significant ~1.7 fold induction of miR-130b **(Fig. 27B)**, indicating that miR-130b is ATF6 inducible.
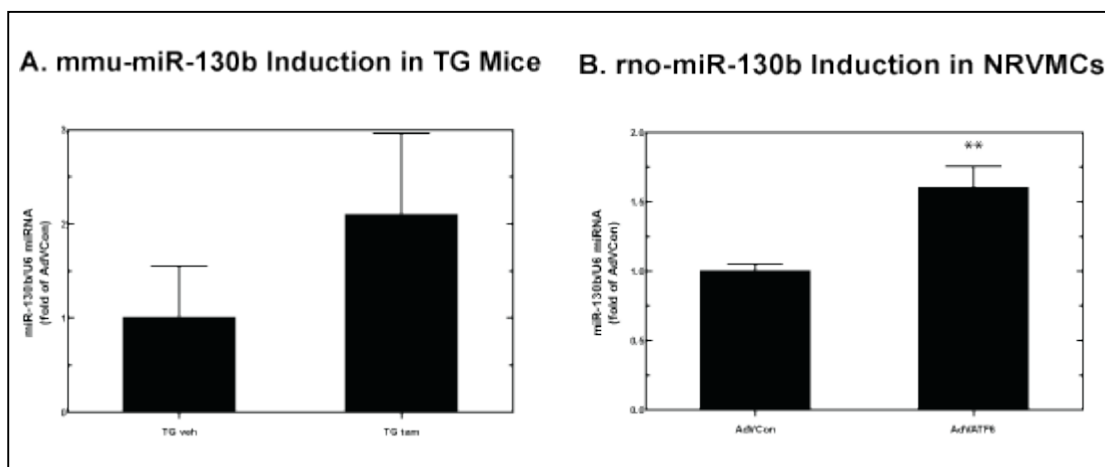
Figure 27. Validation of ATF6-Mediated Induction of miR-130b.

Panel A: To validate ATF6-mediated induction of mir-130b seen in the array, total RNA from cardiac samples used our ATF6 transcript array (TG veh and TG tam) was subjected to Taqman assays using specific stem-loop primers to miR-130b and U6, as a control, and quantified by qRT-PCR. Shown is the fold of miR-130b/U6 miRNA. **Panel B:** To validate ATF6-mediated induction of miR-130b in NRVMCs, cells were infected with AdVCon or AdVATF6, and then a microRNA-enriched RNA fraction was obtained using the miRNEasy kit (Qiagen). This RNA was then subjected to TaqMan assays as in Panel A. Shown is the fold of miR-130b/U6 miRNA, expressed as fold of AdVCon (n=3 cultures per treatment, ** = p<0.01 by Two-Way T-Test).

6.   Assignment of GO Classifications to ATF6-regulated miRNA Targets:

In addition to target mRNA degradation, miRNAs can also regulate gene expression through translational inhibition. In this way, several potential novel targets may not be identified by simply searching the ATF6 transcript array as described above. To determine whether there are novel groups of proteins which may be targeted by ATF6-regulated miRNAs, we assigned GO classifications to the full set of potential targets of each ATF6-regulated miRNA, as identified by TargetScan. A search of significantly-represented GO categories revealed that several members of the TGF family of proteins are potentially targeted by ATF6-regulated miRNAs. The TGF family is known to play a key role in several cellular processes, including proliferation and growth.[88] Specifically, miR-130b targets several members of this family, as shown in **Table 10**. Regulation of TGF signaling by ATF6-regulated miRNAs would represent a novel form of cross-talk between ER stress and TGF signaling.

Table 10. Potential Targets of miR-130b with TGF Family GO Classifications.

Gene Symbol	Protein Name	Mouse TargetScan Score	Rat TargetScan Score
Tgfbr1	TGF-beta receptor type-1 Precursor	0.75	0.75
Tgfbr2	TGF-beta receptor type-2 Precursor	0.89	0.89
Bmpr1b	Bone morphogenetic protein receptor type-1B Precursor	0.52	0.52
Bmpr2	Bone morphogenetic protein receptor type-2 Precursor	0.89	0.89
Acvr1	Activin receptor type-1 Precursor	0.94	0.94
Acvr1c	Activin receptor type-1C Precursor	0.54	N/A
Smad2	Mothers against decapentaplegic homolog 2	0.7	0.7
Smad4	Mothers against decapentaplegic homolog 4	0.5	0.5
Smad5	Mothers against decapentaplegic homolog 5	0.87	0.87

GO classification analysis identified that several predicted targets of miR-130b are members of the TGF signaling pathway.

7.   Conclusions:

In addition to its well-characterized role as a transcriptional regulator, it appears that ATF6 may also serve a role in regulating miRNAs. A whole-genome microarray determined that 381 transcripts were up-regulated in response to ATF6 activation, while 226 were down-regulated, and the proportion of these targets which are direct and indirect targets of ATF6 regulation remains to be identified. Indeed, a subset of the indirect targets may be under the control of ATF6-regulated miRNAs. To this end, we performed a cross-check of the putative targets of ATF6-regulated miRNAs with the known ATF6-regulated transcripts from our array study.[41] As shown in **Table 9**, several targets of up-regulated miRNAs were down-regulated at the transcript level, and vice versa, indicating these ATF6-regulated miRNAs as potential mediators of indirect ATF6 gene regulation. This is consistent with the fact that several of these indirectly-regulated genes do not contain known ER stress elements within their regulatory regions, hence being unlikely direct binding targets of ATF6. To confirm this hypothesis, a validation of the regulation of a subset of these miRNAs by ATF6, as well as their putative transcript targets identified in **Table 9**, is needed.

In addition, there may be an additional subset of genes whose transcript levels are unchanged by ATF6-regulated miRNAs, but whose translation may targeted and affected by these miRNAs. To determine if ATF6-regulated miRNAs may potentially target novel gene families, we assigned GO classifications to all of the potential targets of these miRNAs, and identified several members of the TGF family as being potential targets. One miRNA which potentially targets TGF family members is miR-130b, and we have confirmed its regulation by ATF6. Follow-up studies will aim to

confirm translational regulation of miR-130b targets, with a focus on potential targets belonging to the TGF family of proteins. This would be the first evidence of cross-talk between the ATF6 of the UPR with TGF signaling, and would potentially identify another mechanism by which ATF6 may modulate growth pathways.

IV. Discussion

The data presented herein indicate that activation of ATF6 in the heart has far-reaching effects on gene expression in general, and specifically on mediating the protective properties of the UPR. This work documents the first known ATF6 whole-genome transcript and microRNA arrays, as well as the first known comprehensive ER stress response promoter element search performed on the mouse genome. While it has been previously shown that ATF6 activation in the heart can be protective, the whole-genome transcript array presented here provides a more detailed view of the consequences of ATF6 activation, and will help uncover the specific mechanisms by which ATF6 affords cardioprotection during stress. This work focused on two potential mechanisms of ATF6 action, including RCAN1-mediated inhibition of hypertrophic growth, which could act to modulate the protein folding load on the ER during stress, and induction of Derl3, which enhanced protein quality control, a process which appeared to be critical for survival during stress. The whole-genome array provides a list of additional potential novel gene targets of ATF6, many of which may provide a better understanding of ATF6-mediated protection in the heart.

In addition to growth modulation and protection, these ATF6-regulated genes may provide additional insight into the influence of ATF6 on other cellular processes, as the list of ATF6-regulated genes contains genes which play a role in development (frizzled-related protein, Frzb), metabolism (phospholipid sterol acetyltransferase 1, Psat1) and the immune response (pentraxin-related 3, Ptx3), among other diverse responses. While the majority of ATF6 literature focuses on its role as a mediator of UPR signaling and inducer of ER-localized proteins, it is quite possible that ATF6

may influence additional signaling pathways and biological processes throughout the cell.

It also remains possible that ATF6 may serve as a regulator of miRNA expression, which in turn could have indirect consequences on transcriptional regulation. In part, this would explain the differentially-expressed transcripts from the ATF6 array which do not contain known ER stress response elements. In addition, since ATF6 is not known as a direct repressor of gene expression, there may be a subset of ATF6-inducible miRNAs which influence the inhibition of several transcripts. For instance, several of the transcripts which were down-regulated in the ATF6 transcript array are identified here as putative targets of ATF6-regulated miRNAs found in the miRNA array.

ATF6-regulated miRNAs may also provide some insight into potential ATF6 cross-talk into other signal transduction pathways. One potential example could be the TGFβ family of proteins, which play a role in growth, development, and apoptotic signaling, but which are not known to be regulated by ATF6 or ER stress. Many TGFβ family members are predicted to be targeted by several ATF6-regulated miRNAs. For instance, miR-130b is up-regulated by ~2-fold by ATF6 in the microRNA array, and is predicted to target multiple members of this family, including TGFβ receptors 1 and 2, as well as Smads 2, 4 and 5.

In addition, while this work has identified one possible mechanism of ATF6-mediated hypertrophic attenuation, namely the induction of RCAN1, ATF6 may also mediate attenuation of hypertrophy in part via induction of miRNAs. To date, several miRNAs have been well-characterized in hypertrophic signaling.[89-91] While a

preliminary literature search of the 12 ATF6-regulated miRNAs did not uncover any miRNAs known to play a role in hypertrophic signaling, it remains possible that at least one of these miRNAs may have targets in the hypertrophic growth signaling program, given the marked anti-hypertrophic effect of ATF6 over-expression on agonist-induced NRVMC growth, highlighted in **Chapter B** of the Results.

Another example of ATF6-regulated miRNA action could be attenuation of apoptotic signaling. Previous studies have documented the anti-apoptotic effects of overexpressing ATF6 in the heart,[20,92] as well as the pro-apoptotic effects of knocking down ATF6 in NRVMCs.[40]ATF6 is known as a transcriptional inducer of several protective ER stress response genes, which in turn mediate some of its protective effects. It remains possible, however, that ATF6 could influence apoptotic signaling through mechanisms other than the ER stress response, and these alternative mechanisms could be mediated in part through miRNAs. For instance, we identified predicted targets of the 12 ATF6-regulated miRNAs from our ATF6 miRNA array, and then annotated these potential targets with GO classifications. One potential novel miRNA target is follistatin-like 1 (Fstl1), a secreted protein which is known to have anti-apoptotic effects in the heart.[93,94] Fstl1 transcript levels have been shown to be significantly up-regulated in the heart by *in vivo* stresses such as transverse aortic constriction (TAC), ishchemia/reperfusion, and permanent MI, andFstl1 protein levels were found to be increased both in the heart and in the serum after permanent MI.[94] In this same study, it was shown that overexpression protected NRVMCs from ischemia/reperfusion induced apoptosis, while knockown exacerbated apoptosis.[94] Fstl1 was up-regulated by ~2-fold by ATF6 in the transcript array,[41] and as indicated

in the ATF6 miRNA array, miR-466g, which is predicted to target Fstl1, is coordinately down-regulated, by ~3-fold. This miRNA could represent a novel mechanism by which ATF6 may up-regulate an anti-apoptotic protein not known to play a role in ER stress signaling. Follow-up studies will aim to validate ATF6-mediated regulation of the novel miRNAs mentioned above, as well as the coordinate change in their putative targets, both at the transcript and protein levels.

V.   ATF6-MER Mouse Microarray Results

The following is a list of genes differentially expressed as a result of ATF6 activation in the hearts of ATF6-MER TG mice. All differentially expressed genes are sorted by fold change. Also shown is the gene symbol for each gene. The NCBI Reference Sequence ID, or Accession number for each gene isshown. All genes were sorted into Gene Ontology Biological Process categories.Several of the categories were found to be of interest and the numbers in the Notescolumn refer to genes assigned to the following groupings of Gene Ontology BiologicalProcess categories:

1 = regulation of transcription, DNA-dependent (GO ID 0006355)

2 = protein folding, response to unfolded protein, ER overload response (GO IDs 0006457, 0006986, 0006983)

3 = small GTPase mediated signal transduction (GO ID 0007264)

4 = negative regulation of apoptotis (GO ID 0043066)

5 = cell death (GO IDs 0012501, 0008219)

6 = negative regulators of cell growth (GO IDs 0030308, 0008285, 0001558)

7 = fatty acid and glucose metabolism (GO IDs 0008152, 0015758, 0006094, 0006631)

Known and putative ERSR genes are designated by * and #, respectively.

Table 11. Complete List of Genes Induced by ATF6 Activation in the Heart.

Number	Gene Symbol	RefSeq Transcript ID	Fold Change	Notes
1	Mlstd2	NM_026143	120.90	
2	Spp1	NM_009263	91.47	4
3	Polr3k	NM_025901	69.92	1
4	Alkbh2	NM_175016	47.45	
5	Ptx3	NM_008987	46.31	#
6	Smarcb1	NM_011418	44.98	1, 6
7	Psat1	NM_177420	40.77	7
8	Il6	NM_031168	38.45	4, #
9	Myc	NM_010849	35.36	1
10	Slc15a3	NM_023044	30.96	
11	Cxcl1	NM_008176	25.21	
12	Mthfd2	NM_008638	22.45	
13	Clec4e	NM_019948	22.34	
14	Ccl2	NM_011333	21.74	4
15	Cxcl5	NM_009141	21.56	
16	Vcan	NM_001081249	21.45	
17	Sycp2	NM_177191	21.11	
18	Tk1	NM_009387	20.57	
19	Cdkn1a	NM_007669	20.43	4, 6
20	Derl3	NM_024440	18.50	*
21	Sdf2l1	NM_022324	17.41	#
22	Pdia4	NM_009787	16.37	*
23	Ccl12	NM_011331	14.03	
24	Dnajc3a	NM_008929	12.75	2, *
25	Dnajb11	NM_026400	12.39	2,*
26	Ccl7	NM_013654	12.03	
27	EG574437	NM_001081643	11.90	
28	Rcc2	NM_173867	11.71	
29	Pscdbp	NM_139200	11.54	
30	Chi3l3	NM_009892	11.44	
31	Evi2b	NM_001077496	11.40	
32	Pycr1	NM_144795	10.82	
33	AW011738	XM_001001227	10.56	
34	Plcxd2	XM_001000738	10.55	
35	Gadd45g	NM_011817	10.52	#
36	EG668771	NM_016966	10.30	7
37	Nr4a3	NM_015743	10.23	1
38	2700038G22Rik	XM_899866	10.11	
39	1700012G19Rik	NM_025954	10.09	7
40	Arid4a	NM_001081195	10.08	
41	LOC669660	XM_976375	9.86	
42	Socs3	NM_007707	9.68	*
43	Eif1a	NM_010120	9.66	
44	Ptrh1	NM_178595	9.63	
45	Slc7a5	NM_011404	9.57	
46	Appl1	NM_145221	9.31	
47	Tspyl2	NM_029836	9.29	1
48	Rtn4	NM_024226	9.28	#

Table 11. Complete List of Genes Induced by ATF6 Activation in the Heart.

Number	Gene Symbol	RefSeq Transcript ID	Fold Change	Notes
49	Asns	NM_012055	9.26	7, *
50	P4hb	NM_011032	9.17	2, *
51	BB414484	---	8.92	
52	Cd44	NM_001039150	8.86	
53	Mllt3	NM_027326	8.67	1
54	Arf2	NM_007477	8.52	3
55	2610207I05Rik	NM_001031814	8.45	
56	Cks1b	NM_016904	8.28	
57	AI848100	XM_917085	8.23	
58	ARMET	NM_029103	8.21	*
59	Chac1	NM_026929	8.07	
60	Lrrc49	NM_145616	7.88	
61	Ears2	NM_026140	7.84	
62	Timp1	NM_001044384	7.78	
63	D5Ertd593e	NM_175096	7.56	
64	Il1rn	NM_001039701	7.53	
65	Eda2r	NM_175540	7.46	5
66	Thbs1	NM_011580	7.23	
67	Hspa14	NM_001037542	7.16	
68	Hsp90b1	NM_011631	7.07	2, *
69	Ccr2	NM_009915	6.93	
70	Itgam	NM_001082960	6.88	
71	Tnfrsf12a	NM_013749	6.78	5
72	Hn1l	NM_198937	6.77	
73	Phgdh	NM_016966	6.73	
74	Trib3	NM_144554	6.64	1, *
75	Mxd1	NM_010751	6.47	1
76	Dbf4	NM_013726	6.44	
77	Kpnb1	NM_008379	6.42	
78	Hmox1	NM_010442	6.40	
79	Sptlc2	NM_011479	6.31	
80	Sel1l	NM_001039089	6.30	
81	Zwint	NM_025635	6.28	
82	D16Ertd472e	NM_025967	6.26	
83	Cdk2ap2	NM_026373	6.16	
84	2810474O19Rik	NM_026054	6.05	
85	S100a4	NM_011311	5.99	
86	Azin1	NM_018745	5.96	#
87	Gas5	NR_002840	5.90	#
88	Saa3	NM_011315	5.82	
89	Tubb3	NM_023279	5.80	
90	Zmynd19	NM_026021	5.76	
91	Tubb2b	NM_009450	5.58	
92	Chka	NM_001025566	5.46	
93	Edem1	NM_138677	5.36	2, *
94	Relb	NM_009046	5.35	1, 4
95	Fem1b	NM_010193	5.33	1
96	LOC433261	NM_019768	5.32	1

Table 11. Complete List of Genes Induced by ATF6 Activation in the Heart.

Number	Gene Symbol	RefSeq Transcript ID	Fold Change	Notes
97	Aldh1a2	NM_009022	5.31	7
98	Ebp	NM_007898	5.29	
99	Calr	NM_007591	5.29	2, *
100	G530011O06Rik	NM_001039559	5.22	
101	Trim37	NM_197987	5.21	
102	Kcnq1	NM_008434	5.14	
103	Morf4l2	NM_019768	5.10	1
104	Ints3	NM_145540	5.09	
105	BC013529	NM_145418	5.08	
106	Xpo1	NM_001035226	5.07	
107	Ubfd1	NM_138589	5.05	
108	Uck2	NM_030724	5.03	
109	Cd52	NM_013706	5.02	
110	Rbm15b	NM_175402	4.99	
111	Cxcr6	NM_030712	4.95	
112	Rras2	NM_025846	4.95	3
113	Cxcl2	NM_009140	4.94	
114	Atf4	NM_009716	4.93	1, 7, *
115	Strbp	NM_009261	4.90	
116	Dph5	NM_027193	4.85	7
117	Ncam1	NM_001081445	4.81	
118	Aldh18a1	NM_019698	4.80	
119	Ckap4	NM_175451	4.80	
120	Gm879	NM_001034874	4.80	
121	EG627828	NM_146130	4.78	
122	Tmem158	NM_001002267	4.78	
123	Ms4a6d	NM_022431	4.76	
124	Tgfbi	NM_009369	4.76	
125	Idi1	NM_145360	4.75	
126	Pdia3	NM_007952	4.72	*
127	Hspa5	NM_022310	4.71	2, 4, *
128	Gdf15	NM_011819	4.65	
129	Col3a1	NM_009930	4.64	
130	Zfp697	NM_172863	4.64	
131	Syvn1	NM_028769	4.60	2, 4, *
132	Elk1	NM_007922	4.57	1
133	Ms4a4c	NM_029499	4.57	
134	Plac8	NM_139198	4.56	
135	Kif5b	NM_008448	4.55	
136	Nans	NM_053179	4.53	7
137	Actr3	NM_023735	4.51	
138	Tnrc15	NM_146112	4.49	
139	Snord22	NR_002896	4.48	#
140	Nola2	NM_026631	4.44	
141	Gas2l3	NM_001033331	4.35	
142	Ppp1r3d	NM_001085501	4.33	
143	Fhl1	NM_001077361	4.33	
144	Bex1	NM_009052	4.33	

Table 11. Complete List of Genes Induced by ATF6 Activation in the Heart.

Number	Gene Symbol	RefSeq Transcript ID	Fold Change	Notes
145	Txnrd1	NM_001042513	4.32	#
146	Usp1	NM_146144	4.31	
147	Map3k3	NM_011947	4.29	
148	RCAN1	NM_001081549	4.29	#
149	Arntl	NM_007489	4.27	1
150	Snap23	NM_009222	4.23	
151	2810026P18Rik	XM_925560	4.22	
152	Senp2	NM_029457	4.19	1
153	Tbcb	NM_025548	4.19	2
154	Eif2ak3	NM_010121	4.18	2, *
155	Tes	NM_011570	4.14	
156	Nde1	NM_023317	4.12	
157	Pin1	NM_023371	4.12	2, *
158	2610036L11Rik	XM_488549	4.11	
159	4932431P20Rik	NM_001033230	4.08	1
160	BC049807	NM_001002008	4.08	1
161	Fem1c	NM_173423	4.07	1
162	Tubb2c	NM_146116	4.07	
163	Pgk1	NM_008828	4.04	
164	Itgb1bp3	NM_027120	4.03	
165	Cd53	NM_007651	4.03	
166	Smc2	NM_008017	4.02	
167	D14Wsu89e	NM_001081039	4.01	
168	Slc16a6	NM_001029842	3.98	
169	Hyou1	NM_021395	3.86	2, *
170	Rnd1	NM_172612	3.84	3
171	Ugcgl1	NM_198899	3.70	*
172	Egr1	NM_007913	3.67	1
173	Ikbkg	NM_010547	3.57	1
174	Pcdh7	NM_018764	3.55	
175	Hn1	NM_008258	3.53	
176	Prkg1	NM_001013833	3.51	
177	Rrp12	NM_199447	3.45	
178	Uchl1	NM_011670	3.40	
179	Wfs1	NM_011716	3.38	
180	Wdr68	NM_027946	3.34	
181	Coro1a	NM_009898	3.29	
182	Vcp	NM_009503	3.29	
183	Rhpn2	NM_027897	3.26	
184	Ppp1r14b	NM_008889	3.25	
185	Tuba1c	NM_009448	3.24	
186	Rala	NM_019491	3.18	3
187	Hagh	NM_024284	3.14	
188	Mesdc2	NM_023403	3.14	
189	Pnpo	NM_134021	3.10	
190	Serpinh1	NM_009825	3.10	2, #
191	Cotl1	NM_028071	3.08	
192	Frzb	NM_011356	3.07	

Table 11. Complete List of Genes Induced by ATF6 Activation in the Heart.

Number	Gene Symbol	RefSeq Transcript ID	Fold Change	Notes
193	Rabepk	NM_145522	3.07	
194	Ptpn14	NM_001033287	3.05	
195	Cyb5r3	NM_029787	3.02	
196	Eif2s2	NM_026030	3.02	
197	Gsk3b	NM_019827	3.00	2, 4, #
198	Arid5b	NM_023598	3.00	1
199	1700040I03Rik	NM_028505	2.99	
200	2700049P18Rik	NM_175382	2.98	
201	Prmt2	NM_001077638	2.98	
202	1110014K08Rik	NM_176902	2.98	
203	Bola2	NM_175103	2.96	
204	Efnb2	NM_010111	2.96	
205	Mcm5	NM_008566	2.95	1
206	Xbp1	NM_013842	2.95	1, *
207	Prpf40a	NM_018785	2.94	
208	Flnc	NM_001081185	2.91	
209	Dlgap4	NM_001042487	2.91	
210	Sfpq	NM_023603	2.91	1
211	Nol12	NM_133800	2.89	
212	Dpy19l1	NM_172920	2.89	
213	Mettl1	NM_010792	2.87	
214	Stox2	NM_175162	2.85	
215	Klf6	NM_011803	2.85	1
216	Rhoc	NM_007484	2.84	3
217	2500002L14Rik	NM_025607	2.84	
218	Rfxdc2	NM_001033536	2.83	1
219	Nmt1	NM_008707	2.83	
220	Fkbp11	NM_024169	2.81	2
221	Klhl28	NM_025707	2.81	
222	Srm	NM_009272	2.81	
223	Grn	NM_008175	2.81	
224	Erdr1	NM_133362	2.80	
225	Ormdl2	NM_024180	2.79	
226	Stat3	NM_011486	2.78	1, 7
227	Cttn	NM_007803	2.76	
228	Tmem45a	NM_019631	2.76	
229	Copz1	NM_019817	2.75	
230	Man1a	NM_008548	2.74	7
231	H2-Ke6	NM_013543	2.72	7
232	Enah	NM_001083120	2.68	
233	Fn1	NM_010233	2.68	7
234	Os9	NM_177614	2.67	
235	Acot9	NM_019736	2.67	
236	Gclc	NM_010295	2.66	4
237	Med19	NM_025885	2.66	
238	Ptpre	NM_011212	2.64	
239	Itga7	NM_008398	2.64	
240	Junb	NM_008416	2.64	1

Table 11. Complete List of Genes Induced by ATF6 Activation in the Heart.

Number	Gene Symbol	RefSeq Transcript ID	Fold Change	Notes
241	Nfil3	NM_017373	2.64	1
242	Apex1	NM_009687	2.63	
243	Slc35b4	NM_021435	2.63	
244	Cyb5r1	NM_028057	2.60	
245	Nme6	NM_018757	2.59	
246	1200002N14Rik	NM_027878	2.57	
247	Bmpr2	NM_007561	2.57	
248	Odc1	NM_013614	2.57	
249	Pja2	NM_001025309	2.57	
250	Cdr2	NM_007672	2.56	
251	Rasl11b	NM_026878	2.54	3
252	Sec11a	NM_019951	2.53	#
253	H47	NM_024439	2.52	#
254	Rbm25	NM_025930	2.52	
255	Wdr23	NM_133734	2.52	
256	Trove2	NM_013835	2.51	
257	Nip7	NM_025391	2.51	
258	Heatr5a	NM_177171	2.51	
259	Ppox	NM_008911	2.51	
260	Smurf2	NM_025481	2.51	
261	Slc39a14	NM_144808	2.50	
262	Rap2a	NM_029519	2.49	3
263	Fosl2	NM_008037	2.48	1
264	2010111I01Rik	NM_028079	2.48	
265	Atp2b1	NM_026482	2.48	7
266	Rap2b	NM_028712	2.45	3
267	Ywhaz	NM_011740	2.45	
268	Gmppb	NM_177910	2.44	
269	Rhoa	NM_016802	2.44	3
270	Herpud1	NM_022331	2.43	2, *
271	Incenp	NM_016692	2.41	
272	Ehd4	NM_133838	2.40	
273	3110082I17Rik	NM_028469	2.40	
274	3110050N22Rik	NM_173181	2.40	
275	Slc2a1	NM_011400	2.39	
276	Klhl2	NM_178633	2.39	
277	Ngdn	NM_026890	2.38	
278	Nol10	NM_001008421	2.37	
279	Ing1	NM_011919	2.37	1
280	Mafk	NM_010757	2.37	1
281	Mvp	NM_080638	2.36	
282	Tbccd1	NM_001081368	2.36	
283	Rhobtb3	NM_028493	2.36	
284	LOC433749	XM_485435	2.36	3
285	Cldnd1	NM_171826	2.34	
286	Centg2	NM_001037136	2.34	3
287	Pdap1	NM_001033313	2.34	
288	Pdcd6ip	NM_011052	2.33	

Table 11. Complete List of Genes Induced by ATF6 Activation in the Heart.

Number	Gene Symbol	RefSeq Transcript ID	Fold Change	Notes
289	Pacsin3	NM_028733	2.33	
290	2310061F22Rik	NM_153775	2.33	
291	Klf7	NM_033563	2.33	1
292	Nucks1	NM_175294	2.33	
293	Gcs1	NM_020619	2.32	7
294	Lrrc3b	NM_146052	2.32	
295	St6galnac4	NM_011373	2.32	
296	Dysf	NM_001077694	2.32	
297	Fkbp2	NM_008020	2.32	2
298	2310076L09Rik	NM_025874	2.30	
299	Snurf	NM_033174	2.30	
300	Gprk5	NM_018869	2.28	
301	Sec22b	NM_011342	2.27	
302	1700025G04Rik	NM_197990	2.26	
303	Arl4c	NM_177305	2.26	3
304	Dynll1	NM_019682	2.26	
305	Gars	NM_180678	2.25	
306	AA536743	NM_145923	2.24	
307	A130040M12Rik	NR_002860	2.24	
308	Anxa5	NM_009673	2.23	
309	Mrps18b	NM_025878	2.23	
310	Stt3b	NM_024222	2.23	
311	Tgfb2	NM_009367	2.22	5, 6
312	Pde4b	NM_019840	2.22	
313	Rab6	NM_024287	2.21	3
314	Akap2	NM_001035532	2.21	
315	Lrrc59	NM_133807	2.21	
316	Cnot6	NM_212484	2.21	1
317	Fads3	NM_021890	2.21	
318	Lipa	NM_021460	2.21	
319	Rab20	NM_011227	2.21	3
320	Slc6a6	NM_009320	2.21	
321	Cfl1	NM_007687	2.20	
322	Rnf4	NM_011278	2.20	1
323	Cugbp2	NM_010160	2.19	
324	Ddx54	NM_028041	2.19	1
325	Zbtb44	NM_172765	2.19	1
326	Alg8	NM_199035	2.18	
327	Adamts15	NM_001024139	2.18	
328	Fkbp7	NM_010222	2.16	2
329	Calm1	NM_009790	2.16	
330	Polr1e	NM_022811	2.15	
331	A230046K03Rik	NM_001033375	2.15	
332	Wdr57	NM_025645	2.14	
333	Stmn1	NM_019641	2.14	
334	Tln1	NM_011602	2.14	
335	Sertad3	NM_133210	2.14	1, 6
336	Tmem57	NM_025382	2.14	

Table 11. Complete List of Genes Induced by ATF6 Activation in the Heart.

Number	Gene Symbol	RefSeq Transcript ID	Fold Change	Notes
337	Prr13	NM_025385	2.14	
338	Cds2	NM_138651	2.13	
339	Cib1	NM_011870	2.13	
340	Slc26a2	NM_007885	2.12	
341	Nol5a	NM_024193	2.12	
342	Sfrs9	NM_025573	2.12	
343	Ppp1r12a	NM_027892	2.11	
344	Rrbp1	NM_024281	2.11	
345	Ppap2a	NM_008247	2.11	6
346	Pik3cb	NM_029094	2.11	
347	Tor1aip2	NM_172843	2.11	
348	Spryd3	NM_001033277	2.11	
349	Heatr5b	NM_001081179	2.11	
350	Ralb	NM_022327	2.11	3
351	Dnaja4	NM_021422	2.11	2
352	Tgm2	NM_009373	2.11	
353	Actl6a	NM_019673	2.10	1
354	Rpl14	NM_025974	2.09	
355	Srxn1	NM_029688	2.08	
356	Tubb5	NM_011655	2.08	
357	Psmd11	NM_178616	2.07	
358	D17Wsu104e	NM_080837	2.06	
359	Gna13	NM_010303	2.06	
360	Rrad	NM_019662	2.06	3
361	Taldo1	NM_011528	2.06	7
362	Fstl1	NM_008047	2.06	
363	Pabpn1	NM_019402	2.06	
364	Ap2b1	NM_001035854	2.06	
365	Stip1	NM_016737	2.05	
366	Rps27l	NM_026467	2.05	
367	Sdc2	NM_008304	2.05	
368	1110019N10Rik	NM_026753	2.05	
369	Wdr1	NM_011715	2.05	
370	Popdc3	NM_024286	2.04	
371	2310037I24Rik	NM_133714	2.04	
372	Ccdc86	NM_023731	2.04	
373	Crls1	NM_001024385	2.04	
374	Tfg	NM_019678	2.04	
375	Tial1	NM_009383	2.03	
376	Rwdd4a	NM_203507	2.03	
377	Smad2	NM_010754	2.03	1
378	5730446C15Rik	NM_146096	2.01	
379	BB271151	---	2.01	
380	Dusp27	NM_001033344	2.01	
381	Siah2	NM_009174	2.00	
382	Ifngr2	NM_008338	0.50	
383	Tmed1	NM_010744	0.50	
384	Epha4	NM_007936	0.50	

Table 11. Complete List of Genes Induced by ATF6 Activation in the Heart.

Number	Gene Symbol	RefSeq Transcript ID	Fold Change	Notes
385	Enpp5	NM_032003	0.50	7
386	Galm	NM_176963	0.50	
387	B3galtl	NM_001081204	0.49	
388	Cd59a	NM_007652	0.49	
389	Rtn4ip1	NM_130892	0.49	
390	Klhl24	NM_029436	0.49	
391	Cog6	NM_026225	0.49	
392	Thrsp	NM_009381	0.49	
393	Fgf9	NM_013518	0.49	
394	Ccdc21	NM_144527	0.49	
395	Jam2	NM_023844	0.49	
396	Aig1	NM_025446	0.49	
397	Clasp2	NM_001081960	0.49	
398	Ppm1k	NM_175523	0.49	
399	Mitf	NM_008601	0.48	1
400	Rhobtb1	NM_001081347	0.48	3
401	Entpd5	NM_001026214	0.48	
402	2810405K02Rik	NM_025582	0.48	
403	Auh	NM_016709	0.48	7
404	Peci	NM_011868	0.48	7
405	Wdr33	NM_028866	0.47	
406	Lmod2	NM_053098	0.47	
407	Clip4	NM_030179	0.47	
408	Ppil1	NM_026845	0.47	2
409	Magi2	XM_001000863	0.46	
410	B3gnt1	NM_175383	0.46	
411	3110002H16Rik	NM_029623	0.46	
412	Pigy	NM_025574	0.46	
413	C030044B11Rik	XM_980322	0.46	
414	Lpl	NM_008509	0.46	
415	Art3	NM_181728	0.46	
416	4430402I18Rik	NM_198651	0.46	
417	Ctsh	NM_007801	0.46	
418	Sepp1	NM_001042613	0.45	
419	Clybl	NM_029556	0.45	
420	Klhdc1	NM_178253	0.45	
421	Pex11a	NM_011068	0.45	
422	1810014F10Rik	NM_026928	0.45	
423	Cbr1	NM_007620	0.45	7
424	2410012H22Rik	XM_126343	0.45	
425	Hod	NM_175606	0.45	1
426	Plekhb2	NM_145516	0.45	
427	Ablim1	NM_178688	0.45	
428	Decr1	NM_026172	0.45	7
429	Ccni	NM_017367	0.45	
430	Mgst3	NM_025569	0.45	
431	Coq3	NM_172687	0.44	7
432	Gstt1	NM_008185	0.44	

Table 11. Complete List of Genes Induced by ATF6 Activation in the Heart.

Number	Gene Symbol	RefSeq Transcript ID	Fold Change	Notes
433	2210016H18Rik	---	0.44	
434	Apod	NM_007470	0.44	
435	AV347904	---	0.44	
436	Grb14	NM_016719	0.44	
437	Vapb	NM_019806	0.44	
438	Fahd2a	NM_029629	0.44	7
439	Fgf1	NM_010197	0.44	
440	Snrpn	NM_001082961	0.44	
441	Egflam	NM_178748	0.44	
442	Pcbd2	NM_028281	0.44	
443	Ptpn3	NM_011207	0.44	
444	Bckdhb	NM_199195	0.43	
445	Echs1	NM_053119	0.43	7
446	1810015C04Rik	NM_001034851	0.43	
447	Hrasls	NM_013751	0.43	
448	Neo1	NM_001042752	0.43	
449	Pex19	NM_023041	0.43	
450	Hlf	NM_172563	0.42	1
451	Atp6v0e2	NM_133764	0.42	
452	Mcee	NM_028626	0.42	
453	Pitpnc1	NM_145823	0.42	
454	Mettl7a	NM_027334	0.42	7
455	Ppargc1a	NM_008904	0.42	1, 7
456	Ociad2	NM_026950	0.41	
457	Slc25a11	NM_024211	0.41	
458	Adi1	NM_134052	0.41	
459	Crbn	NM_021449	0.41	
460	BB133024	---	0.41	
461	Slc25a13	NM_015829	0.41	
462	Trmt5	NM_029580	0.41	
463	2310061I04Rik	XM_001000601	0.41	
464	Ccrl2	NM_017466	0.41	
465	Dnaja2	NM_019794	0.41	2
466	Stom	NM_013515	0.41	
467	EG270335	XM_001003067	0.41	
468	Sirt5	NM_178848	0.40	1
469	Bche	NM_009738	0.40	
470	Pank1	NM_023792	0.40	
471	Myh6	NM_010856	0.40	
472	Gramd1b	NM_172768	0.40	
473	Mrpl49	NM_026246	0.40	
474	Cytl1	NM_001081106	0.39	
475	Tarsl2	NM_172310	0.39	
476	Slc22a5	NM_011396	0.39	
477	Cabc1	NM_023341	0.39	1
478	Cog8	NM_139229	0.38	
479	Asb11	NM_026853	0.38	
480	Etfdh	NM_025794	0.38	

Table 11. Complete List of Genes Induced by ATF6 Activation in the Heart.

Number	Gene Symbol	RefSeq Transcript ID	Fold Change	Notes
481	Amacr	NM_008537	0.37	7
482	EG434402	XM_917134	0.37	
483	D930026N18Rik	---	0.37	
484	Slc40a1	NM_016917	0.37	
485	Siae	NM_011734	0.37	
486	Prei4	NM_001042671	0.36	
487	Acsl1	NM_007981	0.36	7
488	Dpep1	NM_007876	0.36	
489	Sesn1	NM_001013370	0.36	
490	Asrgl1	NM_025610	0.36	
491	Mfsd4	NM_172510	0.36	
492	Nit2	NM_023175	0.36	
493	D930001I22Rik	NM_173397	0.36	
494	Pfkfb1	NM_008824	0.35	7
495	Ak3	NM_021299	0.35	
496	Agl	NM_001081326	0.34	
497	Vldlr	NM_013703	0.34	
498	Gpd1	NM_010271	0.34	7
499	Nqo2	NM_020282	0.34	
500	BE952563	---	0.34	
501	Acot11	NM_025590	0.34	7
502	Retsat	NM_026159	0.34	
503	Tfdp2	NM_178667	0.34	1
504	1100001H23Rik	NM_025806	0.33	
505	A2bp1	NM_021477	0.33	
506	Ccdc69	NM_177471	0.33	
507	Myot	NM_001033621	0.33	
508	Slc46a3	NM_027872	0.32	
509	Ndufs4	NM_010887	0.32	
510	4930534B04Rik	NM_181815	0.32	
511	Nmnat1	NM_133435	0.32	
512	Sgcg	NM_011892	0.32	
513	Ednra	NM_010332	0.32	7
514	Ctf1	NM_007795	0.31	
515	Lrrc27	NM_027164	0.31	
516	3632451O06Rik	NM_026142	0.31	
517	1500001A10Rik	NM_026886	0.31	
518	Cpt2	NM_009949	0.31	7
519	Sfxn4	NM_053198	0.31	
520	Pxmp2	NM_008993	0.31	
521	Cutc	NM_025530	0.31	
522	ORF28	NM_138664	0.30	2
523	4930481A15Rik	XM_980129	0.30	
524	2310014G06Rik	NM_001082975	0.30	
525	Hadh	NM_008212	0.30	7
526	Sord	NM_146126	0.30	
527	Rasl2-9	NM_009028	0.29	3
528	Mterfd3	NM_028832	0.29	1

Table 11. Complete List of Genes Induced by ATF6 Activation in the Heart.

Number	Gene Symbol	RefSeq Transcript ID	Fold Change	Notes
529	Aldh5a1	NM_172532	0.29	7
530	Nr0b2	NM_011850	0.29	1
531	Slc16a10	NM_028247	0.29	
532	Slc25a20	NM_020520	0.29	
533	4833417J20Rik	---	0.28	
534	Ucp3	NM_009464	0.27	7
535	Asb15	NM_080847	0.27	1
536	C730029A08Rik	---	0.27	
537	1700040L02Rik	NM_028491	0.26	
538	BQ175377	---	0.25	
539	Rasl10b	NM_001013386	0.25	3
540	Slc25a20	NM_020520	0.25	
541	Asb2	NM_023049	0.25	1
542	Tbl1xr1	NM_030732	0.25	1
543	Rxrg	NM_009107	0.25	1
544	Slc27a1	NM_011977	0.25	7
545	Itgb1bp2	NM_013712	0.25	
546	Fndc5	NM_027402	0.24	
547	Acy3	NM_027857	0.24	7
548	AW989410	---	0.24	
549	Nudt7	NM_024437	0.24	
550	Tcea3	NM_011542	0.24	1
551	Herpud2	NM_020586	0.23	2, *
552	A530016L24Rik	NM_177039	0.23	
553	Asb10	NM_080444	0.23	1
554	Asb15	NM_080847	0.23	
555	1110034G24Rik	XM_001000361	0.23	
556	1700025K23Rik	NM_183254	0.23	
557	Sgca	NM_009161	0.23	
558	Atp1a2	NM_178405	0.23	7

Table 11. Complete List of Genes Induced by ATF6 Activation in the Heart.

Number	Gene Symbol	RefSeq Transcript ID	Fold Change	Notes
559	Acot1	NM_012006	0.23	
560	Csdc2	NM_145473	0.22	1
561	Lrg1	NM_029796	0.22	
562	Gzmm	NM_008504	0.22	
563	Btbd2	XM_001000710	0.22	
564	Kcnj11	NM_010602	0.22	
565	Rad23a	NM_009010	0.21	
566	Wipf3	XM_620310	0.21	
567	Ephx2	NM_007940	0.21	7
568	Gdpd1	NM_025638	0.20	
569	Hhatl	NM_029095	0.20	
570	Gstk1	NM_029555	0.20	
571	Selenbp1	NM_009150	0.20	
572	Adssl1	NM_007421	0.20	
573	Cutl2	NM_007804	0.20	1
574	Fblim1	NM_133754	0.20	
575	Tbc1d10c	NM_178650	0.19	
576	Fah	NM_010176	0.19	1, 7
577	Wdr21	NM_030246	0.19	
578	Asb14	NM_080856	0.19	
579	Mlycd	NM_019966	0.19	7
580	Mme	NM_008604	0.19	
581	Art4	NM_026639	0.19	
582	Kcnv2	NM_183179	0.18	
583	D2hgdh	NM_178882	0.18	
584	Frem2	NM_172862	0.17	
585	Cmbl	NM_181588	0.17	
586	2310076L09Rik	NM_001077348	0.17	
587	Aldob	NM_144903	0.17	7
588	Oplah	NM_153122	0.16	
589	Fbp2	NM_007994	0.16	7
590	Ces3	NM_053200	0.16	
591	Art1	NM_009710	0.16	
592	Inmt	NM_009349	0.15	
593	Cmtm8	NM_027294	0.14	
594	Lrtm1	NM_176920	0.14	
595	Impa2	NM_053261	0.14	
596	Ky	NM_024291	0.14	
597	P2ry1	NM_008772	0.12	
598	BB515119	---	0.11	
599	2310010M20Rik	NM_183283	0.11	
600	Pdlim4	NM_019417	0.10	
601	C730027J19Rik	NM_178758	0.10	7
602	Klf15	NM_023184	0.09	1,7
603	Ogdh	NM_010956	0.08	7
604	Apba3	NM_001081208	0.08	
605	Ttll1	NM_178869	0.06	
606	Slc25a34	NM_001013780	0.06	

Table 11. Complete List of Genes Induced by ATF6 Activation in the Heart.

Number	Gene Symbol	RefSeq Transcript ID	Fold Change	Notes
607	Fn3k	NM_001038699	0.03	

REFERENCES

1.   Herczenik E, Gebbink MF. Molecular and cellular aspects of protein misfolding and disease. *Faseb J*. 2008;22:2115-33.

2.   Faragher RG, Sheerin AN, Ostler EL. Can we intervene in human ageing? *Expert Rev Mol Med*. 2009;11:e27.

3.   Kaufman RJ. Orchestrating the unfolded protein response in health and disease. *J Clin Invest*. 2002;110:1389-98.

4.   Gregersen N, Bross P, Vang S, Christensen JH. Protein misfolding and human disease. *Annu Rev Genomics Hum Genet*. 2006;7:103-24.

5.   Okada K, Minamino T, Tsukamoto Y, Liao Y, Tsukamoto O, Takashima S, Hirata A, Fujita M, Nagamachi Y, Nakatani T, Yutani C, Ozawa K, Ogawa S, Tomoike H, Hori M, Kitakaze M. Prolonged endoplasmic reticulum stress in hypertrophic and failing heart after aortic constriction: possible contribution of endoplasmic reticulum stress to cardiac myocyte apoptosis. *Circulation*. 2004;110:705-12.

6.   Wu J, Kaufman RJ. From acute ER stress to physiological roles of the Unfolded Protein Response. *Cell Death Differ*. 2006;13:374-84.

7.   Zhang K, Kaufman RJ. The unfolded protein response: a stress signaling pathway critical for health and disease. *Neurology*. 2006;66:S102-9.

8.   Fribley A, Zhang K, Kaufman RJ. Regulation of apoptosis by the unfolded protein response. *Methods Mol Biol*. 2009;559:191-204.

9.   Aridor M. Visiting the ER: the endoplasmic reticulum as a target for therapeutics in traffic related diseases. *Adv Drug Deliv Rev*. 2007;59:759-81.

10.   Glembotski CC. The role of the unfolded protein response in the heart. *J Mol Cell Cardiol*. 2008;44:453-9.

11.   Glembotski CC. Endoplasmic reticulum stress in the heart. *Circ Res*. 2007;101:975-84.

12.   Bertolotti A, Zhang Y, Hendershot LM, Harding HP, Ron D. Dynamic interaction of BiP and ER stress transducers in the unfolded-protein response. *Nat Cell Biol*. 2000;2:326-32.

13.   Harding HP, Zhang Y, Ron D. Protein translation and folding are coupled by an endoplasmic-reticulum-resident kinase. *Nature*. 1999;397:271-4.

14. Oyadomari S, Mori M. Roles of CHOP/GADD153 in endoplasmic reticulum stress. *Cell Death Differ*. 2004;11:381-9.

15. McCullough KD, Martindale JL, Klotz LO, Aw TY, Holbrook NJ. Gadd153 sensitizes cells to endoplasmic reticulum stress by down-regulating Bcl2 and perturbing the cellular redox state. *Mol Cell Biol*. 2001;21:1249-59.

16. Sidrauski C, Walter P. The transmembrane kinase Ire1p is a site-specific endonuclease that initiates mRNA splicing in the unfolded protein response. *Cell*. 1997;90:1031-9.

17. Calfon M, Zeng H, Urano F, Till JH, Hubbard SR, Harding HP, Clark SG, Ron D. IRE1 couples endoplasmic reticulum load to secretory capacity by processing the XBP-1 mRNA. *Nature*. 2002;415:92-6.

18. Yoshida H. Unconventional splicing of XBP-1 mRNA in the unfolded protein response. *Antioxid Redox Signal*. 2007;9:2323-33.

19. Urano F, Wang X, Bertolotti A, Zhang Y, Chung P, Harding HP, Ron D. Coupling of stress in the ER to activation of JNK protein kinases by transmembrane protein kinase IRE1. *Science*. 2000;287:664-6.

20. Martindale JJ, Fernandez R, Thuerauf D, Whittaker R, Gude N, Sussman MA, Glembotski CC. Endoplasmic reticulum stress gene induction and protection from ischemia/reperfusion injury in the hearts of transgenic mice with a tamoxifen-regulated form of ATF6. *Circ Res*. 2006;98:1186-93.

21. Thuerauf DJ, Morrison LE, Hoover H, Glembotski CC. Coordination of ATF6-mediated transcription and ATF6 degradation by a domain that is shared with the viral transcription factor, VP16. *J Biol Chem*. 2002;277:20734-9.

22. Yoshida H, Haze K, Yanagi H, Yura T, Mori K. Identification of the cis-acting endoplasmic reticulum stress response element responsible for transcriptional induction of mammalian glucose-regulated proteins. Involvement of basic leucine zipper transcription factors. *J Biol Chem*. 1998;273:33741-9.

23. Kokame K, Kato H, Miyata T. Identification of ERSE-II, a new cis-acting element responsible for the ATF6-dependent mammalian unfolded protein response. *J Biol Chem*. 2001;276:9199-205.

24. Yamamoto K, Yoshida H, Kokame K, Kaufman RJ, Mori K. Differential contributions of ATF6 and XBP1 to the activation of endoplasmic reticulum stress-responsive cis-acting elements ERSE, UPRE and ERSE-II. *J Biochem*. 2004;136:343-50.

25.   Yamamoto K, Suzuki N, Wada T, Okada T, Yoshida H, Kaufman RJ, Mori K. Human HRD1 promoter carries a functional unfolded protein response element to which XBP1 but not ATF6 directly binds. *J Biochem*. 2008;144:477-86.

26.   Yamamoto K, Sato T, Matsui T, Sato M, Okada T, Yoshida H, Harada A, Mori K. Transcriptional induction of mammalian ER quality control proteins is mediated by single or combined action of ATF6alpha and XBP1. *Dev Cell*. 2007;13:365-76.

27.   Belmont PJ, Chen WJ, San Pedro MN, Thuerauf DJ, Gellings Lowe N, Gude N, Hilton B, Wolkowicz R, Sussman MA, Glembotski CC. Roles for Endoplasmic Reticulum-Associated Degradation and the Novel Endoplasmic Reticulum Stress Response Gene Derlin-3 in the Ischemic Heart. *Circ Res*. 2009.

28.   Lee AS. The glucose-regulated proteins: stress induction and clinical applications. *Trends Biochem Sci*. 2001;26:504-10.

29.   Healy SJ, Gorman AM, Mousavi-Shafaei P, Gupta S, Samali A. Targeting the endoplasmic reticulum-stress response as an anticancer strategy. *Eur J Pharmacol*. 2009.

30.   Wang S, Longo FM, Chen J, Butman M, Graham SH, Haglid KG, Sharp FR. Induction of glucose regulated protein (grp78) and inducible heat shock protein (hsp70) mRNAs in rat brain after kainic acid seizures and focal ischemia. *Neurochem Int*. 1993;23:575-82.

31.   Paschen W, Gissel C, Linden T, Althausen S, Doutheil J. Activation of gadd153 expression through transient cerebral ischemia: evidence that ischemia causes endoplasmic reticulum dysfunction. *Brain Res Mol Brain Res*. 1998;60:115-22.

32.   Paschen W, Aufenberg C, Hotop S, Mengesdorf T. Transient cerebral ischemia activates processing of xbp1 messenger RNA indicative of endoplasmic reticulum stress. *J Cereb Blood Flow Metab*. 2003;23:449-61.

33.   Paschen W, Yatsiv I, Shoham S, Shohami E. Brain trauma induces X-box protein 1 processing indicative of activation of the endoplasmic reticulum unfolded protein response. *J Neurochem*. 2004;88:983-92.

34.   Kapoor A, Sanyal AJ. Endoplasmic reticulum stress and the unfolded protein response. *Clin Liver Dis*. 2009;13:581-90.

35.   Thuerauf DJ, Marcinko M, Gude N, Rubio M, Sussman MA, Glembotski CC. Activation of the unfolded protein response in infarcted mouse heart and hypoxic cultured cardiac myocytes. *Circ Res*. 2006;99:275-82.

36. Zhang K, Kaufman RJ. Identification and characterization of endoplasmic reticulum stress-induced apoptosis in vivo. *Methods Enzymol*. 2008;442:395-419.

37. Ron D, Habener JF. CHOP, a novel developmentally regulated nuclear protein that dimerizes with transcription factors C/EBP and LAP and functions as a dominant-negative inhibitor of gene transcription. *Genes Dev*. 1992;6:439-53.

38. Yoshida H, Okada T, Haze K, Yanagi H, Yura T, Negishi M, Mori K. ATF6 activated by proteolysis binds in the presence of NF-Y (CBF) directly to the cis-acting element responsible for the mammalian unfolded protein response. *Mol Cell Biol*. 2000;20:6755-67.

39. Nakanishi K, Sudo T, Morishima N. Endoplasmic reticulum stress signaling transmitted by ATF6 mediates apoptosis during muscle development. *J Cell Biol*. 2005;169:555-60.

40. Doroudgar S, Thuerauf DJ, Marcinko MC, Belmont PJ, Glembotski CC. Ischemia activates the ATF6 branch of the endoplasmic reticulum stress response. *J Biol Chem*. 2009;284:29735-45.

41. Belmont PJ, Tadimalla A, Chen WJ, Martindale JJ, Thuerauf DJ, Marcinko M, Gude N, Sussman MA, Glembotski CC. Coordination of growth and endoplasmic reticulum stress signaling by regulator of calcineurin 1 (RCAN1), a novel ATF6-inducible gene. *J Biol Chem*. 2008;283:14012-21.

42. Vega RB, Bassel-Duby R, Olson EN. Control of cardiac growth and function by calcineurin signaling. *J Biol Chem*. 2003;278:36981-4.

43. Ruddon RW, Bedows E. Assisted protein folding. *J Biol Chem*. 1997;272:3125-8.

44. Austin RC. The Unfolded Protein Response in Health and Disease. *Antioxid Redox Signal*. 2009.

45. Meunier L, Usherwood YK, Chung KT, Hendershot LM. A subset of chaperones and folding enzymes form multiprotein complexes in endoplasmic reticulum to bind nascent proteins. *Mol Biol Cell*. 2002;13:4456-69.

46. Sitia R, Braakman I. Quality control in the endoplasmic reticulum protein factory. *Nature*. 2003;426:891-4.

47. Vembar SS, Brodsky JL. One step at a time: endoplasmic reticulum-associated degradation. *Nat Rev Mol Cell Biol*. 2008;9:944-57.

48.	Ellgaard L, Helenius A. Quality control in the endoplasmic reticulum. *Nat Rev Mol Cell Biol*. 2003;4:181-91.

49.	Wiertz EJ, Jones TR, Sun L, Bogyo M, Geuze HJ, Ploegh HL. The human cytomegalovirus US11 gene product dislocates MHC class I heavy chains from the endoplasmic reticulum to the cytosol. *Cell*. 1996;84:769-79.

50.	Schmitz A, Herrgen H, Winkeler A, Herzog V. Cholera toxin is exported from microsomes by the Sec61p complex. *J Cell Biol*. 2000;148:1203-12.

51.	Nakatsukasa K, Huyer G, Michaelis S, Brodsky JL. Dissecting the ER-associated degradation of a misfolded polytopic membrane protein. *Cell*. 2008;132:101-12.

52.	van Rooij E, Marshall WS, Olson EN. Toward microRNA-based therapeutics for heart disease: the sense in antisense. *Circ Res*. 2008;103:919-28.

53.	Lu M, Zhang Q, Deng M, Miao J, Guo Y, Gao W, Cui Q. An analysis of human microRNA and disease associations. *PLoS One*. 2008;3:e3420.

54.	Cui Q, Yu Z, Purisima EO, Wang E. Principles of microRNA regulation of a human cellular signaling network. *Mol Syst Biol*. 2006;2:46.

55.	Cui Q, Yu Z, Pan Y, Purisima EO, Wang E. MicroRNAs preferentially target the genes with high transcriptional regulation complexity. *Biochem Biophys Res Commun*. 2007;352:733-8.

56.	Sassen S, Miska EA, Caldas C. MicroRNA: implications for cancer. *Virchows Arch*. 2008;452:1-10.

57.	Leung AK, Sharp PA. microRNAs: a safeguard against turmoil? *Cell*. 2007;130:581-5.

58.	Tadimalla A, Belmont PJ, Thuerauf DJ, Glassy MS, Martindale JJ, Gude N, Sussman MA, Glembotski CC. Mesencephalic astrocyte-derived neurotrophic factor is an ischemia-inducible secreted endoplasmic reticulum stress response protein in the heart. *Circ Res*. 2008;103:1249-58.

59.	Chen WH, Sun LT, Tsai CL, Song YL, Chang CF. Cold-stress induced the modulation of catecholamines, cortisol, immunoglobulin M, and leukocyte phagocytosis in tilapia. *Gen Comp Endocrinol*. 2002;126:90-100.

60.	Efron B, Tibshirani R. Statistical Data Analysis in the Computer Age. *Science*. 1991;253:390-395.

61. Sadoshima J, Jahn L, Takahashi T, Kulik TJ, Izumo S. Molecular characterization of the stretch-induced adaptation of cultured cardiac cells. An in vitro model of load-induced cardiac hypertrophy. *J Biol Chem*. 1992;267:10551-60.

62. Ashburner M, Ball CA, Blake JA, Botstein D, Butler H, Cherry JM, Davis AP, Dolinski K, Dwight SS, Eppig JT, Harris MA, Hill DP, Issel-Tarver L, Kasarskis A, Lewis S, Matese JC, Richardson JE, Ringwald M, Rubin GM, Sherlock G. Gene ontology: tool for the unification of biology. The Gene Ontology Consortium. *Nat Genet*. 2000;25:25-9.

63. DenBoer LM, Hardy-Smith PW, Hogan MR, Cockram GP, Audas TE, Lu R. Luman is capable of binding and activating transcription from the unfolded protein response element. *Biochem Biophys Res Commun*. 2005;331:113-9.

64. Thuerauf DJ, Marcinko M, Belmont PJ, Glembotski CC. Effects of the isoform-specific characteristics of ATF6 alpha and ATF6 beta on endoplasmic reticulum stress response gene expression and cell viability. *J Biol Chem*. 2007;282:22865-78.

65. Wu H, Peisley A, Graef IA, Crabtree GR. NFAT signaling and the invention of vertebrates. *Trends Cell Biol*. 2007;17:251-60.

66. Rothermel BA, Vega RB, Williams RS. The role of modulatory calcineurin-interacting proteins in calcineurin signaling. *Trends Cardiovasc Med*. 2003;13:15-21.

67. Fuentes JJ, Genesca L, Kingsbury TJ, Cunningham KW, Perez-Riba M, Estivill X, de la Luna S. DSCR1, overexpressed in Down syndrome, is an inhibitor of calcineurin-mediated signaling pathways. *Hum Mol Genet*. 2000;9:1681-90.

68. Terai K, Hiramoto Y, Masaki M, Sugiyama S, Kuroda T, Hori M, Kawase I, Hirota H. AMP-activated protein kinase protects cardiomyocytes against hypoxic injury through attenuation of endoplasmic reticulum stress. *Mol Cell Biol*. 2005;25:9554-75.

69. Yamamoto K, Yoshida H, Kokame K, Kaufman RJ, Mori K. Differential contributions of ATF6 and XBP1 to the activation of endoplasmic reticulum stress-responsive cis-acting elements ERSE, UPRE and ERSE-II. *J Biochem (Tokyo)*. 2004;136:343-50.

70. Pu WT, Ma Q, Izumo S. NFAT transcription factors are critical survival factors that inhibit cardiomyocyte apoptosis during phenylephrine stimulation in vitro. *Circ Res*. 2003;92:725-31.

71. Thuerauf DJ, Hoover H, Meller J, Hernandez J, Su L, Andrews C, Dillmann WH, McDonough PM, Glembotski CC. Sarco/endoplasmic reticulum calcium ATPase-2 expression is regulated by ATF6 during the endoplasmic reticulum stress response: intracellular signaling of calcium stress in a cardiac myocyte model system. *J Biol Chem*. 2001;276:48309-17.

72. Hanford DS, Thuerauf DJ, Murray SF, Glembotski CC. Brain natriuretic peptide is induced by alpha 1-adrenergic agonists as a primary response gene in cultured rat cardiac myocytes. *J Biol Chem*. 1994;269:26227-33.

73. Molkentin JD, Dorn, G.W. Cytoplasmic Signaling Pathways That Regulate Cardiac Hypertrophy. *Annu. Rev. Physiol.* 2001;63:391-426.

74. Oda Y, Okada T, Yoshida H, Kaufman RJ, Nagata K, Mori K. Derlin-2 and Derlin-3 are regulated by the mammalian unfolded protein response and are required for ER-associated degradation. *J Cell Biol*. 2006;172:383-93.

75. Soto C, Estrada LD. Protein misfolding and neurodegeneration. *Arch Neurol*. 2008;65:184-9.

76. Skovronsky DM, Lee VM, Trojanowski JQ. Neurodegenerative diseases: new concepts of pathogenesis and their therapeutic implications. *Annu Rev Pathol*. 2006;1:151-70.

77. Thuerauf DJ, Morrison L, Glembotski CC. Opposing roles for ATF6alpha and ATF6beta in endoplasmic reticulum stress response gene induction. *J Biol Chem*. 2004;279:21078-84.

78. Oyadomari S, Koizumi A, Takeda K, Gotoh T, Akira S, Araki E, Mori M. Targeted disruption of the Chop gene delays endoplasmic reticulum stress-mediated diabetes. *J Clin Invest*. 2002;109:525-32.

79. Sifers RN, Brashears-Macatee S, Kidd VJ, Muensch H, Woo SL. A frameshift mutation results in a truncated alpha 1-antitrypsin that is retained within the rough endoplasmic reticulum. *J Biol Chem*. 1988;263:7330-5.

80. Lilley BN, Ploegh HL. Multiprotein complexes that link dislocation, ubiquitination, and extraction of misfolded proteins from the endoplasmic reticulum membrane. *Proc Natl Acad Sci U S A*. 2005;102:14296-301.

81. Plemper RK, Egner R, Kuchler K, Wolf DH. Endoplasmic reticulum degradation of a mutated ATP-binding cassette transporter Pdr5 proceeds in a concerted action of Sec61 and the proteasome. *J Biol Chem*. 1998;273:32848-56.

82.   Fasanaro P, Greco S, Lorenzi M, Pescatori M, Brioschi M, Kulshreshtha R, Banfi C, Stubbs A, Calin GA, Ivan M, Capogrossi MC, Martelli F. An integrated approach for experimental target identification of hypoxia-induced miR-210. *J Biol Chem*. 2009.

83.   Divakaran V, Mann DL. The emerging role of microRNAs in cardiac remodeling and heart failure. *Circ Res*. 2008;103:1072-83.

84.   Williams AH, Liu N, van Rooij E, Olson EN. MicroRNA control of muscle development and disease. *Curr Opin Cell Biol*. 2009;21:461-9.

85.   Lee Y, Kim M, Han J, Yeom KH, Lee S, Baek SH, Kim VN. MicroRNA genes are transcribed by RNA polymerase II. *Embo J*. 2004;23:4051-60.

86.   Megraw M, Baev V, Rusinov V, Jensen ST, Kalantidis K, Hatzigeorgiou AG. MicroRNA promoter element discovery in Arabidopsis. *Rna*. 2006;12:1612-9.

87.   Megraw M, Hatzigeorgiou AG. MicroRNA promoter analysis. *Methods Mol Biol*;592:149-61.

88.   Herpin A, Lelong C, Favrel P. Transforming growth factor-beta-related proteins: an ancestral and widespread superfamily of cytokines in metazoans. *Dev Comp Immunol*. 2004;28:461-85.

89.   van Rooij E, Sutherland LB, Liu N, Williams AH, McAnally J, Gerard RD, Richardson JA, Olson EN. A signature pattern of stress-responsive microRNAs that can evoke cardiac hypertrophy and heart failure. *Proc Natl Acad Sci U S A*. 2006;103:18255-60.

90.   Wang N, Zhou Z, Liao X, Zhang T. Role of microRNAs in cardiac hypertrophy and heart failure. *IUBMB Life*. 2009;61:566-71.

91.   Barry SP, Davidson SM, Townsend PA. Molecular regulation of cardiac hypertrophy. *Int J Biochem Cell Biol*. 2008;40:2023-39.

92.   Toth A, Nickson P, Mandl A, Bannister ML, Toth K, Erhardt P. Endoplasmic reticulum stress as a novel therapeutic target in heart diseases. *Cardiovasc Hematol Disord Drug Targets*. 2007;7:205-18.

93.   Walsh K. Adipokines, myokines and cardiovascular disease. *Circ J*. 2009;73:13-8.

94.   Oshima Y, Ouchi N, Sato K, Izumiya Y, Pimentel DR, Walsh K. Follistatin-like 1 is an Akt-regulated cardioprotective factor that is secreted by the heart. *Circulation*. 2008;117:3099-108.